

Supplementary Information for

Controlled introduction of functional groups at one P atom in [Cp*Fe(η^5 -P₅)] and release of functionalised phosphines

Stephan Reichl¹, Felix Riedelberger¹, Martin Piesch¹, Gábor Balázs¹, Michael Seidl¹,
Manfred Scheer^{1*}

¹Institute of Inorganic Chemistry, University of Regensburg; Universitätsstraße 31, 93053 Regensburg, Germany.

*Corresponding author. Email: Manfred.Scheer@chemie.uni-regensburg.de

This PDF file includes:

1. Experimental details	2
2. NMR spectroscopic characterization	9
3. Crystallographic details	33
4. Additional information	54
5. Computational details	59
6. References	61

Experimental details

General methods:

All manipulations were carried out under an inert atmosphere of dried argon using standard Schlenk and glove box techniques. 1,2-dimethoxyethane (DME) was dried and deoxygenated by distillation under argon atmosphere from sodium. All other solvents were dried using a MB SPS-800 device of the company MBRAUN and stored over molecular sieve. NMR spectra were recorded on a Bruker Avance III 400/600 MHz NMR spectrometer. Chemical shifts were measured at ambient temperature and are given in ppm; they are referenced to TMS for ^1H and 85% H_3PO_4 for ^{31}P as external standard. Signal multiplicities are described using common abbreviations: s (singlet), d (doublet), t (triplet), q (quartet), quint (quintet), m (multiplet) and br (broad). LIFDI-/FD-/EI-MS spectra (LIFDI = liquid injection field desorption ionization, FD = field desorption, EI = electron ionization) were measured on a JEOL AccuTOF GCX. ESI-MS spectra (ESI = Electrospray ionization) were measured on an Agilent Q-TOF 6540 UHD. Elemental analysis (CHN) was determined using a Vario micro cube instrument. A glass stirring bar was used in reactions with potassium benzyl.

The compounds potassium benzyl (KBn , KC_7H_7), $[\text{K}(\text{DME})_2]_2[\text{Cp}^*\text{Fe}(\eta^4\text{-P}_5)]$ (**I'**), $[\text{Cp}^*\text{Fe}(\eta^5\text{-P}_5)]$ (**I**), $[\text{Li}(\text{DME})_3][\text{Cp}^*\text{Fe}(\eta^4\text{-P}_5\text{Me})]$ (**1a**) and $[\text{Li}(12\text{c}4)_2][\text{Cp}^*\text{Fe}(\eta^4\text{-P}_5'\text{Bu})]$ (**1b**), were synthesized according to literature procedures¹⁻⁴. Modified Synthesis of KPPh_2 : Deprotonation of PPh_2H with KH in DME and stored as a stock solution at 8 °C.

Unless otherwise noted, all other materials were obtained from commercial suppliers and used without purification.

DFT calculations were carried out using the ORCA program⁵. The geometries were optimised using the B3LYP⁶⁻⁹ functional together with the *def2-TZVP* basis set¹⁰ and the RIJCOSX¹¹ approximation. The dispersion effects have been incorporated by using the charge dependent atom-pairwise dispersion correction D4¹² as implemented in Orca.

CV / SQV measurements were conducted via the following setup: glass carbon-, Pt- and Ag electrodes; 0.01 mmol analyte, 500 mg $[\text{NBu}_4]\text{[PF}_6]$ as conductive salt, 5 mL solvent (o-DFB), ferrocene for reference.

Crystals suitable for single crystal X-ray diffraction analysis were obtained as described below. The diffraction data were collected either on a Gemini Ultra diffractometer equipped with an Atlas^{S2} CCD detector and with a fine-focus sealed Cu-K α X-ray tube, on a XtaLAB Synergy R, DW system diffractometer equipped with a HyPix-Arc 150 detector and a rotating-anode Cu-K α X-ray tube or a GV50 diffractometer equipped with a Titan^{S2} CCD detector and a micro-focus Cu-K α X-ray tube. Data collection and reduction were performed with CrysAlisPro software package. The structures were solved with Olex2¹³, using ShelXT¹⁴ and a least-square refinement on P^2 was carried out with ShelXL¹⁵. All non-hydrogen atoms were refined anisotropically. Hydrogen atoms at the carbon atoms were located in idealized positions and refined with isotropic displacement parameters according to the riding model. The images of the molecular structures were made using Olex2.¹³ All NMR simulations were conducted with the *WinDaisy* application within the NMR software *Top Spin* 4.1.1 by *Bruker*.

Synthetic protocols:

Synthesis of $[K(18c6)(THF)][Cp^*Fe(\eta^4-P_5-C\equiv CPh)]$ (**1c**):

Benzyl potassium (0.29 mmol, 37.8 mg, 1 eq) was dissolved in THF and 0.29 mmol (0.50 mL, 1 eq) of a 0.58 molar solution of ethynylbenzene in THF was added. Thereby the color changed from red to colorless. Afterwards this solution was added to a solution of 100 mg (0.29 mmol, 1 eq) $[Cp^*Fe(\eta^5-P_5)]$ (**I**) at $-80^\circ C$ in THF. The solution was slowly warmed up to ambient temperatures and stirred overnight. All volatiles were removed in vacuum and the brown residue was washed three times with 10 mL *n*-hexane. 38 mg (0.145 mmol, 1 eq) 18-crown-6 was dissolved in THF 5 mL, added to the brown residue, layered with 20 mL *n*-hexane and stored at $4^\circ C$. After two weeks metallic dark green blocks of $[K(18c6)(thf)][Cp^*Fe(\eta^4-P_5)-C\equiv C-Ph]$ (**1c**) were formed.

Yield: 124.0 mg (0.151 mmol, 27 %). 1H NMR (THF-d₈, 293 K): δ [ppm] = 7.25 (m, 3 H, -Ph), 7.15 (m, 2 H, -Ph), 3.87 (s, 33 H, 18c6), 3.87 (33 H, THF), 2.01 (m, 3 H, THF), 1.73 (s, 15 H, $C_5(CH_3)_5$). $^{31}P\{^1H\}$ NMR (THF-d₈, 293 K): δ [ppm] = 35.5 (m, 1 P, P_A), 26.1 (m, 2 P, P_{B,B'}), -60.3 (m, 2 P, P_{x,x'}). ^{31}P NMR (THF-d₈, 293 K): δ [ppm] = 35.5 (m, 1 P, P_A), 26.1 (m, 2 P, P_{B,B'}), -60.3 (m, 2 P, P_{x,x'}). (ESI-MS (DME): 446.96 (100 %, $[M]^+$), 478.95 (16 %, $[M-O_2]^+$). Elemental analysis (calcd., found for $C_{34}H_{52}FeKO_7P_5$): C (49.64, 49.66), H (6.37, 6.39).

Alternative route: Compound **I** (0.87 mmol, 300.0 mg, 1 eq) and Li-C≡CPh (0.87 mmol, 94.0 mg, 1 eq) were dissolved together in THF at r.t. Within the next 30 minutes, the green color of the solution got darker. After letting the solution stir overnight, the solvent was removed under reduced pressure and a 0.8102 molar solution of 12c4 in DME (1.74 mmol, 2.15 mL, 2 eq) was added. The solution was layered with 10 mL of *n*-Hexane and stored at r.t. Crystals suitable for XRD were obtained as green plates after one week. The analytical data matches the anion of **1c**.

Yield: 497.0 mg (0.69 mmol, 79 %). 1H NMR (THF-d₈, 293 K): δ [ppm] = 7.31 (m, 3 H, -Ph), 7.17 (m, 2 H, -Ph), 4.06 (s, 16 H, 12c4), 3.67 (6 H, DME), 3.51 (m, 4 H, DME), 1.73 (s, 15 H, $C_5(CH_3)_5$). $^{31}P\{^1H\}$ NMR (THF-d₈, 293 K): δ [ppm] = 35.7 (m, 1 P, P_A), 26.0 (m, 2 P, P_{B,B'}), -59.3 (m, 2 P, P_{x,x'}). ^{31}P NMR (THF-d₈, 293 K): δ [ppm] = 35.7 (m, 1 P, P_A), 26.0 (m, 2 P, P_{B,B'}), -59.3 (m, 2 P, P_{x,x'}). For coupling constants, see Table S1).

Reaction of $[Li(12c4)_2][Cp^*Fe(\eta^4-P_5'Bu)]$ (**1a**) with 1,3-dibromopropane:

A solution of *in situ* generated **1a** ($[Cp^*Fe(\eta^5-P_5)]$ (**I**): 2.9 mmol, 1 g, 1 eq; $'BuLi$ in *n*-pentane: 0.4 mmol, v = 0.97 mL, c = 1.028 mol·L⁻¹, 1 eq) in 20 mL THF was added to a 0.917 molar solution of 1,3-dibromopropane in DME (2 mmol, 2.18 mL, 2 eq) at room temperature. A colour change from brown to green occurred and a colourless solid was formed. The mixture was stirred for 18 hours. The solvent was removed under reduced pressure. The residue was dissolved in dichloromethane, silica is added, and the solvent was removed *in vacuo*. The preabsorbed reaction mixture was purified via column chromatography (SiO₂, hexane, 15 x 3 cm). Using a mixture of hexane/toluene (8:2), a first green fraction ($[Cp^*Fe(\eta^4-P_5'Bu(CH_2)_3Br)]$ (**2a**), followed by a brown one ($[(Cp^*Fe)_2\{\mu,\eta^{4:4}-P_5'Bu(CH_2)_3P_5'Bu\}]$) (**3a**) can be eluted. The solvent of both fractions was removed under reduced pressure. $[Cp^*Fe(\eta^4-P_5'Bu(CH_2)_3Br)]$ (**2a**) can be isolated as dark green needles after one day in a concentrated *n*-hexane solution, stored at $-30^\circ C$. $[(Cp^*Fe)_2\{\mu,\eta^{4:4}-P_5'Bu(CH_2)_3P_5'Bu\}]$ (**3a**) can be obtained as brown needles after one week via layering a dichloromethane (3 mL) solution with acetonitrile (10 mL) and stored at $-30^\circ C$.

Data for $[Cp^*Fe(\eta^4-P_5'Bu(CH_2)_3Br)]$ (**2a**):

Yield: 917.0 mg (1.69 mmol, 58 %). 1H NMR (CD₂Cl₂, 293 K): δ [ppm] = 3.62 (t, 2 H, $J_{H-H} = 6.34$ Hz, -(CH₂)₂CH₂-Br), 2.70 (m, 2 H, -(CH₂)₂CH₃), 2.56 (m, 2 H, -(CH₂)₂CH₃), 1.63 (s, 15 H, $C_5(CH_3)_5$), 0.59 (d, 9 H, $^3J_{P-H} = 14.54$ Hz, -C(CH₃)₃). $^{31}P\{^1H\}$ NMR (CD₂Cl₂, 293 K): δ [ppm] = 165.1 (m, 1 P, P_A), 40.2 (m, 2 P, P_{M,M'}), -121.6 (m, 2 P, P_{x,x'}). ^{31}P NMR (CD₂Cl₂, 293 K): δ [ppm] = 165.1 (m, 1 P, P_A), 40.2 (m, 2 P,

$P_{M,M'}$), -121.6 (m, 2 P, $P_{x,x'}$). For coupling constants, see Table S2. **LIFDI-MS** (toluene): m/z = 523.90 (100 %, $[M]^+$). Elemental analysis (calcd., found for $C_{17}H_{30}FeBrP_5$): C (47.26, 47.61), H (7.40, 7.49).

Data for $[(Cp^*Fe)_2\{\mu,\eta^{4:4}-P_5'Bu(CH_2)_3P_5'Bu\}]$ (3a/3a'):

Yield: 390.0 mg (0.46 mmol, 32 %).

3a: **1H NMR** (CD_2Cl_2 , 293 K): δ [ppm] = 2.92 (m, 6 H, $-(CH_2)_3-$), 1.69 (s, 30 H, $C_5(CH_3)_5$), 0.69 (d, 18 H, $^3J_{P-H}$ = 14.32 Hz, $-C(CH_3)_3$), **$^{31}P\{^1H\}$ NMR** (CD_2Cl_2 , 293 K): δ [ppm] = 162.4 (m, 1 P, P_A), 44.6 (m, 2 P, $P_{M,M'}$), -120.1 (m, 2 P, $P_{x,x'}$). **^{31}P NMR** (CD_2Cl_2 , 293 K): δ [ppm] = 162.4 (m, 1 P, P_A), 44.6 (m, 2 P, $P_{M,M'}$), -120.1 (m, 2 P, $P_{x,x'}$). For coupling constants, see Table S7.

3a': **1H NMR** (CD_2Cl_2 , 293 K): δ [ppm] = 2.75 (m, 1 H, $-(CH_2)_3-$), 2.61 (m, 2 H, $-(CH_2)_3-$), 1.77 (s, 8 H, $C_5(CH_3)_5$), 1.69 (s, 8 H, $C_5(CH_3)_5$), 0.66 (d, 5 H, $^3J_{P-H}$ = 13.83 Hz, $-C(CH_3)_3$), 0.64 (d, 5 H, J_{P-H} = 14.33 Hz, $-C(CH_3)_3$). **$^{31}P\{^1H\}$ NMR** (CD_2Cl_2 , 293 K): δ [ppm] = 162.4 (m, 1 P, P_A), 44.6 (m, 2 P, $P_{M,M'}$), -120.1 (m, 2 P, $P_{x,x'}$). **^{31}P NMR** (CD_2Cl_2 , 293 K): δ [ppm] = 162.4 (m, 1 P, P_A), 44.6 (m, 2 P, $P_{M,M'}$), -120.1 (m, 2 P, $P_{x,x'}$). **LIFDI-MS** (toluene): m/z = 847.93 (100 %, $[M]^+$). Elemental analysis (calcd., found for $C_{31}H_{54}Fe_2P_{10}$): C (43.87, 43.61), H (6.42, 6.36). The given Proton NMR Spectrum (Fig. S7) and corresponding signals belong to an attempt to maximize **2b'** (see Additional Information) and does not correspond to the ratio in of **3a** / **3a'** in solid state (see Crystallographic details).

Reaction of $[Li(dme)_3][Cp^*Fe(\eta^4-P_5Me)]$ (1b) with 1,3-dibromopropane:

A solution of *in situ* generated **1b** ($[Cp^*Fe(\eta^5-P_5)]$ (I): 0.4 mmol, 138.4 mg, 1 eq; MeLi in Et_2O : 0.4 mmol, v = 0.50 mL, c = 0.802 mol·L⁻¹, 1 eq) in 15 mL THF was added to a 0.917 molar solution of 1,3-dibromopropane in DME (0.8 mmol, 0.9 mL, 2 eq). A colour change from brown to green occurred and a colourless solid was formed. The mixture was stirred for one hour. The solvent was removed under reduced pressure. The residue was dissolved in dichloromethane, silica is added and the solvent was removed *in vacuo*. The preabsorbed reaction mixture was purified via column chromatography (SiO_2 , hexane, 15 x 2 cm). Using a mixture of hexane/dichloromethane (10:1), a first green fraction ($[Cp^*Fe(\eta^4-P_5Me(CH_2)_3Br)]$ (**2b**), followed by a brown one ($[(Cp^*Fe)_2\{\mu,\eta^{4:4}-P_5Me(CH_2)_3P_5Me\}]$) (**3b**) can be eluted. The solvent of both fractions was removed under reduced pressure. $[Cp^*Fe(\eta^4-P_5Me(CH_2)_3Br)]$ (**2b**) can be isolated as dark green needles after one day in a concentrated *n*-hexane solution, stored at -30 °C. $[(Cp^*Fe)_2\{\mu,\eta^{4:4}-P_5Me(CH_2)_3P_5Me\}]$ (**3b**) can be obtained after one week as brown needles via layering a dichloromethane solution (3 mL) with acetonitrile (10 mL) and stored at -30°C.

Data for $[Cp^*Fe(\eta^4-P_5Me(CH_2)_3Br)]$ (2b):

Yield: 77.7 mg (0.161 mmol, 40 %). **1H NMR** (C_6D_6 , 293 K): δ [ppm] = 2.88 (t, 2 H, J_{H-H} = 6.28 Hz, $-(CH_2)_2CH_2Br$), 2.05 (m, 2 H, $-(CH_2)_2CH_2Br$), 1.75 (m, 2 H, $-(CH_2)_2CH_2Br$), 1.63 (s, 15 H, $C_5(CH_3)_5$), 0.04 (d, 3 H, $-CH_3$, $^2J_{P-H}$ = 10.57 Hz). **$^{31}P\{^1H\}$ NMR** (C_6D_6 , 293 K): δ [ppm] = 128.9 (m, 1 P, P_A), 32.0 (m, 2 P, $P_{M,M'}$), -130.3 (m, 2 P, $P_{x,x'}$). **^{31}P NMR** (C_6D_6 , 293 K): δ [ppm] = 128.9 (m, 1 P, P_A), 32.0 (m, 2 P, $P_{M,M'}$), -130.3 (m, 2 P, $P_{x,x'}$). For coupling constants, see Table S3. **FD-MS** (toluene): m/z = 481.91 (100 %, $[M]^+$). Elemental analysis (calcd., found for $C_{15}H_{24}FeBrP_5$): C (34.82, 34.77), H (5.01, 4.90).

Data for $[(Cp^*Fe)_2\{\mu,\eta^{4:4}-P_5Me(CH_2)_3P_5Me\}]$ (3b):

Yield: 100.9 mg (0.132 mmol, 33 %).

1H NMR (C_6D_6 , 293 K): δ [ppm] = 2.27 (m, 2 H, $-(CH_2)_3-$), 1.86 (m, 1 H, $-(CH_2)_3-$), 1.67 (s, 15 H, $C_5(CH_3)_5$), 0.19 (d, 3 H, $^2J_{P-H}$ = 10.48 Hz, $-CH_3$). **$^{31}P\{^1H\}$ NMR** (C_6D_6 , 293 K): δ [ppm] = 127.4 (m, 1 P, P_A), 32.6 (m, 2 P, $P_{M,M'}$), -129.5 (m, 2 P, $P_{x,x'}$). **^{31}P NMR** (C_6D_6 , 293 K): δ [ppm] = 127.4 (m, 1 P, P_A), 32.6 (m, 2 P, $P_{M,M'}$), -129.5 (m, 2 P, $P_{x,x'}$). For coupling constants, see Table S8.

LIFDI-MS (toluene): m/z = 763.94 (100 %, $[M]^+$). analysis (calcd., found for $C_{25}H_{42}Fe_2P_{10}$): C (39.30, 39.05), H (5.54, 5.55).

Synthesis of $[Cp^*Fe\{\eta^4-P_5(-C\equiv CPh)Me\}]$ (2c):

An *in situ* generated solution of **1c** ($[Cp^*Fe(\eta^5-P_5)]$ (I): 0.6 mmol, 207.6 mg, 1 eq; Li-C≡CPh: 0.6 mmol, m = 64.8 mg, 1 eq) in 15 mL THF was cooled to -80°C and a 1.116 molar solution of MeI in Et_2O

(0.6 mmol, 0.54 mL, 1 eq) was added. The mixture was allowed to stir overnight and reach room temperature, thereby the solution turned brownish/red. The solvent was removed under reduced pressure. The residue was dissolved in dichloromethane, silica is added, and the solvent was removed *in vacuo*. The preabsorbed reaction mixture was purified via column chromatography (SiO₂, hexane, 7 x 1 cm). Using a mixture of hexane/dichloromethane (8:1), a first green fraction, can be eluted. A second red one showed decomposition within the workup and could not be further characterized. The solvent of the first fraction was removed under reduced pressure. of [Cp*Fe{η⁴-P₅(-C≡CPh)Me}] (**2b**) can be isolated as dark green plates after one week in a concentrated CH₂Cl₂ solution, layered with *n*-hexane and stored at -30 °C.

Yield: 180.0 mg (0.389 mmol, 65 %). ¹H NMR (C₆D₆, 293 K): δ [ppm] = 6.89 (m, 2 H, -Ph), 6.79 (m, 1 H, -Ph), 6.68 (m, 1 H, -Ph), 2.17 (m, 3 H, -CH₃), 1.56 (s, 15 H, C₅(CH₃)₅). ³¹P{¹H} NMR (C₆D₆, 293 K): δ [ppm] = 76.2 (m, 1 P, P_A), 39.6 (m, 2 P, P_{M,M'}), -83.2 (m, 2 P, P_{x,x'}). ³¹P NMR (C₆D₆, 293 K): δ [ppm] = 76.2 (m, 1 P, P_A), 39.6 (m, 2 P, P_{G,G'}), -83.2 (m, 2 P, P_{x,x'}). For coupling constants, see **Table S4. FD-MS** (toluene): *m/z* = 461.04 (100 %, [M]⁺). Elemental analysis (calcd., found for C₁₉H₂₃FeP₅): C (49.38, 49.16), H (5.02, 5.02).

Synthesis of [Cp*Fe{η⁴-P₅Me(CH₂)₃CN}] (**2d**):

A solution of **1a** (0.16 mmol, 100 mg, 1 eq) in 10 mL DME was cooled to -50 °C and a 0.1093 molar solution of 4-Bromobutyronitrile in DME (0.2 mmol, 1.43 mL, 1 eq) was added. The mixture was allowed to stir overnight and reach room temperature, thereby a colourless solid is formed. The solvent was removed under reduced pressure and a brown solution was extracted with 10 mL toluene and filtered over diatomaceous earth. The solvent was reduced, layered with *n*-pentane and stored at -30 °C.

Compound **2d** was isolated as dark blocks after one week.

Yield: 233 mg (0.12 mmol, 72 %). ¹H NMR (CD₂Cl₂, 293 K): δ [ppm] = 1.93 (m, 2 H, -(CH₂)₂CH₂CN), 1.62 (s, 15 H, C₅(CH₃)₅), 1.43 (t, 2 H, J_{H-H} = 6.66 Hz, -(CH₂)₂CH₂CN), 1.28 (m, 2 H, -(CH₂)₂CH₂CN), -0.01 (d, 3 H, ²J_{P-H} = 10.41 Hz, -CH₃). ³¹P{¹H} NMR (CD₂Cl₂, 293 K): δ [ppm] = 127.3 (m, 1 P, P_A), 32.0 (m, 2 P, P_{M,M'}), -129.6 (m, 2 P, P_{1x,x'}). ³¹P NMR (CD₂Cl₂, 293 K): δ [ppm] = 127.3 (m, 1 P, P_A), 32.0 (m, 2 P, P_{M,M'}), -129.6 (m, 2 P, P_{1x,x'}). For coupling constants, see **Table S5. LIFDI-MS** (toluene): *m/z* = 428.99 (100 %, [M]⁺). Elemental analysis (calcd., found for C₁₅H₂₄FeP₅N): C (41.99, 42.25), H (5.64, 5.61), N (3.26, 3.09).

Reaction of [Li(dme)₃][Cp*Fe(η⁴-P₅Me)] (**1b**) with 1,4-dibromobutane:

A solution of *in situ* generated **1b** ([Cp*Fe(η⁵-P₅)] (**I**): 0.58 mmol, 200.6 mg, 1 eq; MeLi in Et₂O: 0.58 mmol, v = 0.72 mL, c = 0.802 mol·L⁻¹, 1 eq) in 15 mL THF was added to a 0.0968 molar solution of 1,4-dibromopropane in DME (1.16 mmol, 12.0 mL, 2 eq) at room temperature. The mixture was stirred for one hour. The solvent was removed under reduced pressure. The residue was dissolved in dichloromethane, silica is added and the solvent was removed *in vacuo*. The preabsorbed reaction mixture was purified via column chromatography (SiO₂, hexane, 10 x 2 cm). Using a mixture of hexane/dichloromethane (8:1), a first green fraction ([Cp*Fe(η⁴-P₅Me(CH₂)₄Br)] (**2e**) can be eluted. Compound **2e** can be obtained as dark brown needles from a concentrated cyclo-hexane solution, stored at 8 °C.

Increasing the amount of dichloromethane up to a ratio of 1:1 (hexane), yields [(Cp*Fe)₂{μ,η^{4,4}-P₅Me(CH₂)₄P₅Me}] (**3c**) as a green-brown fraction. Compound **3c** can be obtained after one week as green plates via layering a dichloromethane solution (3 mL) with hexane (10 mL) and stored at -30°C.

Data for [Cp*Fe(η⁴-P₅Me(CH₂)₄Br)] (**2e**):

Yield: 124.2 mg (0.250 mmol, 43 %). ¹H NMR (C₆D₆, 293 K): δ [ppm] = 2.88 (t, 2 H, J_{H-H} = 6.06 Hz, -(CH₂)₂CH₂-Br), 1.87 (m, 2 H, -(CH₂)₂CH₂-Br), 1.63 (s, 15 H, C₅(CH₃)₅), 1.47 (m, 4 H, -(CH₂)₂CH₂-Br), 0.11 (d, 3 H, ²J_{P-H} = 10.61 Hz, -CH₃). ³¹P{¹H} NMR (C₆D₆, 293 K): δ [ppm] = 130.8 (m, 1 P, P_A), 32.0 (m, 2 P, P_{M,M'}), -130.8 (m, 2 P, P_{x,x'}). ³¹P NMR (C₆D₆, 293 K): δ [ppm] = 130.8 (m, 1 P, P_A), 32.0 (m, 2 P, P_{M,M'}),

–130.8 (m, 2 P, $P_{x,x'}$). For coupling constants, see **Table S6**. **LIFDI-MS** (toluene): m/z = 496.00 (100 %, [M] $^+$). Elemental analysis (calcd., found for $C_{15}H_{26}FeBrP_5$): C (36.25, 37.70), H (5.27, 5.08). elemental analysis failed after several attempts of the isolated crystals.

Data for $[(Cp^*Fe)_2\{\mu,\eta^{4:4}-P_5Me(CH_2)_4P_5Me\}]$ (3c):

Yield: 106.7 mg (0.137 mmol, 24 %). **1H NMR** (C_6D_6 , 293 K): δ [ppm] = 2.10 (m, 4 H, -(CH_2) $_4$ –), 1.68 (s, 30 H, $C_5(CH_3)_5$), 2.92 (m, 4 H, -(CH_2) $_4$ –), 0.23 (d, 6 H, J_{P-H} = 10.55 Hz, - CH_3). **$^{31}P\{^1H\}$ NMR** (C_6D_6 , 293 K): δ [ppm] = 130.1 (m, 1 P, P_A), 32.9 (m, 2 P, $P_{M,M'}$), –130.1 (m, 2 P, $P_{x,x'}$). **^{31}P NMR** (C_6D_6 , 293 K): δ [ppm] = 130.1 (m, 1 P, P_A), 32.9 (m, 2 P, $P_{M,M'}$), –130.1 (m, 2 P, $P_{x,x'}$). For coupling constants, see **Table S9**. **LIFDI-MS** (toluene): m/z = 777.92 (100 %, [M] $^+$). analysis (calcd., found for $C_{26}H_{44}Fe_2P_{10}$): C (40.14, 39.82), H (5.70, 5.57).

Synthesis of $[(Cp^*Fe)_2\{\mu,\eta^{4:4}-P_5'Bu(CH_2)_3P_5Me\}]$ (4):

Compound **1b** (0.1 mmol, 63.8 mg, 1 eq) and **2a** (0.1 mmol, 52.5 mg, 1 eq) were dissolved separately in 10 mL THF. The solution of **1b** was added to **2a**. A colourless solid was formed and the suspension was allowed to stir for 1 hour. The solvent was removed under reduced pressure and a brown solution was extracted with 5 mL toluene and filtered over diatomaceous earth. The solvent was removed *in vacuo*. The brown residue was dissolved in 2 mL THF, layered with 4 mL *n*-pentane and stored at –30 °C. $[(Cp^*Fe)_2\{\mu,\eta^{4:4}-P_5'Bu(CH_2)_3P_5Me\}]$ (4) was formed as dark green blocks after one day.

Yield: 64.5 mg (0.08 mmol, 80 %). **1H NMR** (CD_2Cl_2 , 293 K): δ [ppm] = 2.79 (m, 4 H, -(CH_2) $_2$ CH_3), 2.44 (m, 2 H, -(CH_2) $_2$ CH_3), 1.67 (s, 15 H, $C_5(CH_3)_5$), 1.66 (s, 15 H, $C_5(CH_3)_5$), 0.79 (d, 3 H, J_{P-H} = 10.67 Hz, - CH_3), 0.64 (d, 9 H, J_{P-H} = 14.54 Hz, - $C(CH_3)_3$). **$^{31}P\{^1H\}$ NMR** (CD_2Cl_2 , 293 K): δ [ppm] = 164.3 (m, 1 P, P_{1A}), 128.9 (m, 1 P, P_{2A}), 41.0 (m, 2 P, $P_{1M,M'}$), 29.8 (m, 2 P, $P_{2M,M'}$), –120.3 (m, 2 P, $P_{1x,x'}$), –129.9 (m, 2 P, $P_{2x,x'}$). **$^{31}P\{^1H\}$ NMR** (CD_2Cl_2 , 293 K): δ [ppm] = 164.3 (m, 1 P, P_{1A}), 128.9 (m, 1 P, P_{2A}), 41.0 (m, 2 P, $P_{1M,M'}$), 29.8 (m, 2 P, $P_{2M,M'}$), –120.3 (m, 2 P, $P_{1x,x'}$), –129.9 (m, 2 P, $P_{2x,x'}$). For coupling constants, see **Table S10, S11**. **LIFDI-MS** (toluene): m/z = 806.02 (100 %, [M] $^+$). Elemental analysis (calcd., found for $C_{28}H_{48}Fe_2P_{10}$): C (41.72, 41.49), H (6.42, 5.79).

Synthesis of $[(Cp^*Fe\{\eta^4-P_5'Bu(CH_2)_3PPh_2\})$ (5):

Complex **2a** (0.5 mmol, 262.5 mg, 1 eq) was dissolved in 10 mL THF and cooled to –80 °C and a 0.233 molar solution of $KPPPh_2$ in DME (2.2 mL, 1 eq) was added dropwise. The mixture was allowed to stir overnight and reach room temperature, thereby a colour solid was formed. The solvent was removed *in vacuo*, the brown residue was solved in hexane and purified via column chromatography (SiO_2 , hexane, 5 × 2 cm). Using a mixture of hexane/toluene (1:1) yields $[Cp^*Fe(\eta^4-P_5'Bu(CH_2)_3PPh_2)]$ (8) as a brown greenish fraction. The solvent was removed under reduced pressure and the brown residue is dissolved in 15 mL *n*-pentane. Compound **8** can be obtained spectroscopically pure as dark green crystals by slow removal of the solvent under reduced pressure at room temperature.

Yield: 237.1 mg (0.375 mmol, 75 %).

1H NMR (C_6D_6 , 293 K): δ [ppm] = 7.48 (m, 8H, -(CH_2) $_3$ PPh_2), 7.11 (m, 8 H, -(CH_2) $_3$ PPh_2), 2.50 (m, 2 H, -(CH_2) $_3$ PPh_2), 2.18 (m, 2 H, -(CH_2) $_3$ PPh_2), 2.10 (m, 2 H, -(CH_2) $_3$ PPh_2), 1.59 (s, 15 H, $C_5(CH_3)_5$), 0.29 (d, 9 H, J_{P-H} = 14.12 Hz, - $C(CH_3)_3$). **$^{31}P\{^1H\}$ NMR** (C_6D_6 , 293 K): δ [ppm] = 164.9 (m, 1 P, P_A), 42.6 (m, 2 P, $P_{M,M'}$), –17.9 (s, 1 P, PPh_2), –121.7 (m, 2 P, $P_{x,x'}$). **^{31}P NMR** (C_6D_6 , 293 K): δ [ppm] = 164.9 (m, 1 P, P_A), 42.6 (m, 2 P, $P_{M,M'}$), –17.9 (s, 1 P, PPh_2), –121.7 (m, 2 P, $P_{x,x'}$). For coupling constants, see **Table S12**. **LIFDI-MS** (toluene): m/z = 630.05 (100 %, [M] $^+$). Elemental analysis (calcd., found for $C_{29}H_{40}FeP_6$): C (55.23, 55.71), H (6.40, 6.18).

Synthesis of $P'BuBn((CH_2)_4Ph)$ (6):

Complex **2a** (0.18 mmol, 94.5 mg, 1 eq) and KBn (0.36 mmol, 46.8 mg, 2 eq) were dissolved separately in 10 mL THF and cooled to –80 °C. One equivalent of the KBn solution was added dropwise (a $^{31}P\{^1H\}$ NMR was recorded of the reaction mixture) (see Fig. S60). The mixture was allowed to stir for one hour, thereby

a colourless solid was formed (*). The solution was again cooled to -80°C . and the second equivalent of the KBn solution was added. The reaction mixture was stirred for an additional hour. The solvent was removed under reduced pressure. The brownish oily residue was extracted with 3×10 mL of *n*-pentane and filtered over diatomaceous earth. The solvent was removed *in vacuo*. Compound **6** can be isolated as a slightly brownish oil.

Yield: 37.5 mg (0.12 mmol, 67 %).

$^1\text{H NMR}$ (C_6D_6 , 293 K): δ [ppm] = 7.21 (m, 3 H, -Ph), 7.08 (m, 7 H, -Ph), 2.77 (dd, 1 H, ${}^2J_{\text{P}-\text{H}} = 14.12$ Hz, ${}^3J_{\text{P}-\text{H}} = 1.74$ Hz, P- $\underline{\text{CH}_2}$ -Ph), 2.45 (dd, 1 H, ${}^2J_{\text{P}-\text{H}} = 13.43$ Hz, ${}^3J_{\text{P}-\text{H}} = 3.18$ Hz, P- $\underline{\text{CH}_2}$ -Ph), 2.37 (t, 2 H, ${}^2J_{\text{H}-\text{H}} = 7.69$ Hz, ${}^3J_{\text{P}-\text{H}} = 1.74$ Hz, - $\underline{\text{CH}_2}$ -Ph), 1.51 (m, 2 H, -(CH_2)₃-Ph), 1.30 (m, 3 H, -(CH_2)₃-Ph), 1.20 (m, 2 H, -(CH_2)₃-Ph), 0.97 (d, 9 H, $J_{\text{P}-\text{H}} = 14.12$ Hz, -C(CH_3)₃). **$^{31}\text{P}\{{}^1\text{H}\} \text{NMR}$** (C_6D_6 , 293 K): δ [ppm] = 4.5 (s). **$^{31}\text{P NMR}$** (C_6D_6 , 293 K): δ [ppm] = 4.5 (s, br). **$^{13}\text{C}\{{}^1\text{H}\} \text{NMR}$** (C_6D_6 , 293 K): δ [ppm] = 142.4 (s, Ph), 139.7 (d, ${}^2J_{\text{P}-\text{C}} = 7.8$ Hz, Ph), 129.4 (d, ${}^3J_{\text{P}-\text{C}} = 6.8$ Hz, Ph), 128.3 (d, ${}^2J_{\text{P}-\text{C}} = 9.8$ Hz, Ph), 128.2 (d, ${}^3J_{\text{P}-\text{C}} = 6.2$ Hz, Ph), 125.6 (s, Ph), 125.5 (d, ${}^4J_{\text{P}-\text{C}} = 2.2$ Hz, Ph), 35.6 (s, -(CH_2)-Ph), 33.0 (d, ${}^1J_{\text{P}-\text{C}} = 12.0$ Hz, P-($\underline{\text{CH}_2}$)-Ph), 32.3 (d, ${}^1J_{\text{P}-\text{C}} = 22.3$ Hz, P-($\underline{\text{CH}}$)-(CH_3)₂-Ph), 27.8 (d, $J_{\text{P}-\text{C}} = 14.7$ Hz), 27.2 (d, $J_{\text{P}-\text{C}} = 14.7$ Hz), 27.2 (d, $J_{\text{P}-\text{C}} = 19.1$ Hz), 27.1 (d, $J_{\text{P}-\text{C}} = 13.2$ Hz), 23.9 (d, ${}^2J_{\text{P}-\text{C}} = 20.5$ Hz, P-C(CH_3)₃).

Synthesis of SP^tBuBn((CH_2)₄Ph) (6'):

Compound **6** was synthesised *in situ* according to previous experimental details (0.18 mmol, 1 eq) and dissolved in 5 mL of *n*-pentane. Sulfur (0.18 mmol, 5.8 mg, 1 eq) was dissolved in 2 mL of *n*-pentane and added to compound **6** at room temperature. The reaction mixture is stirred for one hour. The solvent is reduced *in vacuo* and stored at -30°C . Compound **6'** can be isolated as colourless blocks after three days. Yield: 51.7 mg (0.15 mmol, 83 %).

$^1\text{H NMR}$ (C_6D_6 , 293 K): δ [ppm] = 7.35 (m, 2 H, -Ph), 7.05 (m, 7 H, -Ph), 2.86 (d, 1 H, ${}^2J_{\text{P}-\text{H}} = 6.37$ Hz, P- $\underline{\text{CH}_2}$ -Ph), 2.86 (d, 1 H, ${}^2J_{\text{P}-\text{H}} = 6.37$ Hz, P- $\underline{\text{CH}_2}$ -Ph), 2.83 (d, 1 H, ${}^2J_{\text{P}-\text{H}} = 3.84$ Hz, P- $\underline{\text{CH}_2}$ -Ph), 2.28 (m, 2 H, - $\underline{\text{CH}_2}$ -Ph), 1.59 (m, 2 H, -(CH_2)₃-Ph), 1.35 (m, 3 H, -(CH_2)₃-Ph), 1.11 (m, 2 H, -(CH_2)₃-Ph), 0.98 (d, 9 H, $J_{\text{P}-\text{H}} = 15.25$ Hz, -C(CH_3)₃). **$^{31}\text{P}\{{}^1\text{H}\} \text{NMR}$** (C_6D_6 , 293 K): δ [ppm] = 63.5 (s). **$^{31}\text{P NMR}$** (C_6D_6 , 293 K): δ [ppm] = 63.5 (s, br). **$^{13}\text{C}\{{}^1\text{H}\} \text{NMR}$** (C_6D_6 , 293 K): δ [ppm] = 142.2 (s, Ph), 132.9 (d, ${}^2J_{\text{P}-\text{C}} = 7.5$ Hz, Ph), 130.2 (d, ${}^3J_{\text{P}-\text{C}} = 4.7$ Hz, Ph), 128.3 (d, ${}^2J_{\text{P}-\text{C}} = 7.0$ Hz, Ph), 126.8 (d, ${}^4J_{\text{P}-\text{C}} = 3.0$ Hz, Ph), 125.7 (s, Ph), 35.8 (d, ${}^1J_{\text{P}-\text{C}} = 41.8$ Hz, P-($\underline{\text{CH}_2}$)-Ph), 35.4 (s, -(CH_2)-Ph), 33.9 (d, ${}^1J_{\text{P}-\text{C}} = 47.8$ Hz, P-($\underline{\text{CH}}$)-(CH₃)₂-Ph), 32.9 (d, $J_{\text{P}-\text{C}} = 14.0$ Hz), 25.6 (d, ${}^2J_{\text{P}-\text{C}} = 20.5$ Hz, P-C(CH_3)₃), 24.7 (d, $J_{\text{P}-\text{C}} = 0.2$ Hz), 22.9 (d, $J_{\text{P}-\text{C}} = 3.6$ Hz).

GC-MS (CH_2Cl_2): $m/z = 344.17$ (15 %, [M]⁺), 91.06 (100 %, [Bn]⁺), 57.07 (15 %, [Bu]⁺), 312.20 (5 %, [M-S]⁺). Elemental analysis (calcd., found for $\text{C}_{21}\text{H}_{29}\text{SP}$): C (73.22, 70.23), H (8.49, 7.50), S (9.31, 12.01).

Synthesis of [$\text{Cp}^*\text{Fe}\{\eta^4-\text{P}_5((\text{CH}_2)_3\text{CN})_2\}$] (7):

Complex **I** (0.15 mmol, 90.7 mg, 1 eq) was dissolved in DME, cooled to -50°C and a 0.1093 molar solution of 4-Bromobutyronitrile in DME (0.3 mmol, 2.75 mL, 2 eq) was added. Thereby the colour change to red/brown and a colourless solid formed. The solution was allowed to stir over night. The solvent was removed under reduced pressure and the brown residue was washed with 3×10 mL of *n*-pentane. The residue was dissolved in 5 mL of toluene, filtered over diatomaceous earth, layered with 5 mL of *n*-pentane and stored at -30°C . Compound **7** can be isolated as dark green blocks after washing with 10 mL of *n*-hexane in order to remove residues of **I'**.

Yield: 46.0 mg (0.096 mmol, 64 %).

$^1\text{H NMR}$ (C_6D_6 , 293 K): δ [ppm] = 2.02 (m, 2 H, -(CH_2)₂CH₂CN), 1.63 (s, 15 H, C₅(CH₃)₅), 1.48 (t, 2 H, -(CH_2)₂CH₂CN, $J_{\text{H}-\text{H}} = 6.52$ Hz), 1.32 (m, 2 H, -(CH_2)₂CH₂CN), 1.05 (t, 2 H, -(CH_2)₂CH₂CN, $J_{\text{H}-\text{H}} = 6.70$ Hz), 0.59 (m, 2 H, -(CH_2)₂CH₂CN), 0.25 (m, 2 H, -(CH_2)₂CH₂CN). **$^{31}\text{P}\{{}^1\text{H}\} \text{NMR}$** (C_6D_6 , 293 K): δ [ppm] = 133.7 (m, 1 P, P_A), 37.0 (m, 2 P, P_{M,M'}), -129.2 (m, 2 P, P_{x,x'}). **$^{31}\text{P NMR}$** (C_6D_6 , 293 K): δ [ppm] = 133.7 (m, 1 P, P_A), 37.0 (m, 2 P, P_{M,M'}), -129.2 (m, 2 P, P_{x,x'}). For coupling constants, see **Table S13. LIFDI-MS** (toluene): $m/z = 482.01$ (100 %, [M]⁺), 964.05 (2 %, [M]₂⁺). Elemental analysis (calcd., found for $\text{C}_{18}\text{H}_{27}\text{FeP}_5\text{N}_2$): C (44.84, 45.34), H (5.64, 5.23), N (5.81, 6.00).

Synthesis of [{Cp*Fe{η⁴-P₅((CH₂)₃CN)₂}ZnBr₂₈):

Compound **7** (0.15 mmol, 72.3 mg, 1 eq) and ZnBr₂ (0.15 mmol, 72.3 mg, 1 eq) were dissolved separately in 10 mL THF. The solution of **7** was added to ZnBr₂. A colour change was not observed and the solution was allowed to stir for 1 hour. The solvent was removed under reduced pressure and a brown oil was dissolved in 3 mL CH₂Cl₂, layered with 10 mL toluene and stored at room temperature. [{Cp*Fe{η⁴-P₅((CH₂)₃CN)₂}ZnBr₂] (**8**) was formed as dark green/brownish plates after three days.

Yield: 86.5 mg (0.122 mmol, 81 %).

¹H NMR (THF-d₈, 293 K): δ [ppm] = 2.78 (m, 2 H, -(CH₂)₂CH₂CN), 2.69 (t, 2 H, -(CH₂)₂CH₂CN, J_{H-H} = 6.88 Hz), 2.21 (t, 2 H, -(CH₂)₂CH₂CN, J_{H-H} = 6.88 Hz), 2.17 (m, 2 H, -(CH₂)₂CH₂CN), 1.63 (s, 15 H, C₅(CH₃)₅), 1.20 (m, 2 H, -(CH₂)₂CH₂CN), 1.06 (m, 2 H, -(CH₂)₂CH₂CN). **³¹P{¹H} NMR** (C₆D₆, 293 K): δ [ppm] = 137.9 (m, 1 P, P_A), 36.3 (m, 2 P, P_{M,M'}), -130.3 (m, 2 P, P_{x,x}). **³¹P NMR** (C₆D₆, 293 K): δ [ppm] = 137.9 (m, 1 P, P_A), 36.3 (m, 2 P, P_{M,M'}), -130.3 (m, 2 P, P_{x,x}). For coupling constants, see **Table S14. LIFDI-MS (o-DFB):** m/z = 482.01 (100 %, [7]⁺). Elemental analysis (calcd., found for C₁₈H₂₇FeP₅N₂ZnBr₂): C (30.69, 30.98), H (3.87, 3.91), N (3.78, 3.93).

NMR spectroscopic characterization

^1H NMR Spectra:

[K(18c6)(thf)][Cp^{*}Fe(η^4 -P₅-C≡CPh)] (**1c**)

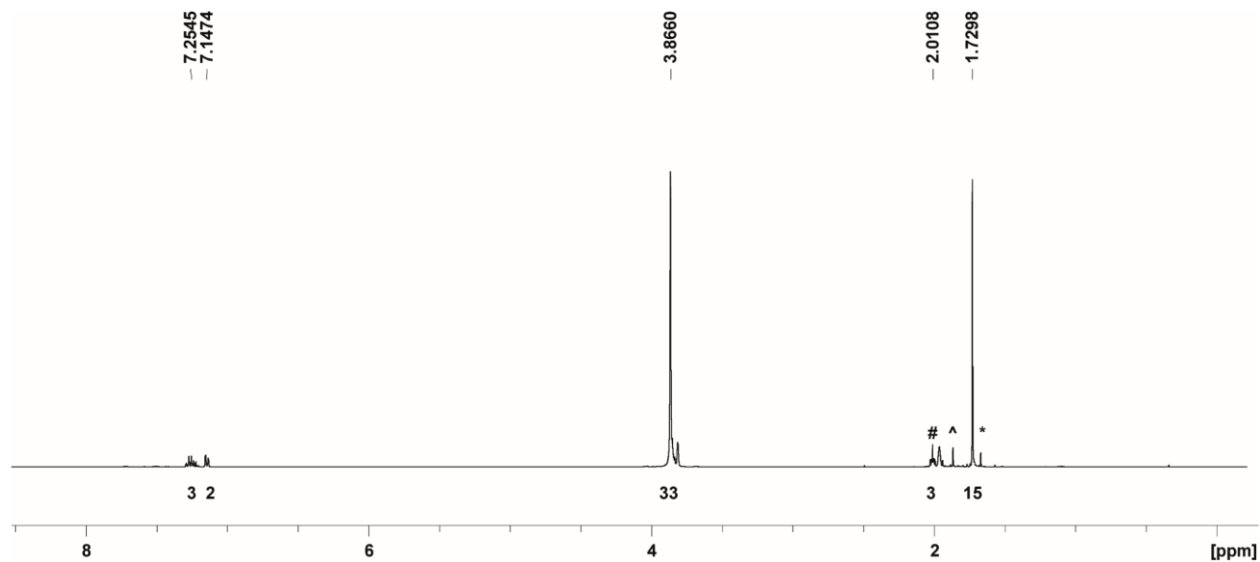


Fig. S1. Experimental ^1H NMR (400.13 MHz, THF-d₈) spectrum of **1c** (# = THF, ^ = unidentified impurity, * = I).

[Cp^{*}Fe(η^4 -P₅'Bu(CH₂)₃Br)] (**2a**)

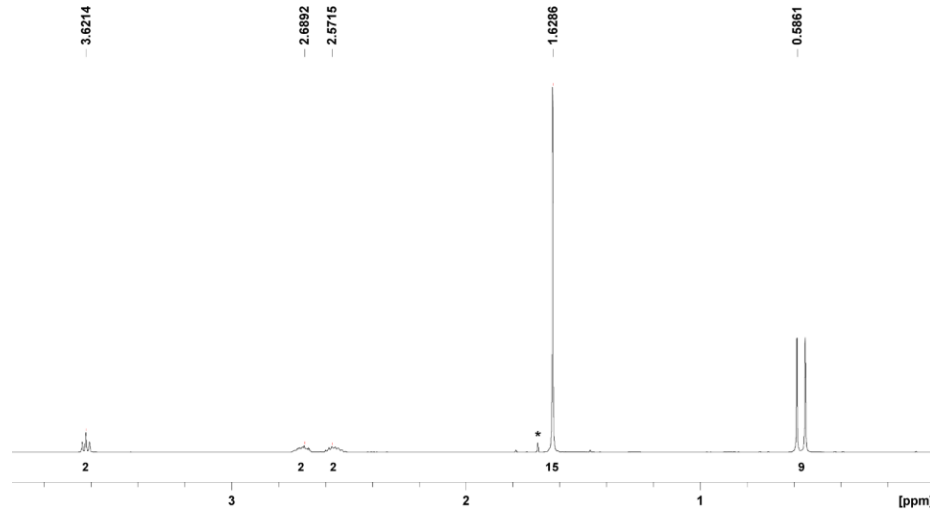


Fig. S2. Experimental ^1H NMR (400.13 MHz, CD₂Cl₂) spectrum of **2a** (* = I).

$[\text{Cp}^*\text{Fe}(\eta^4\text{-P}_5\text{Me}(\text{CH}_2)_3\text{Br})] \textbf{(2b)}$

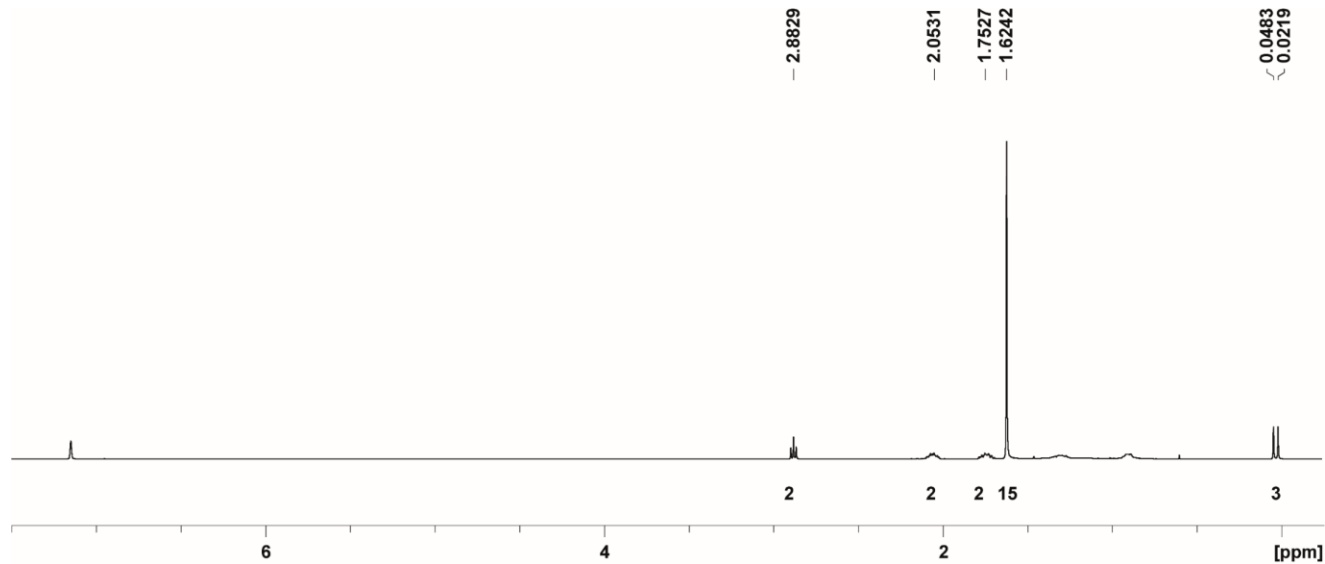


Fig. S3. Experimental ^1H NMR (400.13 MHz, C_6D_6) spectrum of **2b**.

$[\text{Cp}^*\text{Fe}(\eta^4\text{-P}_5(-\text{C}\equiv\text{CPh})\text{Me})] \textbf{(2c)}$

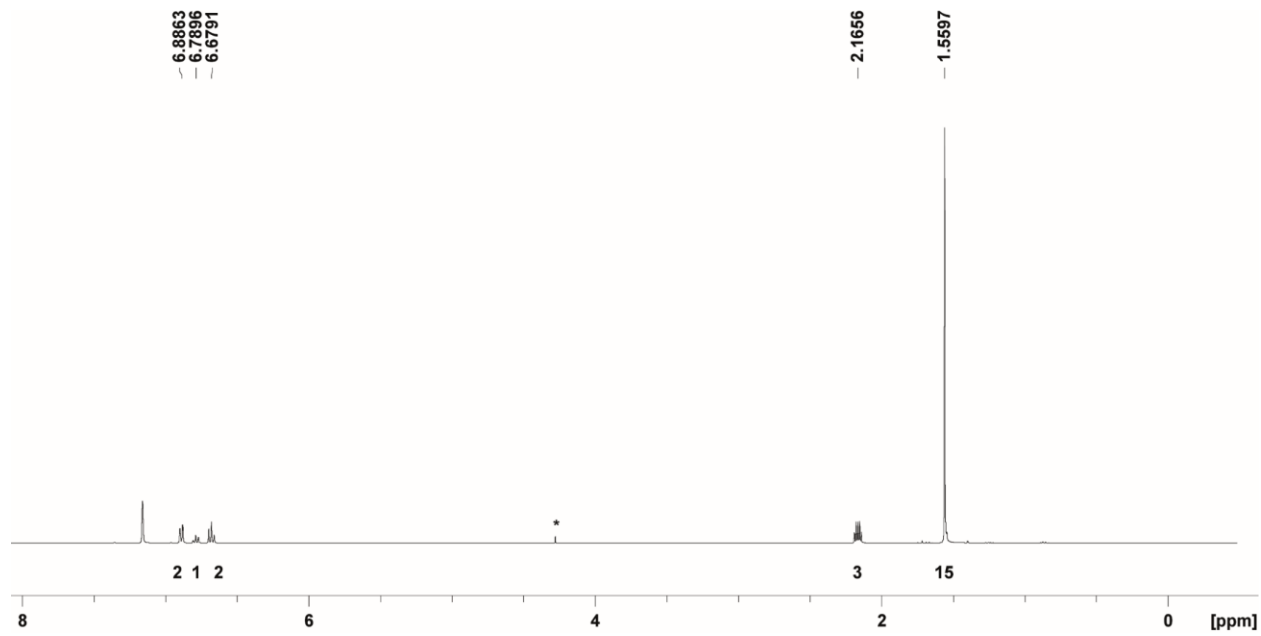


Fig. S4. Experimental ^1H NMR (400.13 MHz, C_6D_6) spectrum of **2c** (* = CH_2Cl_2).

$[\text{Cp}^*\text{Fe}\{\eta^4\text{-P}_5\text{Me}(\text{CH}_2)_3\text{CN}\}]$ (**2d**)

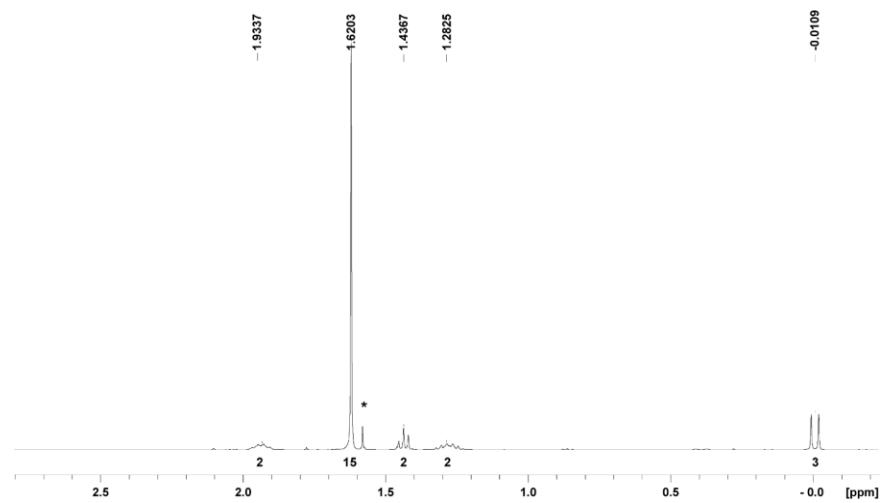


Fig. S5. Experimental ^1H NMR (400.13 MHz, C_6D_6) spectrum of **2d** (* = I).

$[\text{Cp}^*\text{Fe}\{\eta^4\text{-P}_5\text{Me}(\text{CH}_2)_4\text{Br}\}]$ (**2e**)

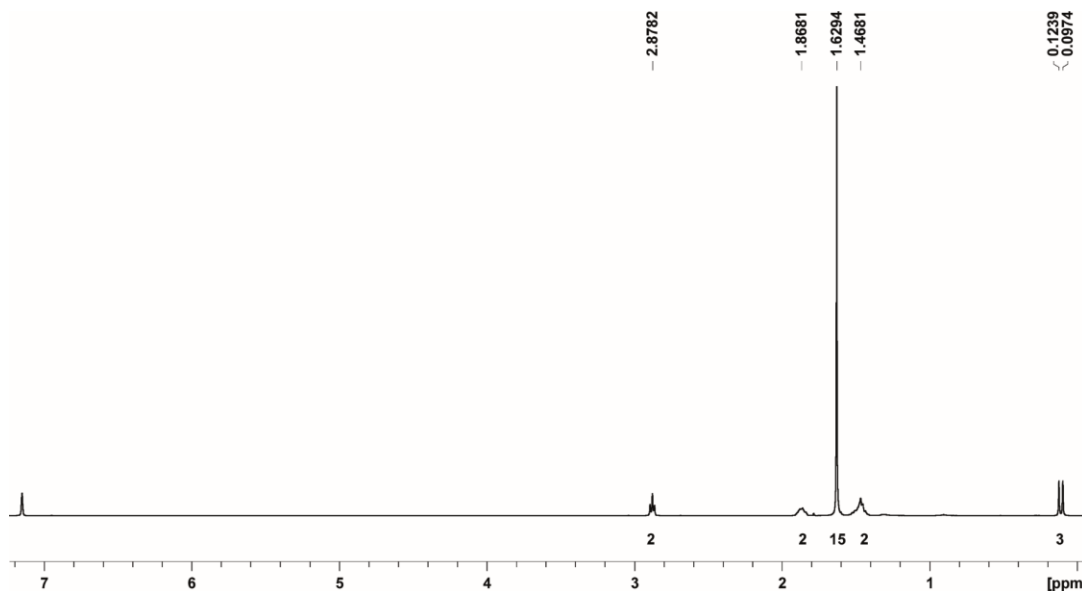


Fig. S6. Experimental ^1H NMR (400.13 MHz, C_6D_6) spectrum of **2e**.

$[(\text{Cp}^*\text{Fe})_2\{\mu,\eta^{4:4}\text{-P}_5^t\text{Bu}(\text{CH}_2)_3\text{P}_5^t\text{Bu}\}]$ (**3a/3a'**)

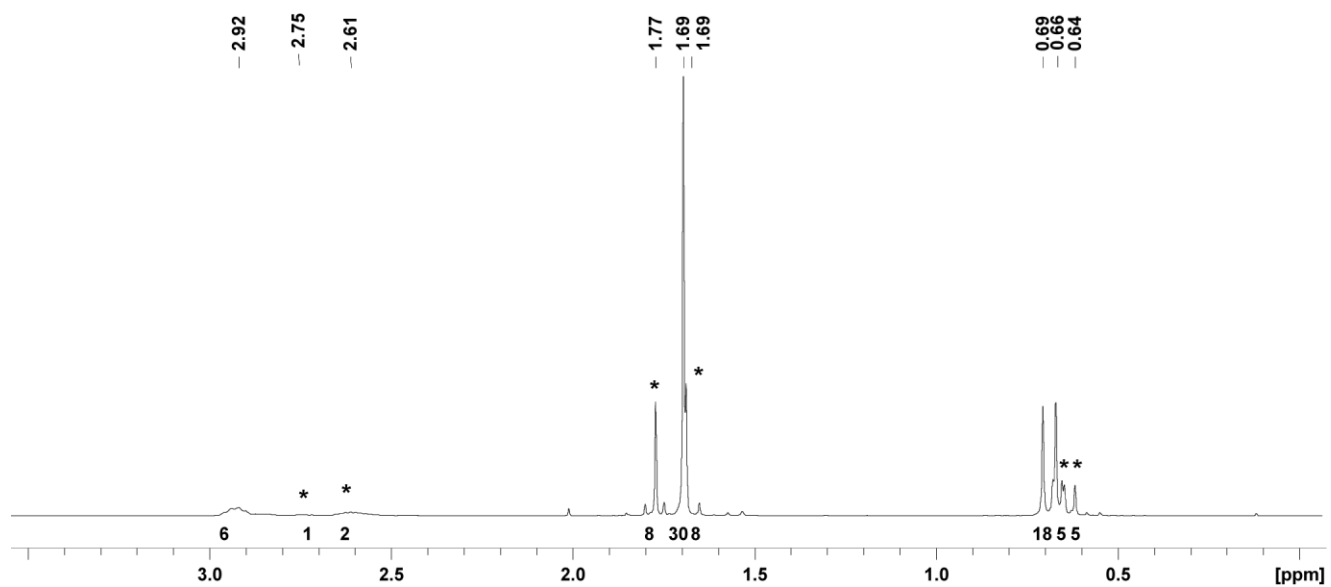


Fig. S7. Experimental ^1H NMR (400.13 MHz, CD_2Cl_2) spectrum of **3a** ($*$ = $3\text{a}'$).

$[(\text{Cp}^*\text{Fe})_2\{\mu,\eta^{4:4}\text{-P}_5\text{Me}(\text{CH}_2)_3\text{P}_5\text{Me}\}]$ (**3b**)

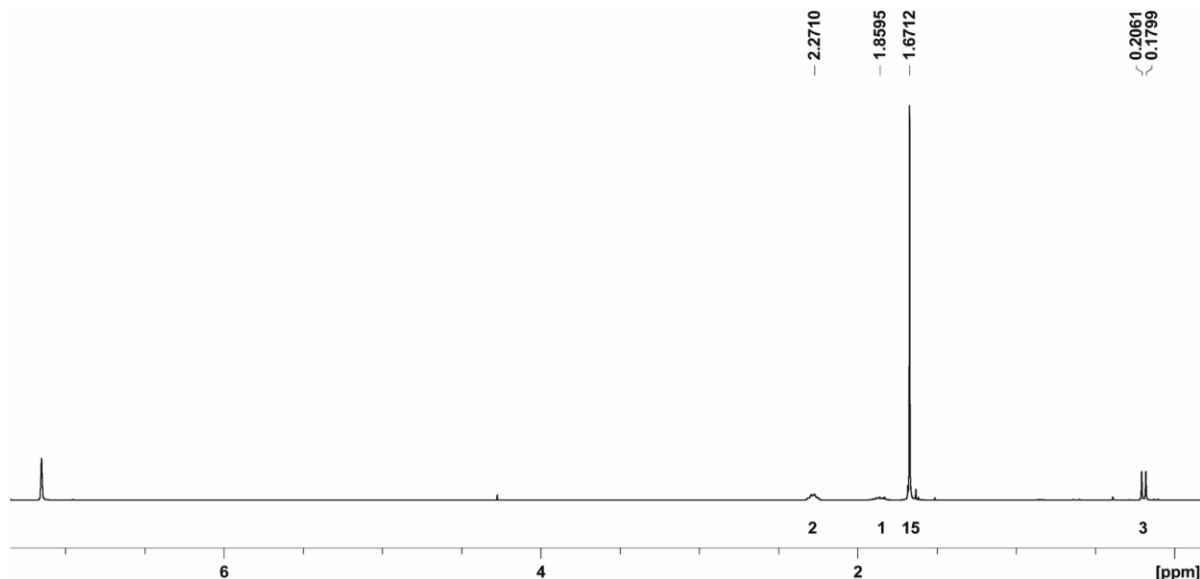


Fig. S8. Experimental ^1H NMR (400.13 MHz, CD_2Cl_2) spectrum of **3b**.

$[(\text{Cp}^*\text{Fe})_2\{\mu,\eta^{4:4}\text{-P}_5\text{Me}(\text{CH}_2)_4\text{P}_5\text{Me}\}]$ (**3c**)

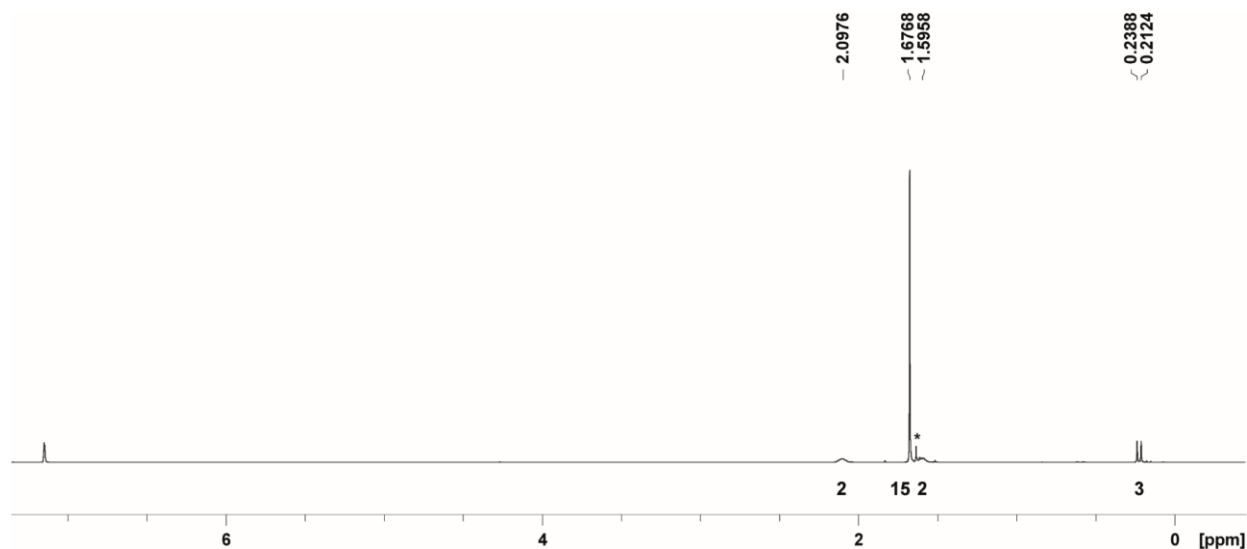


Fig. S9. Experimental ^1H NMR (400.13 MHz, CD_2Cl_2) spectrum of **3c** (* = CH_2Cl_2 ; * = **3c'**).

$[(\text{Cp}^*\text{Fe})_2\{\mu,\eta^{4:4}\text{-P}_5^t\text{Bu}(\text{CH}_2)_3\text{P}_5\text{Me}\}]$ (**4**)

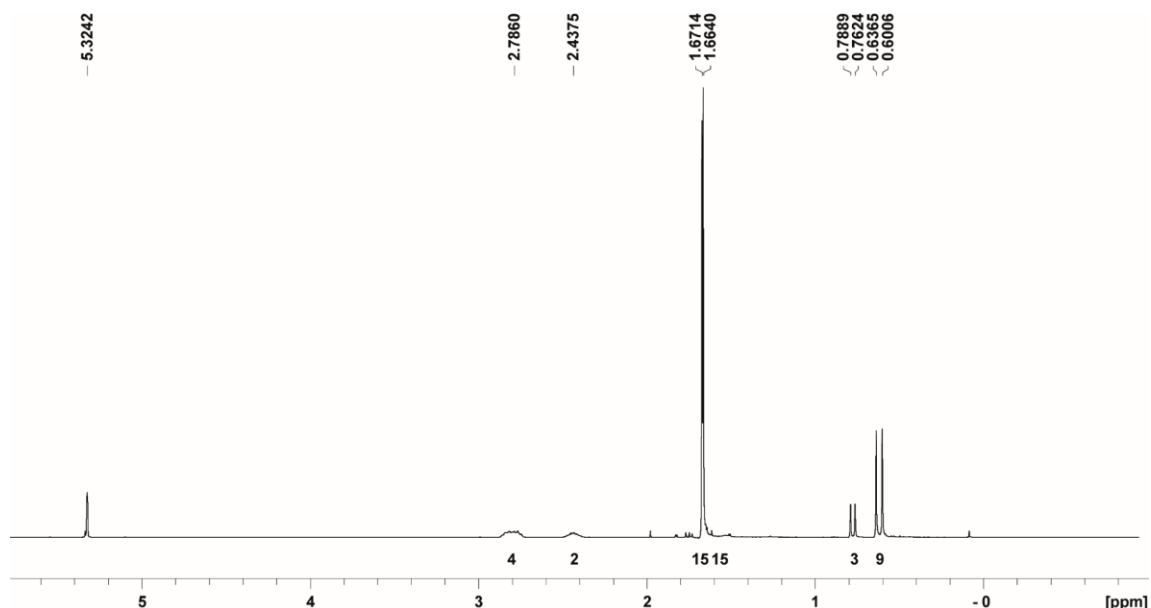


Fig. S10. Experimental ^1H NMR (400.13 MHz, CD_2Cl_2) spectrum of **4**.

$[\text{Cp}^*\text{Fe}\{\eta^4\text{-P}_5^t\text{Bu}(\text{CH}_2)_3\text{PPh}_2\}]$ (**5**)

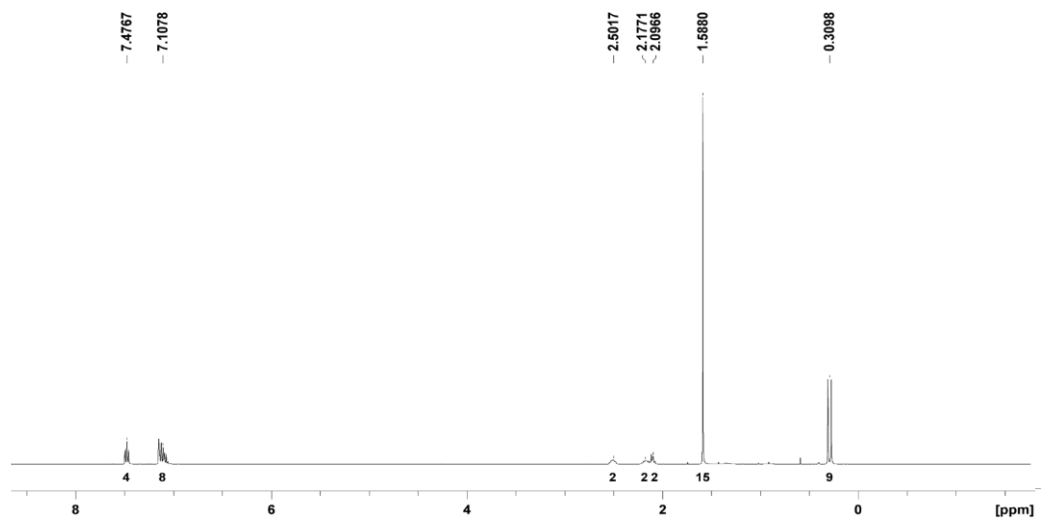


Fig. S11. Experimental ^1H NMR (400.13 MHz, C_6D_6) spectrum of **5**.

$^t\text{BuPBn}((\text{CH}_2)_3\text{Bn})$ (**6**)

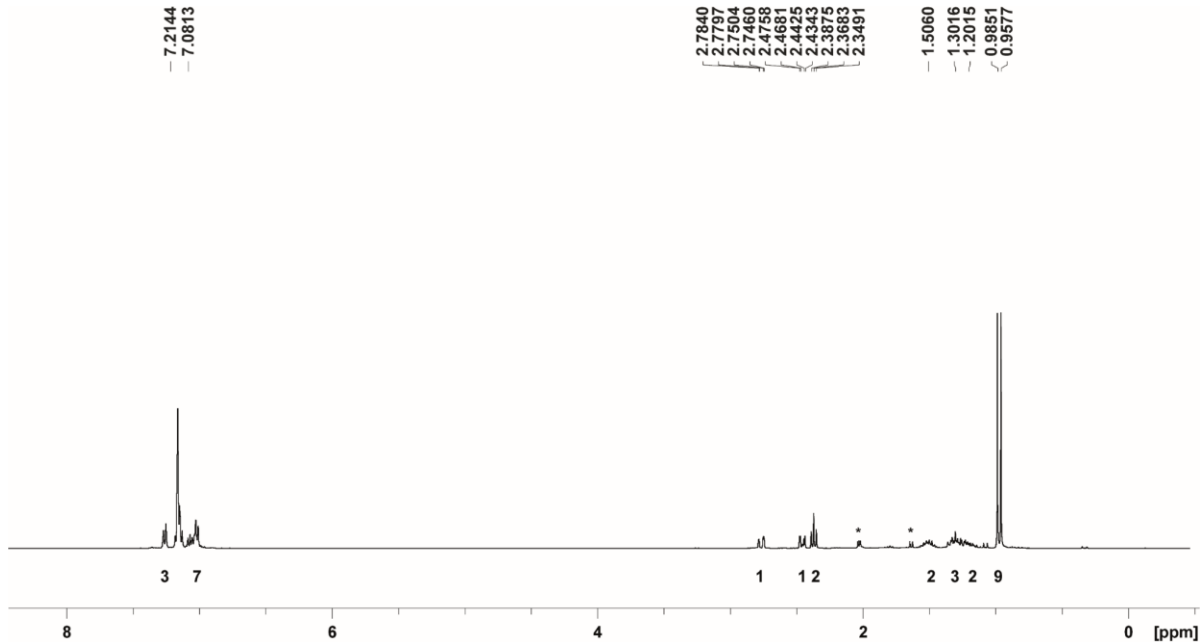


Fig. S12. Experimental ^1H NMR (400.13 MHz, C_6D_6) spectrum of **6** (* = unidentified sideproduct).

$\text{SP}'\text{BuBn}((\text{CH}_2)_3\text{Bn})$ (**6'**)

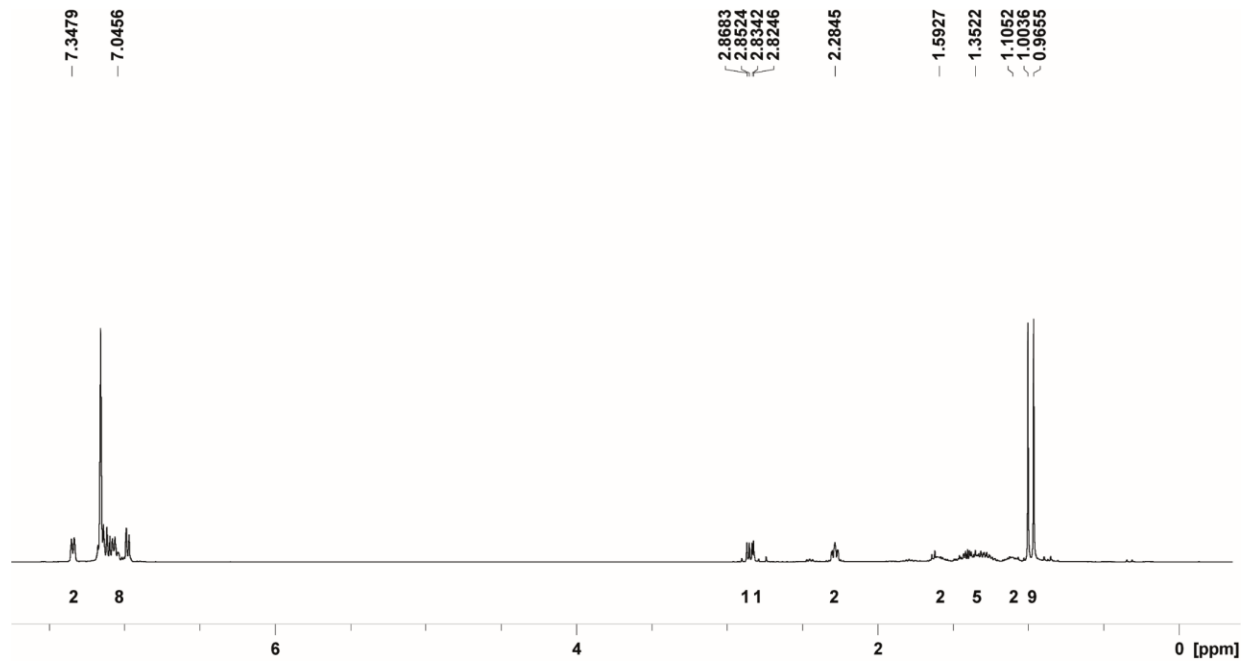


Fig. S13. Experimental ^1H NMR (400.13 MHz, C_6D_6) spectrum of **6'**.

$[\text{Cp}'^*\text{Fe}\{\eta^4\text{-P}_5((\text{CH}_2)_3\text{CN})_2\}]$ (**7**)

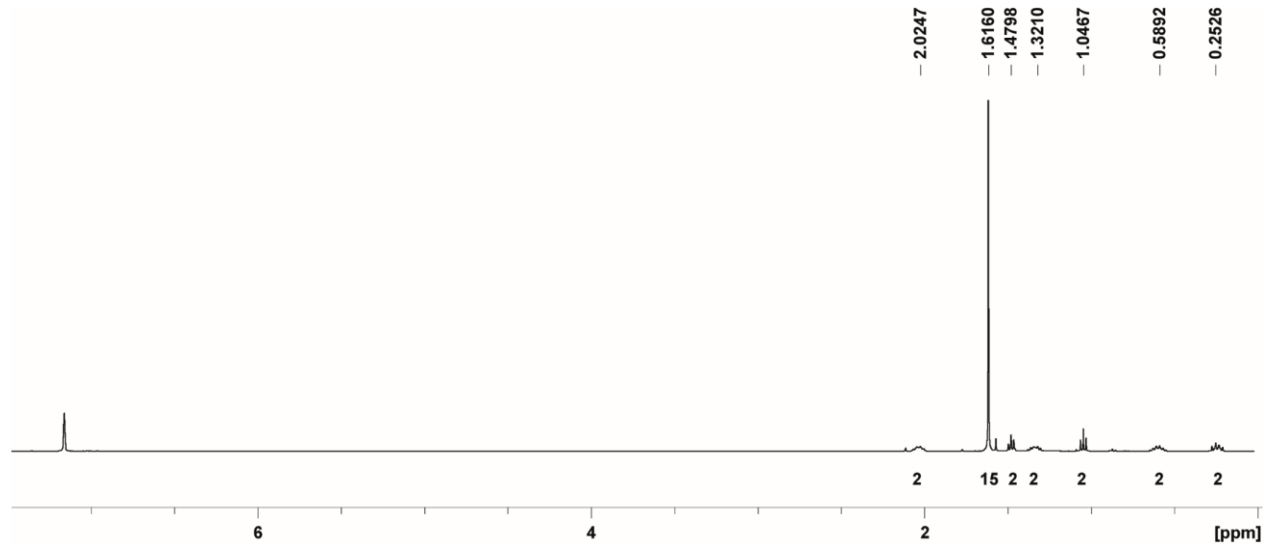


Fig. S14. Experimental ^1H NMR (400.13 MHz, C_6D_6) spectrum of **7**.

$[\text{Cp}^*\text{Fe}\{\eta^4\text{-P}_5((\text{CH}_2)_3\text{CN})_2\}\text{ZnBr}_2]$ (**8**)

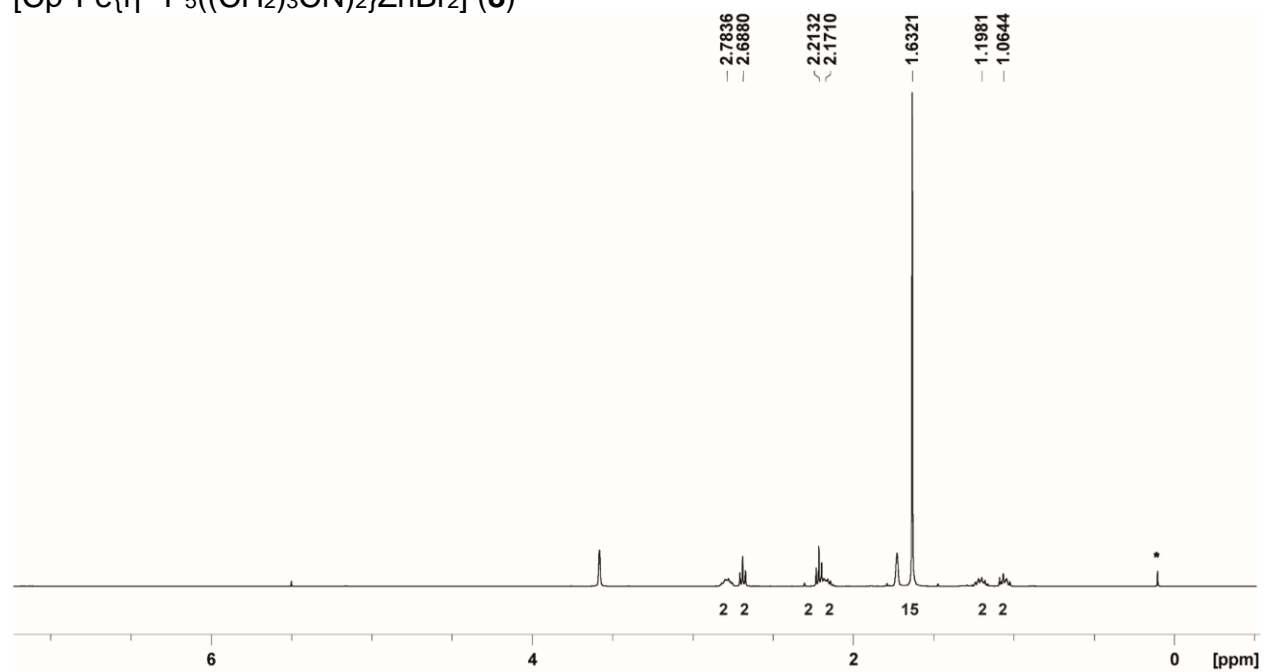


Fig. S15. Experimental ^1H NMR (400.13 MHz, THF- d_8) spectrum of **8** (* = grease).

^{31}P NMR Spectra:

[K(18c6)(thf)][Cp*Fe(η^4 -P₅-C≡CPh)] (**1c**)

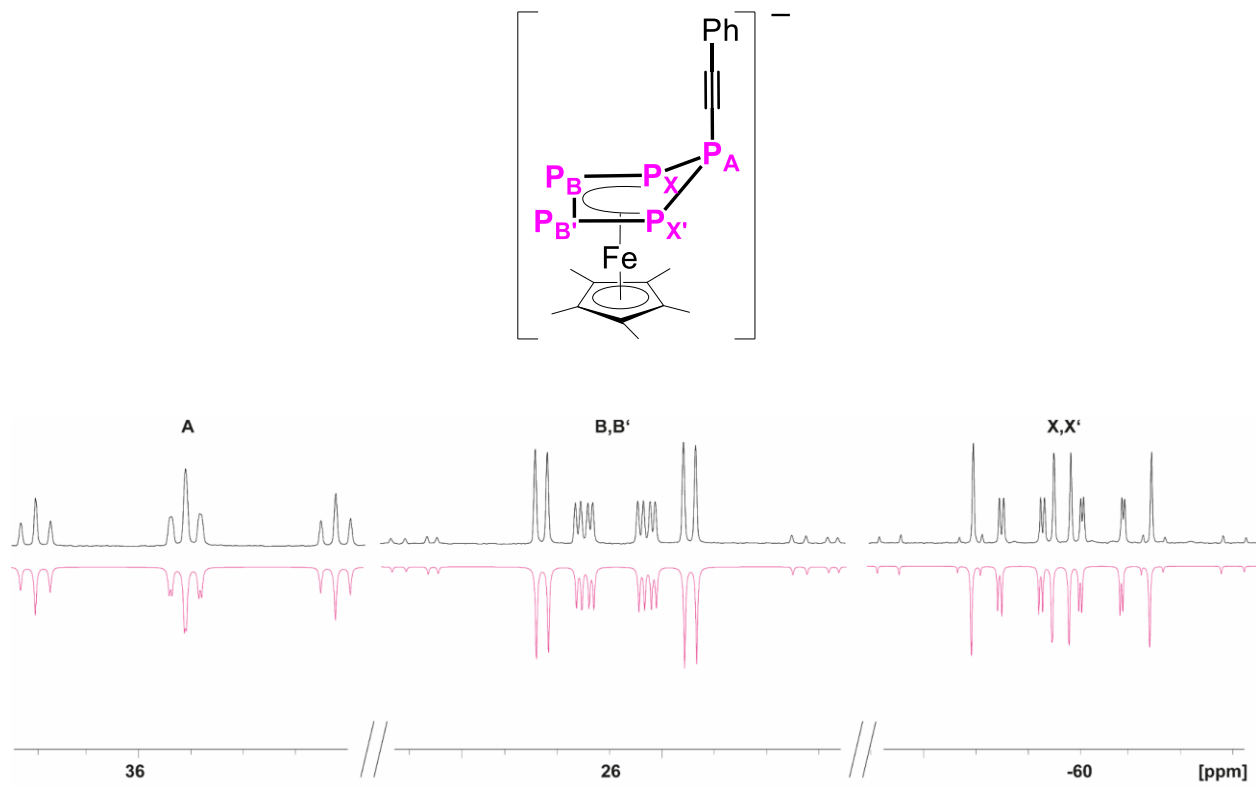


Fig. S16. Experimental (top) and simulated (bottom) $^{31}\text{P}\{{}^1\text{H}\}$ NMR (161.98 MHz, THF-d₈) spectrum of the anion of **1c**. (for a better resolution, **1c** was reacted with Li-C≡CPh in THF-d₈).

Table S1. Chemical shifts and coupling constants obtained from the simulation (R-factor = 2.43 %) in Figure S16.

J [Hz]				δ [ppm]	
${}^1J_{\text{P}_\text{A},\text{P}_\text{X}}$	305.0	${}^1J_{\text{P}_\text{B},\text{P}_\text{X}}$	377.5	X, X'	-59.3
${}^1J_{\text{P}_\text{A},\text{P}_\text{X}'}$	301.58	${}^1J_{\text{P}_\text{B}',\text{P}_\text{X}'}$	377.5		
${}^2J_{\text{P}_\text{A},\text{P}_\text{B}}$	-48.37	${}^2J_{\text{P}_\text{B}',\text{P}_\text{X}}$	-21.25	B, B'	26.0
${}^2J_{\text{P}_\text{A},\text{P}_\text{B}'}$	-31.74	${}^2J_{\text{P}_\text{B}',\text{P}_\text{X}'}$	-2.30		
${}^1J_{\text{P}_\text{B},\text{P}_\text{B}'}$	418.99	${}^2J_{\text{P}_\text{X},\text{P}_\text{X}'}$	-48.37	A	35.7

[Cp*Fe{η⁴-P₅'Bu(CH₂)₃Br}] (2a)

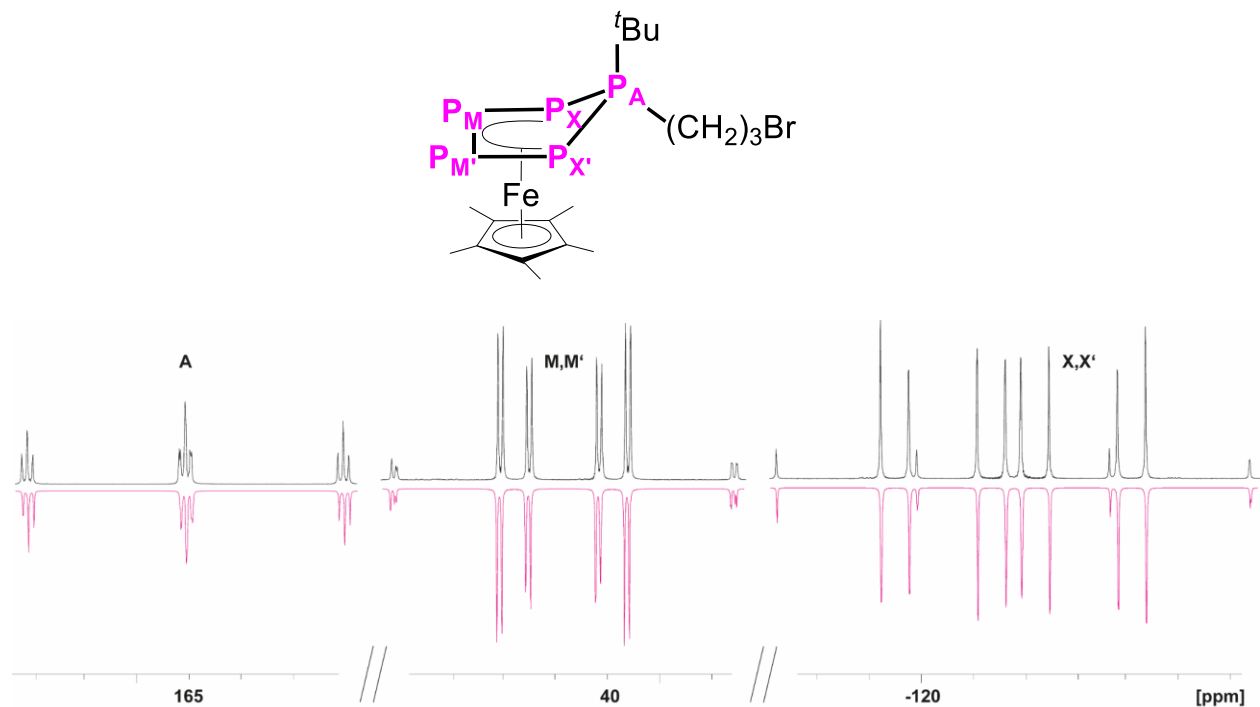


Fig. S17. Experimental (top) and simulated (bottom) ³¹P NMR (161.98 MHz, CD₂Cl₂) spectrum of **2a**.

Table S2. Chemical shifts and coupling constants obtained from the simulation (R-factor = 0.27 %) in Figure S17.

<i>J</i> [Hz]		<i>δ</i> [ppm]	
¹ J _{P_A,P_X}	410.20	¹ J _{P_A,P_X}	410.20
¹ J _{P_A,P_{X'}}	410.36	¹ J _{P_A,P_{X'}}	410.36
² J _{P_A,P_M}	14.77	² J _{P_A,P_{M'}}	14.77
² J _{P_A,P_{M'}}	13.31	² J _{P_A,P_M}	13.31
¹ J _{P_M,P_{M'}}	386.77	¹ J _{P_M,P_{M'}}	386.77

$[\text{Cp}^*\text{Fe}\{\eta^4\text{-P}_5\text{Me}(\text{CH}_2)_3\text{Br}\}]$ (**2b**)

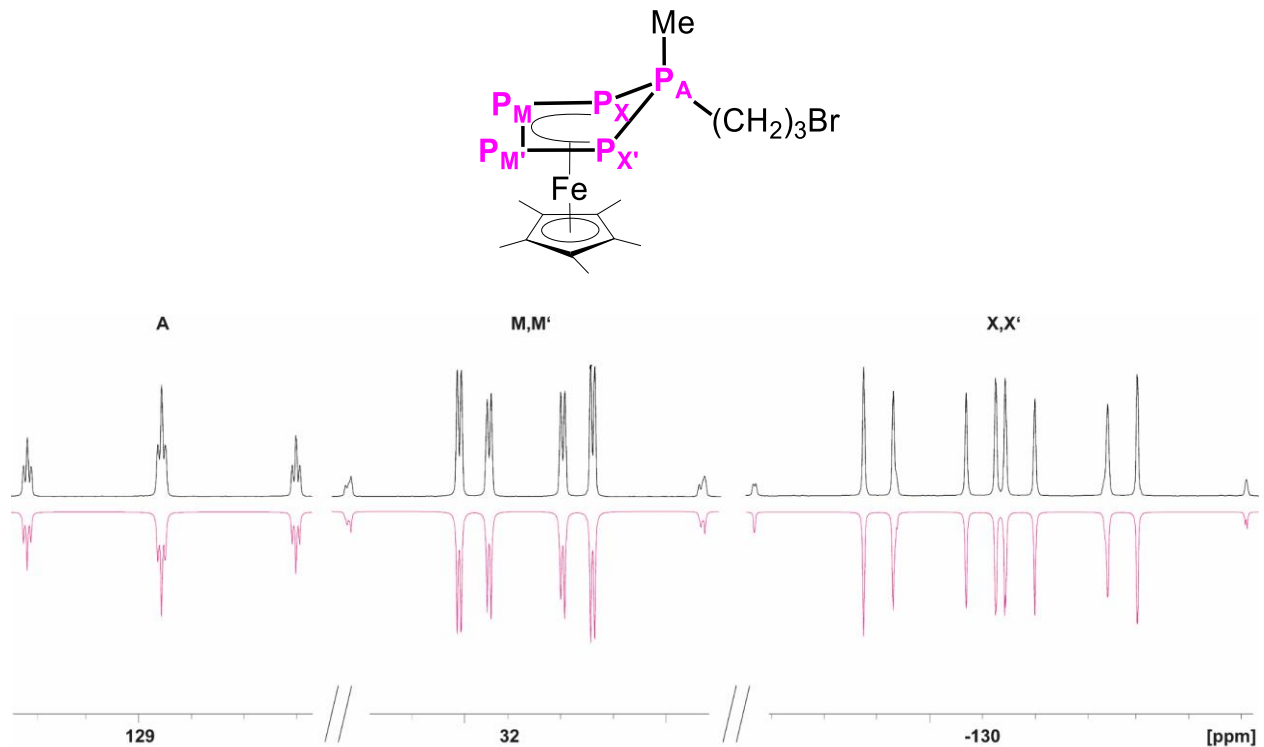


Fig. S18. Experimental (top) and simulated (bottom) $^{31}\text{P}\{^1\text{H}\}$ NMR (161.98 MHz, C_6D_6) spectrum of **2b**.

Table S3. Coupling constants obtained from the simulation (R-factor = 2.02 %) in Figure S18.

	J [Hz]		δ [ppm]	
$^1J_{\text{P}_A,\text{P}_X}$	387.09	$^1J_{\text{P}_{\text{M}'},\text{P}_X}$	399.39	X, X' -130.3
$^1J_{\text{P}_A,\text{P}_X'}$	387.32	$^1J_{\text{P}_{\text{M}'},\text{P}_X'}$	398.72	
$^2J_{\text{P}_A,\text{P}_M}$	-10.20	$^2J_{\text{P}_{\text{M}'},\text{P}_X}$	-38.00	M, M' 32.0
$^2J_{\text{P}_A,\text{P}_{\text{M}'}}$	-11.42	$^2J_{\text{P}_{\text{M}'},\text{P}_X'}$	-37.62	
$^1J_{\text{P}_{\text{M}'},\text{P}_{\text{M}'}}$	379.54	$^2J_{\text{P}_X,\text{P}_X'}$	2.56	A 128.9

[Cp*Fe{η⁴-P₅(-C≡CPh)Me}] (**2c**)

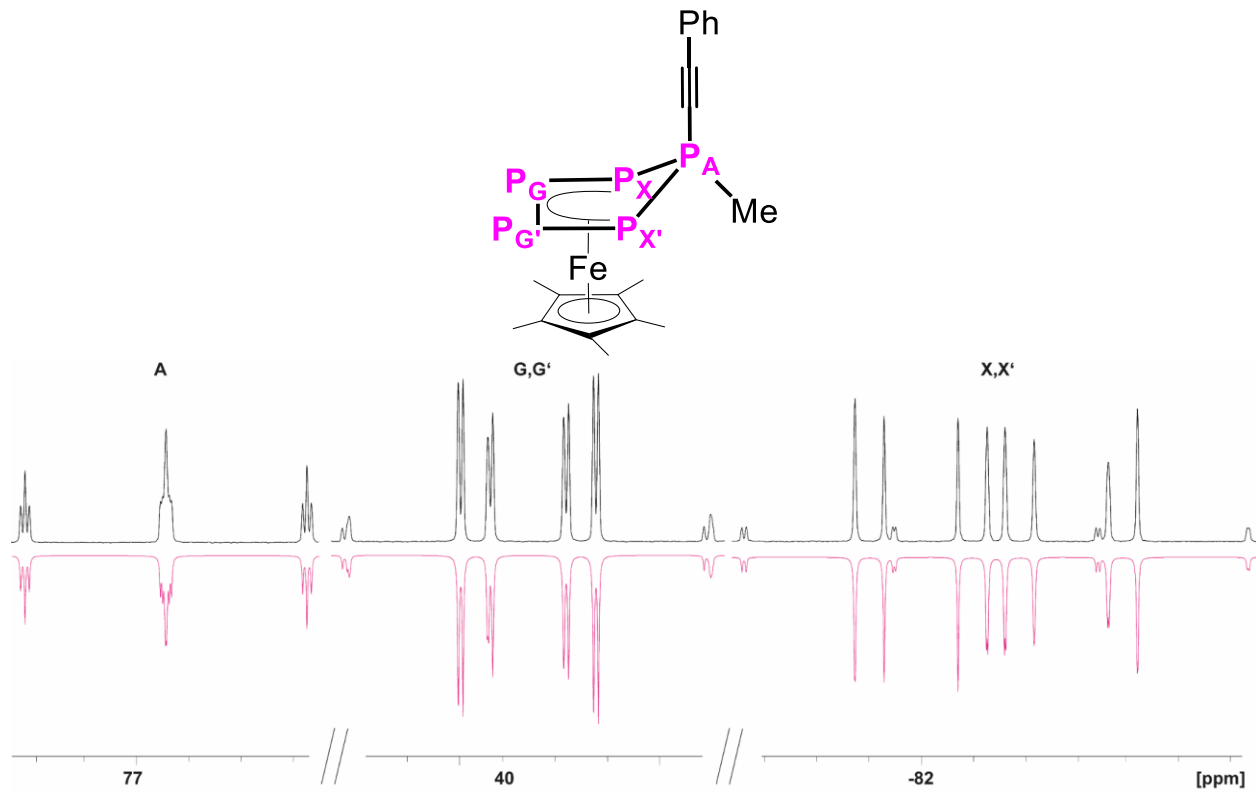


Fig. S19. Experimental (top) and simulated (bottom) ³¹P{¹H} NMR (161.98 MHz, C₆D₆) spectrum of **2c**.

Table S4. Coupling constants obtained from the simulation (R-factor = 2.68 %) in Figure S19.

	<i>J</i> [Hz]		<i>δ</i> [ppm]	
¹ J _{P_A,P_X}	414.97	¹ J _{P_G,P_X}	405.75	X, X' -83.2
¹ J _{P_A,P_{X'}}	414.31	¹ J _{P_{G'},P_{X'}}	406.26	
² J _{P_A,P_G}	13.19	² J _{P_{G'},P_X}	-40.72	G, G' 39.6
² J _{P_A,P_{G'}}	12.39	² J _{P_G,P_{X'}}	-41.16	
¹ J _{P_G,P_{G'}}	386.38	² J _{P_X,P_{X'}}	5.07	A 76.2

[Cp*Fe(η^4 -P₅Me(CH₂)₃CN)] (2d)

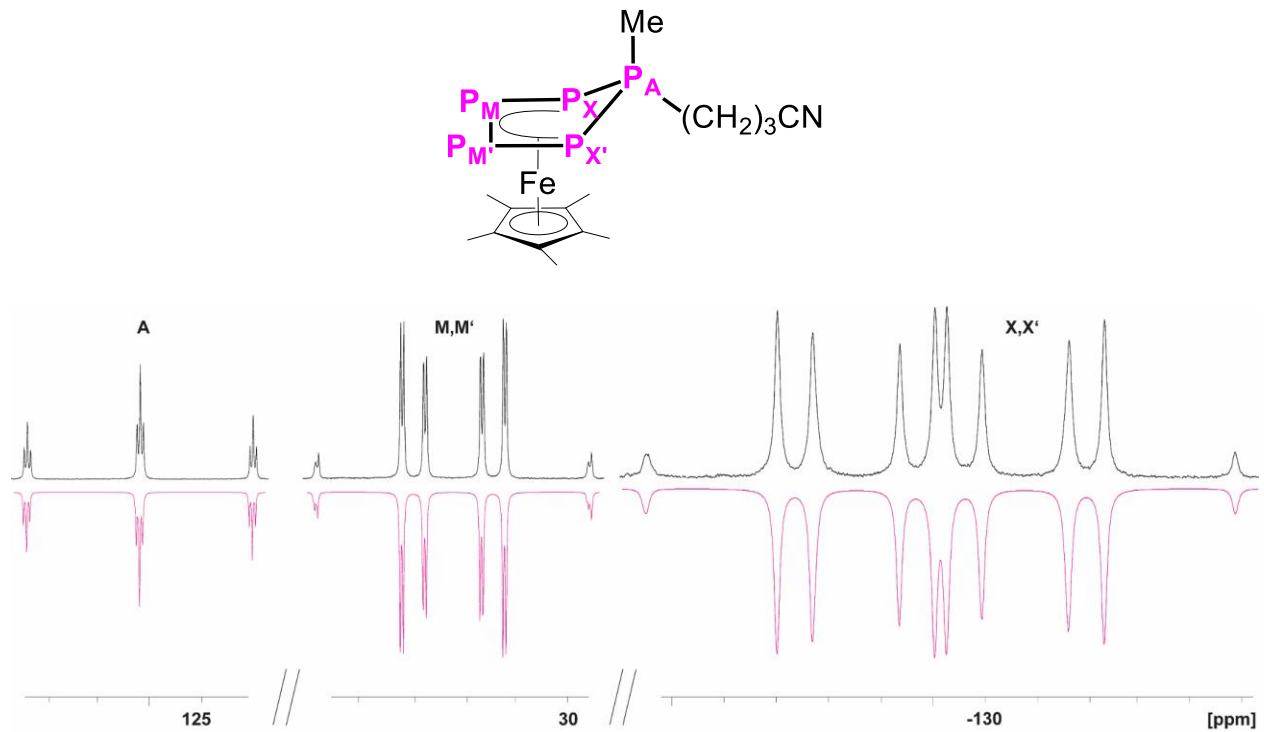


Fig. S20. Experimental (top) and simulated (bottom) $^{31}\text{P}\{\text{¹H}\}$ NMR (161.98 MHz, C₆D₆) spectrum of **2d**.

Table S5. Coupling constants obtained from the simulation (R-factor = 0.85 %) in Figure S20.

J [Hz]		δ [ppm]	
$^1J_{\text{P}_\text{A},\text{P}_\text{X}}$	388.43	$^1J_{\text{P}_\text{M},\text{P}_\text{X}}$	402.00
$^1J_{\text{P}_\text{A},\text{P}_\text{X}'}$	387.79	$^1J_{\text{P}_\text{M}',\text{P}_\text{X}'}$	396.52
$^2J_{\text{P}_\text{A},\text{P}_\text{M}}$	10.38	$^2J_{\text{P}_\text{M}',\text{P}_\text{X}}$	-41.41
$^2J_{\text{P}_\text{A},\text{P}_\text{M}'}$	11.35	$^2J_{\text{P}_\text{M},\text{P}_\text{X}'}$	-35.78
$^1J_{\text{P}_\text{M},\text{P}_\text{M}'}$	381.21	$^2J_{\text{P}_\text{X},\text{P}_\text{X}'}$	2.56
		A	127.3
		X, X'	-129.6
		M, M'	32.0

$[\text{Cp}^*\text{Fe}\{(\eta^4\text{-P}_5\text{Me}(\text{CH}_2)_4\text{Br})\}]$ (**2e**)

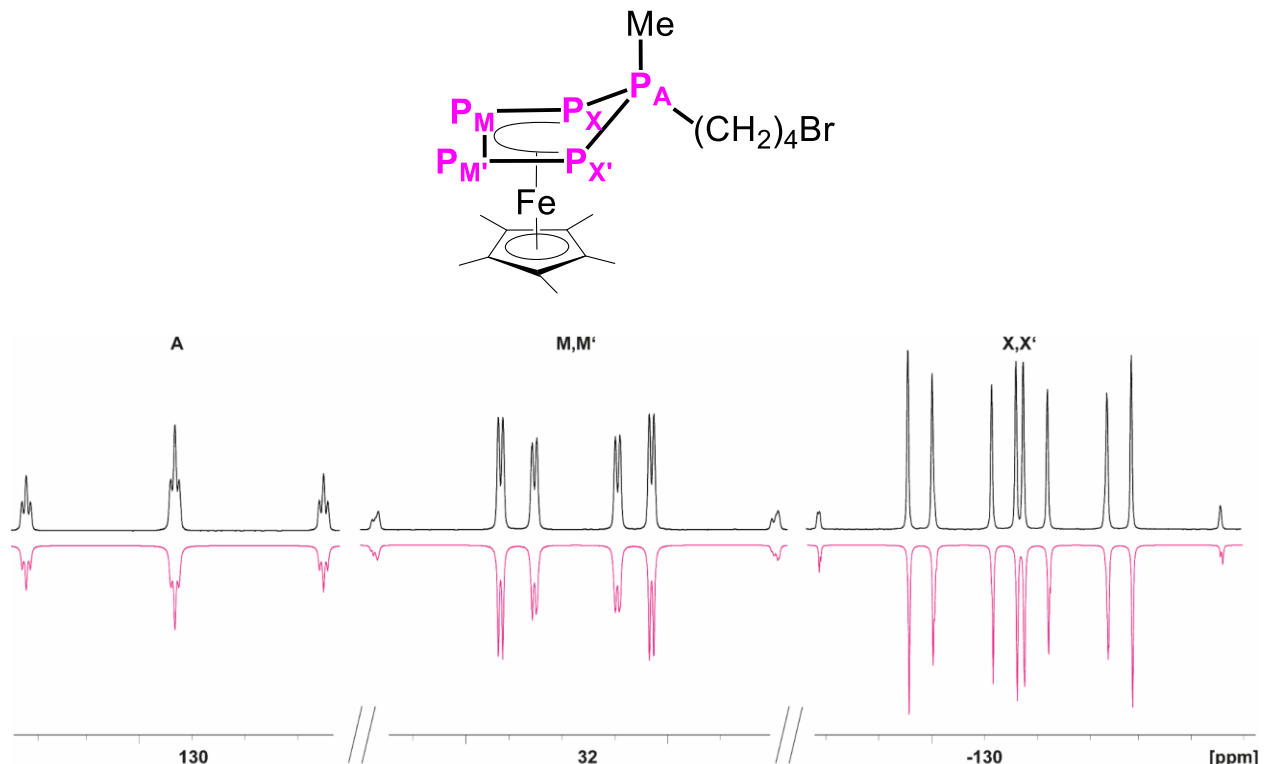


Fig. S21. Experimental (top) and simulated (bottom) $^{31}\text{P}\{^1\text{H}\}$ NMR (161.98 MHz, C_6D_6) spectrum of **2e**.

Table S6. Coupling constants obtained from the simulation (R-factor = 3.15 %) in Figure S21.

J [Hz]				δ [ppm]	
$^1J_{\text{P}_A,\text{P}_X}$	385.4	$^1J_{\text{P}_{\text{M}},\text{P}_X}$	402.6	X, X'	-130.8
$^1J_{\text{P}_A,\text{P}_{X'}}$	385.7	$^1J_{\text{P}_{\text{M}'},\text{P}_{X'}}$	395.4		
$^2J_{\text{P}_A,\text{P}_M}$	-10.4	$^2J_{\text{P}_{\text{M}'},\text{P}_X}$	-41.0	M, M'	31.9, 32.0
$^2J_{\text{P}_A,\text{P}_{M'}}$	-11.1	$^2J_{\text{P}_{\text{M}'},\text{P}_X}$	-34.0		
$^1J_{\text{P}_{\text{M}},\text{P}_{\text{M}'}}$	380.3	$^2J_{\text{P}_X,\text{P}_{X'}}$	-2.8	A	130.8

$[(\text{Cp}^*\text{Fe})_2\{\mu,\eta^{4:4}\text{-P}_5^t\text{Bu}(\text{CH}_2)_3\text{P}_5^t\text{Bu}\}]$ (**3a/3a'**)

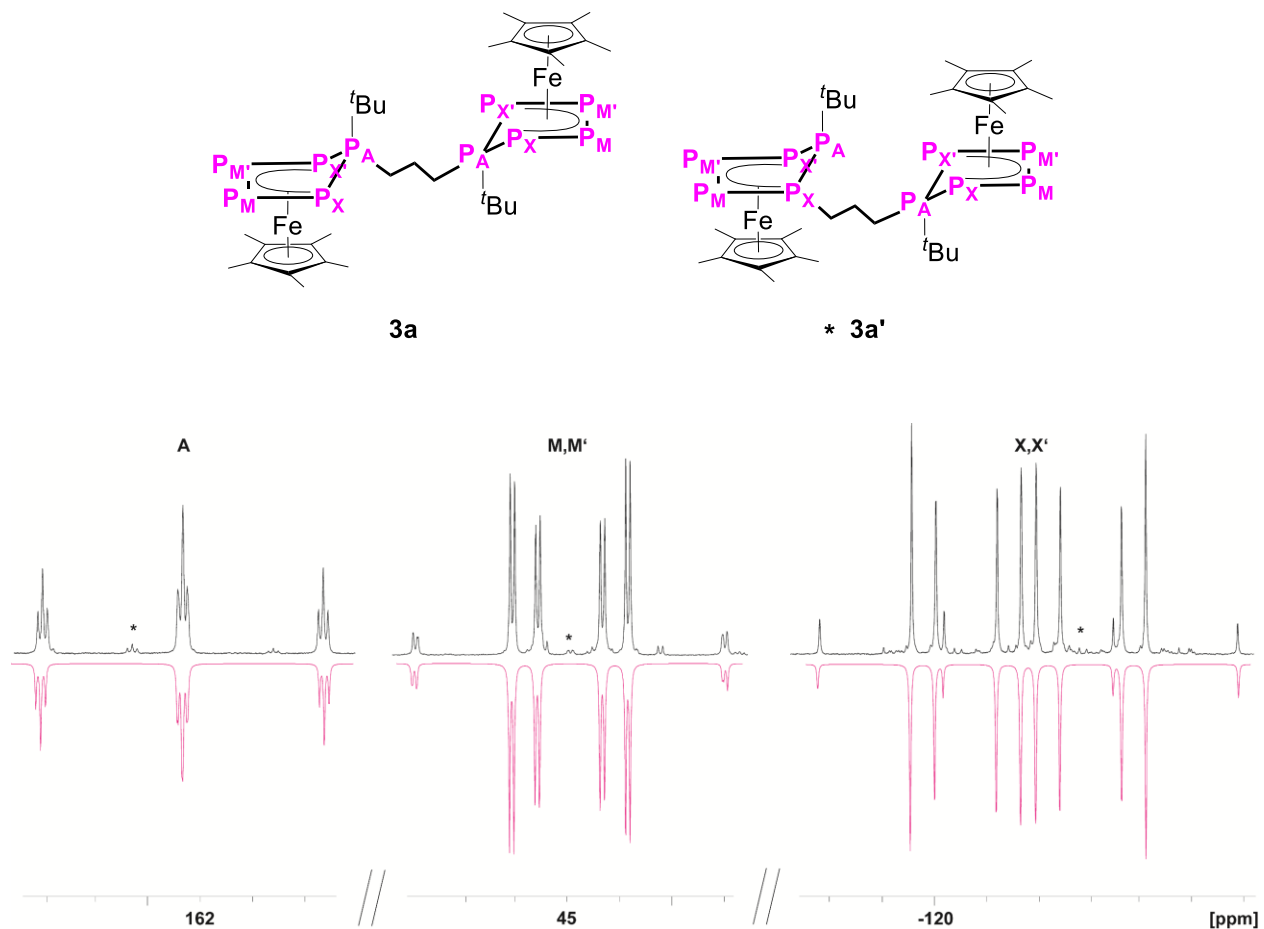


Fig. S22. Experimental (top) and simulated (bottom) $^{31}\text{P}\{^1\text{H}\}$ NMR (161.98 MHz, CD_2Cl_2) spectrum of **3a** (* = **3a'**).

Table S7. Chemical shifts and coupling constants obtained from the simulation (R-factor = 1.05 %) in Figure S22.

J [Hz]				δ [ppm]	
$^1J_{\text{P}_A,\text{P}_X}$	403.07	$^1J_{\text{P}_{M'},\text{P}_X}$	404.00	X, X'	-120.14
$^1J_{\text{P}_A,\text{P}_{X'}}$	403.07	$^1J_{\text{P}_{M'},\text{P}_{X'}}$	404.00		
$^2J_{\text{P}_A,\text{P}_M}$	14.41	$^2J_{\text{P}_{M'},\text{P}_X}$	-37.51	M, M'	44.64
$^2J_{\text{P}_A,\text{P}_{M'}}$	14.41	$^2J_{\text{P}_{M'},\text{P}_{X'}}$	-37.51		
$^1J_{\text{P}_M,\text{P}_{M'}}$	385.06	$^2J_{\text{P}_X,\text{P}_{X'}}$	2.00	A	162.43

Three Signals of **3a'** overlay with the Signals of **3a**. Due to the low intensity of **3a'** and the overlay, a simulation was not possible.

$[(\text{Cp}^*\text{Fe})_2\{\mu,\eta^{4:4}\text{-P}_5\text{Me}(\text{CH}_2)_3\text{P}_5\text{Me}\}]$ (**3b**)

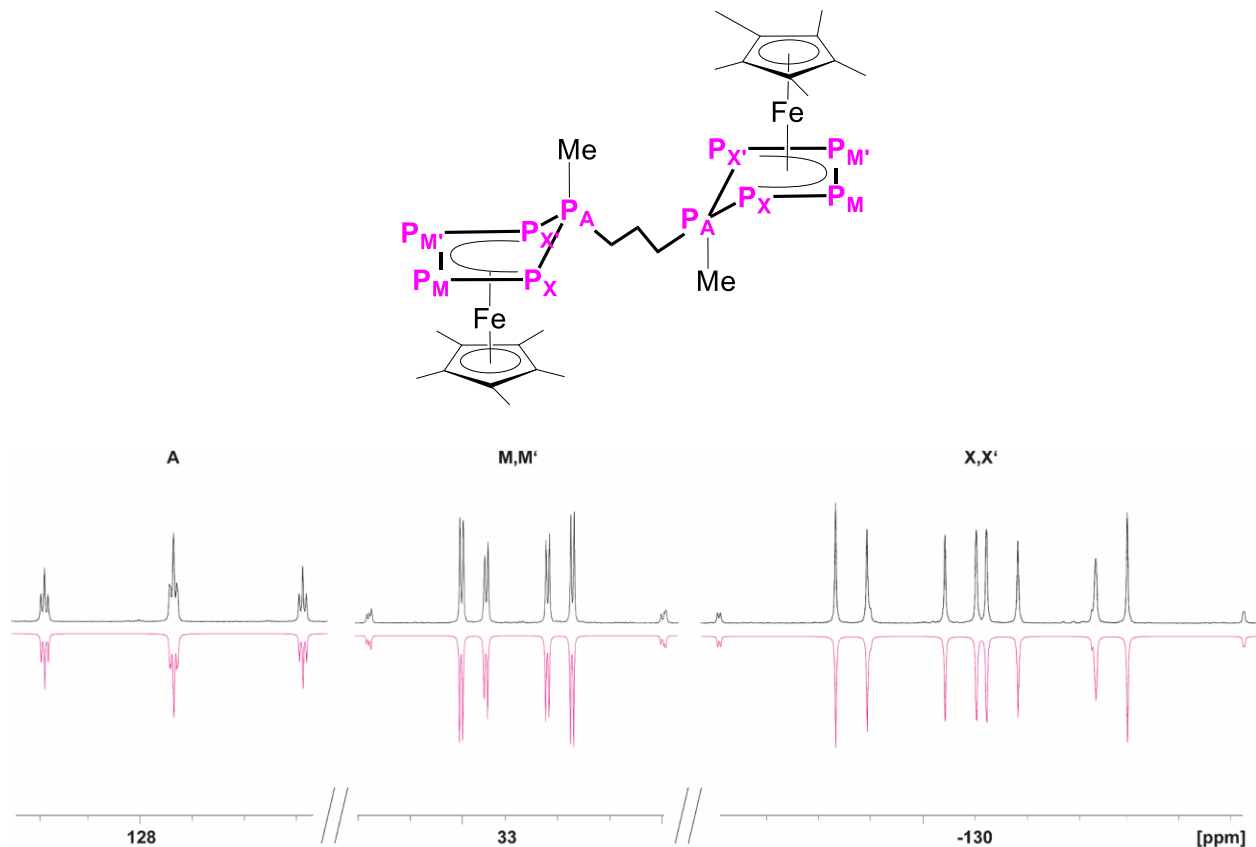


Fig. S23. Experimental (top) and simulated (bottom) ${}^3\text{P}\{{}^1\text{H}\}$ NMR (161.98 MHz, C_6D_6) spectrum of **3b**.

Table S8. Coupling constants obtained from the simulation (R-factor = 0.43 %) in Figure S23.

	J [Hz]		δ [ppm]	
${}^1J_{\text{P}_A,\text{P}_X}$	386.34	${}^1J_{\text{P}_M,\text{P}_X}$	401.41	X, X' -129.6
${}^1J_{\text{P}_A,\text{P}_X'}$	387.07	${}^1J_{\text{P}_M',\text{P}_X'}$	396.75	
${}^2J_{\text{P}_A,\text{P}_M}$	10.32	${}^2J_{\text{P}_M',\text{P}_X}$	-40.64	M, M' 32.6
${}^2J_{\text{P}_A,\text{P}_M'}$	11.16	${}^2J_{\text{P}_M,\text{P}_X'}$	-36.00	
${}^1J_{\text{P}_M,\text{P}_M'}$	379.19	${}^2J_{\text{P}_X,\text{P}_X'}$	3.21	A 127.4

$[(\text{Cp}^*\text{Fe})_2\{\mu,\eta^{4:4}\text{-P}_5\text{Me}(\text{CH}_2)_4\text{P}_5\text{Me}\}]$ (**3c/3c'**)

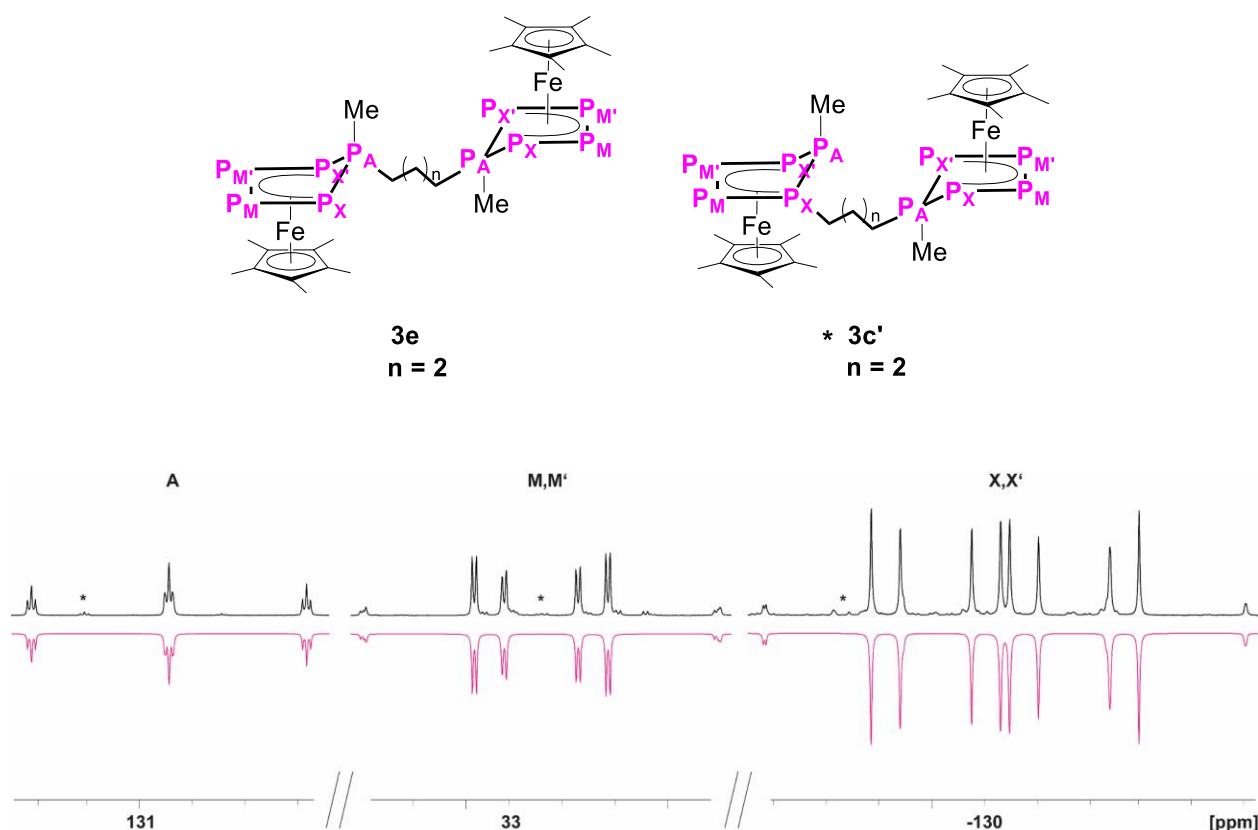


Fig. S24. Experimental (top) and simulated (bottom) $^{31}\text{P}\{^1\text{H}\}$ NMR (161.98 MHz, C_6D_6) spectrum of **3c** ($*$ = $\text{3c}'$).

Table S9. Coupling constants obtained from the simulation (R-factor = 1.06 %) in Figure S24.

J [Hz]		δ [ppm]	
$^1J_{\text{P}_A,\text{P}_X}$	386.37	$^1J_{\text{P}_M,\text{P}_X}$	400.10
$^1J_{\text{P}_A,\text{P}_X'}$	386.60	$^1J_{\text{P}_M',\text{P}_X'}$	398.96
$^2J_{\text{P}_A,\text{P}_M}$	11.02	$^2J_{\text{P}_M',\text{P}_X}$	-37.19
$^2J_{\text{P}_A,\text{P}_M'}$	11.27	$^2J_{\text{P}_M,\text{P}_X'}$	-38.77
$^1J_{\text{P}_M,\text{P}_M'}$	378.84	$^2J_{\text{P}_X,\text{P}_X'}$	3.49
		A	130.8

Three Signals of **3c'** overlay with the signals of **3c**. Due to the low intensity of **3c'** and the overlay, a simulation was not possible.

$[(\text{Cp}^*\text{Fe})_2\{\mu,\eta^{4:4}\text{-P}_5^t\text{Bu}(\text{CH}_2)_3\text{P}_5\text{Me}\}]$ (**4**)

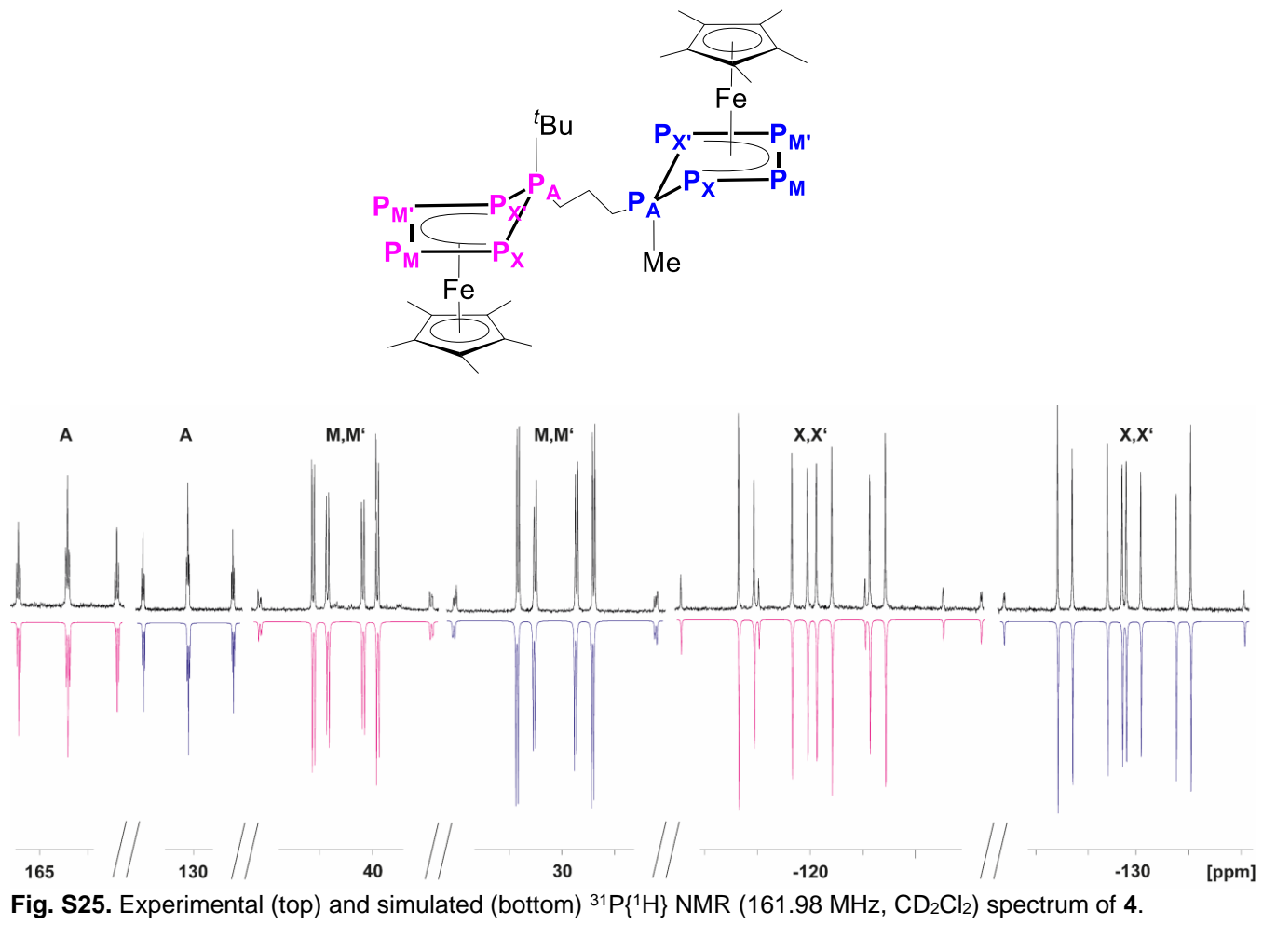


Fig. S25. Experimental (top) and simulated (bottom) $^{31}\text{P}\{^1\text{H}\}$ NMR (161.98 MHz, CD_2Cl_2) spectrum of **4**.

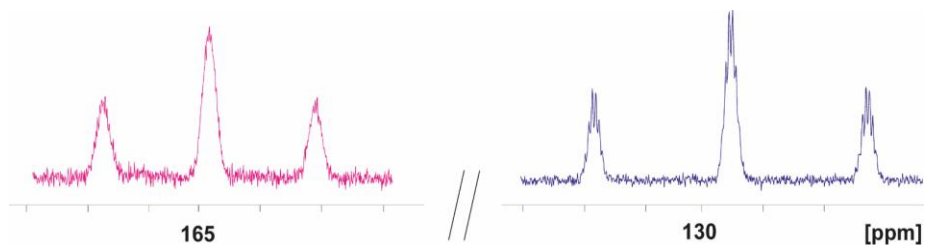


Fig. S26. View frame of the essential part of the experimental ^{31}P NMR (161.98 MHz, CD_2Cl_2) spectrum of **4**.

$\text{P}_5^t\text{Bu-R}$:

Table S10. Chemical shifts and coupling constants obtained from the simulation (R-factor = 3.79 %) in Figure S25.

	J [Hz]		δ [ppm]	
$^1J_{\text{P}_A, \text{P}_X}$	411.79	$^1J_{\text{P}_M, \text{P}_X}$	402.75	X, X' -120.3
$^1J_{\text{P}_A, \text{P}_X'}$	411.53	$^1J_{\text{P}_{M'}, \text{P}_X'}$	404.17	

$^2J_{P_A, P_M}$	14.41	$^2J_{P_{M'}, P_X}$	-38.32	M, M'	41.0
$^2J_{P_A, P_{M'}}$	14.28	$^2J_{P_{M'}, P_{X'}}$	-39.65		
$^1J_{P_M, P_{M'}}$	386.85	$^2J_{P_X, P_{X'}}$	-0.52	A	164.3

P₅Me-R:

Table S11. Coupling constants obtained from the simulation (R-factor = 3.79 %) in Figure S24.

J [Hz]				δ [ppm]	
$^1J_{P_A, P_X}$	384.39	$^1J_{P_{M'}, P_X}$	396.00	X, X'	-129.9
$^1J_{P_A, P_{X'}}$	383.85	$^1J_{P_{M'}, P_{X'}}$	400.37		
$^2J_{P_A, P_M}$	10.69	$^2J_{P_{M'}, P_X}$	-35.00	M, M'	29.8
$^2J_{P_A, P_{M'}}$	10.95	$^2J_{P_M, P_{X'}}$	-39.00		
$^1J_{P_M, P_{M'}}$	385.85	$^2J_{P_X, P_{X'}}$	3.03	A	128.9

$[\text{Cp}^*\text{Fe}\{\eta^4\text{-P}_5^t\text{Bu}(\text{CH}_2)_3\text{PPh}_2\}]$ (**5**)

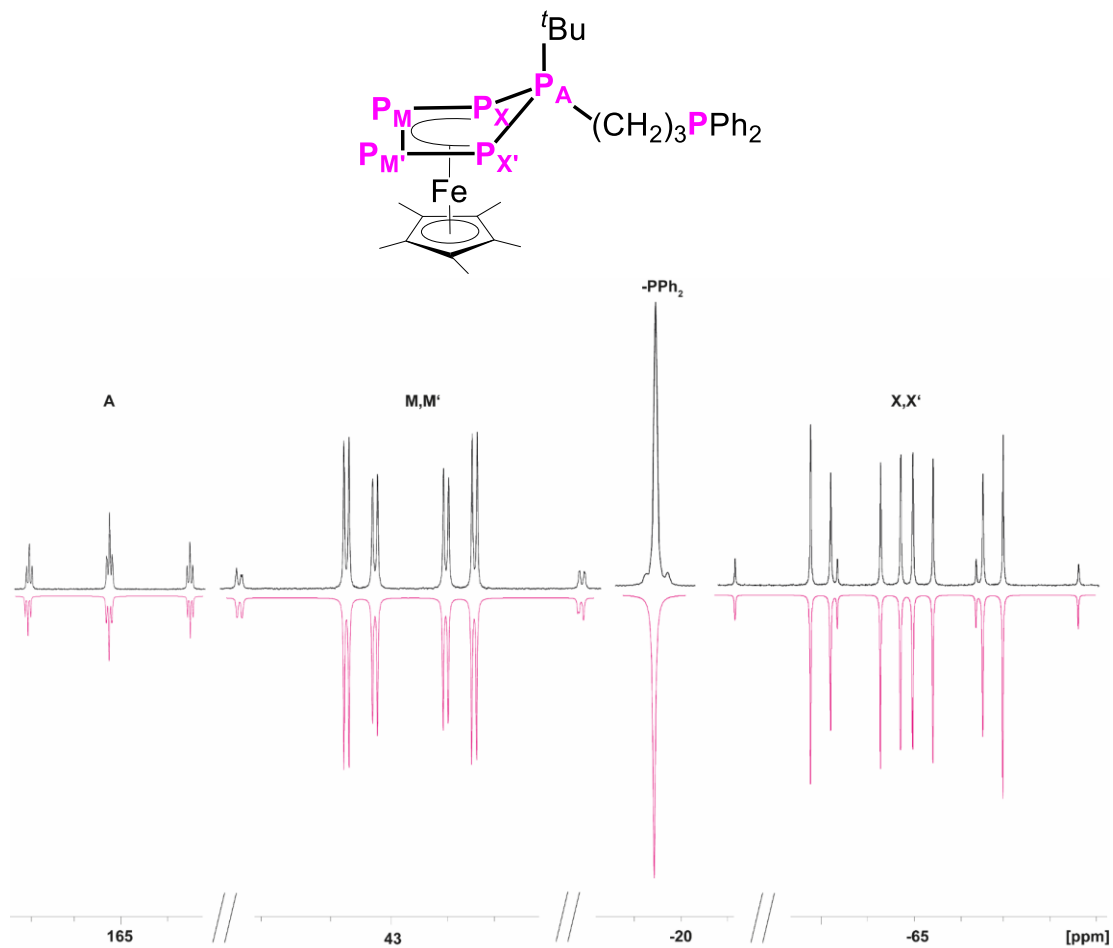


Fig. S27. Experimental (top) and simulated (bottom) $^{31}\text{P}\{^1\text{H}\}$ NMR (161.98 MHz, C_6D_6) spectrum of **5**.

Table S12. Coupling constants obtained from the simulation (R-factor = 8.07 %) in Figure S27.

J [Hz]			δ [ppm]	
$^1\text{J}_{\text{PA},\text{PX}}$	412.20	$^1\text{J}_{\text{PM},\text{PX}}$	400.99	X, X' -121.65
$^1\text{J}_{\text{PA},\text{PX}'}$	412.09	$^1\text{J}_{\text{PM}',\text{PX}'}$	403.85	
$^2\text{J}_{\text{PA},\text{PM}}$	14.25	$^2\text{J}_{\text{PM}',\text{PX}}$	-37.84	M, M' 42.57
$^2\text{J}_{\text{PA},\text{PM}'}$	14.26	$^2\text{J}_{\text{PM},\text{PX}'}$	-40.90	
$^1\text{J}_{\text{PM},\text{PM}'}$	383.98	$^2\text{J}_{\text{PX},\text{PX}'}$	-0.344	A 164.88
				PPh ₂ -17.87

*t*BuPBn((CH₂)₃Bn) (**6**)

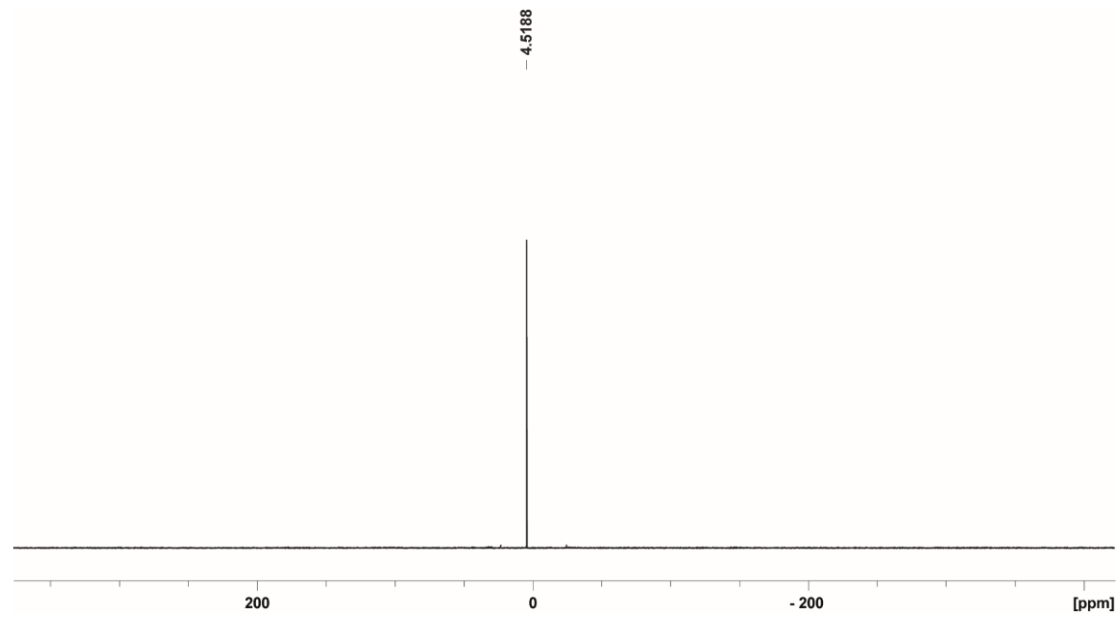


Fig. S28. Experimental ³¹P{¹H} NMR (161.98 MHz, C₆D₆) spectrum of **6**.

SP*t*BuBn((CH₂)₃Bn) (**6'**)

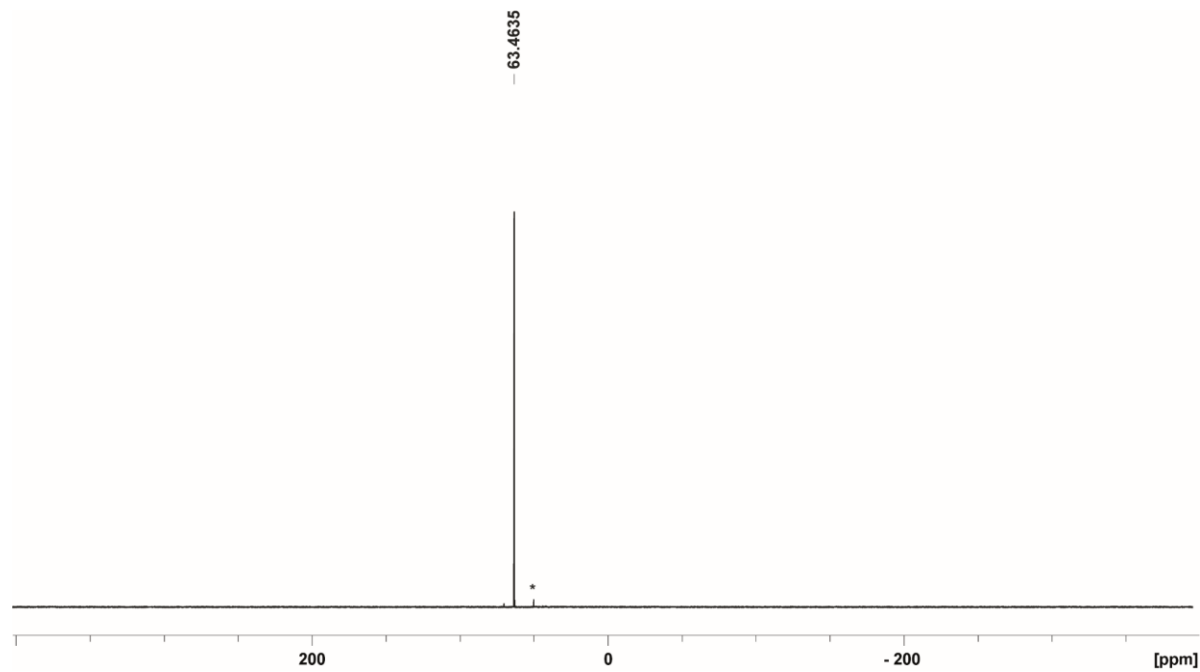


Fig. S29. Experimental ³¹P{¹H} NMR (161.98 MHz, C₆D₆) spectrum of **6'** (* = OP*t*BuBn((CH₂)₃Bn)).

$[\text{Cp}^*\text{Fe}\{\eta^4\text{-P}_5((\text{CH}_2)_3\text{CN})_2\}]$ (7)

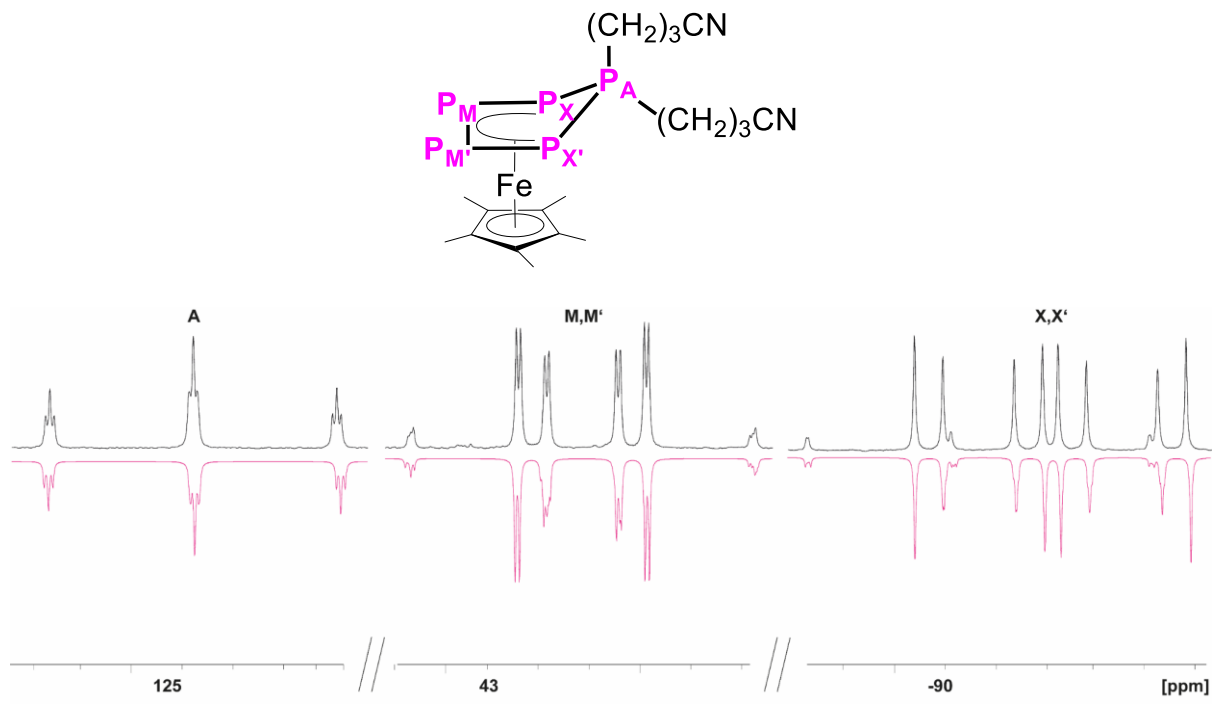


Fig. S30. Experimental (top) and simulated (bottom) $^{31}\text{P}\{^1\text{H}\}$ NMR (161.98 MHz, C_6D_6) spectrum of 7.

Table S13. Coupling constants obtained from the simulation ($\text{R-factor} = 2.41 \%$) in Figure S30.

J [Hz]				δ [ppm]	
$^1J_{\text{P}_\text{A},\text{P}_\text{X}}$	409.62	$^1J_{\text{P}_\text{M},\text{P}_\text{X}}$	400.00	X, X'	-129.2
$^1J_{\text{P}_\text{A},\text{P}_\text{X}'}$	409.76	$^1J_{\text{P}_\text{M}',\text{P}_\text{X}'}$	407.00		
$^2J_{\text{P}_\text{A},\text{P}_\text{M}}$	11.37	$^2J_{\text{P}_\text{M}',\text{P}_\text{X}}$	-35.28	M, M'	37.0
$^2J_{\text{P}_\text{A},\text{P}_\text{M}'}$	11.51	$^2J_{\text{P}_\text{M},\text{P}_\text{X}'}$	-42.64		
$^1J_{\text{P}_\text{M},\text{P}_\text{M}'}$	379.00	$^2J_{\text{P}_\text{X},\text{P}_\text{X}'}$	1.50	A	133.7

$[\text{Cp}^*\text{Fe}\{\eta^4\text{-P}_5((\text{CH}_2)_3\text{CN})_2\}\text{ZnBr}_2]$ (**8**)

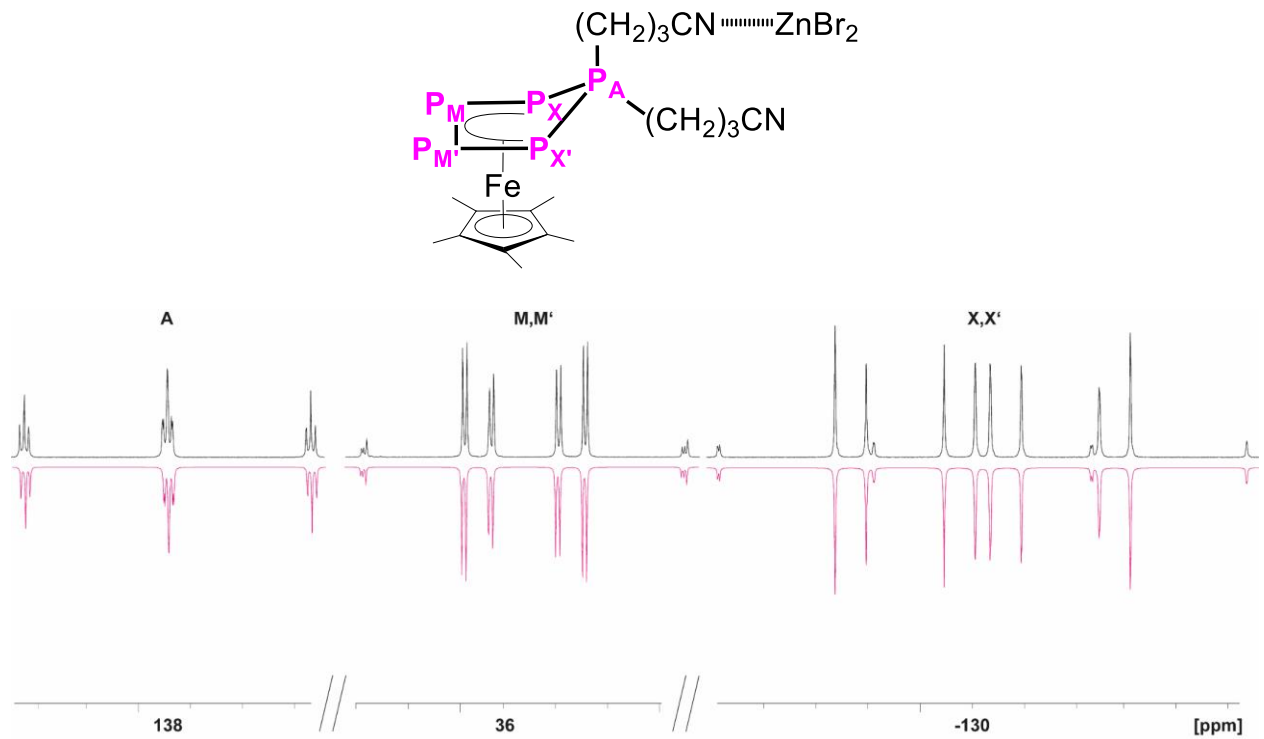


Fig. S31. Experimental (top) and simulated (bottom) $^{31}\text{P}\{^1\text{H}\}$ NMR (161.98 MHz, THF- d_8) spectrum of **8**.

Table S14. Coupling constants obtained from the simulation (R-factor = 0.39 %) in Figure S31.

J [Hz]		δ [ppm]	
$^1J_{\text{P}_A,\text{P}_X}$	398.68	$^1J_{\text{P}_M,\text{P}_X}$	397.74
$^1J_{\text{P}_A,\text{P}_X'}$	398.62	$^1J_{\text{P}_M',\text{P}_X'}$	400.27
$^2J_{\text{P}_A,\text{P}_M}$	12.41	$^2J_{\text{P}_M',\text{P}_X}$	-37.83
$^2J_{\text{P}_A,\text{P}_M'}$	12.63	$^2J_{\text{P}_M,\text{P}_X'}$	-40.16
$^1J_{\text{P}_M,\text{P}_M'}$	378.88	$^2J_{\text{P}_X,\text{P}_X'}$	2.26
		A	137.9
X, X'			-130.3
M, M'			36.3

^{13}C NMR spectra:

$t\text{BuPb}((\text{CH}_2)_3\text{Bn})$ (**6**)

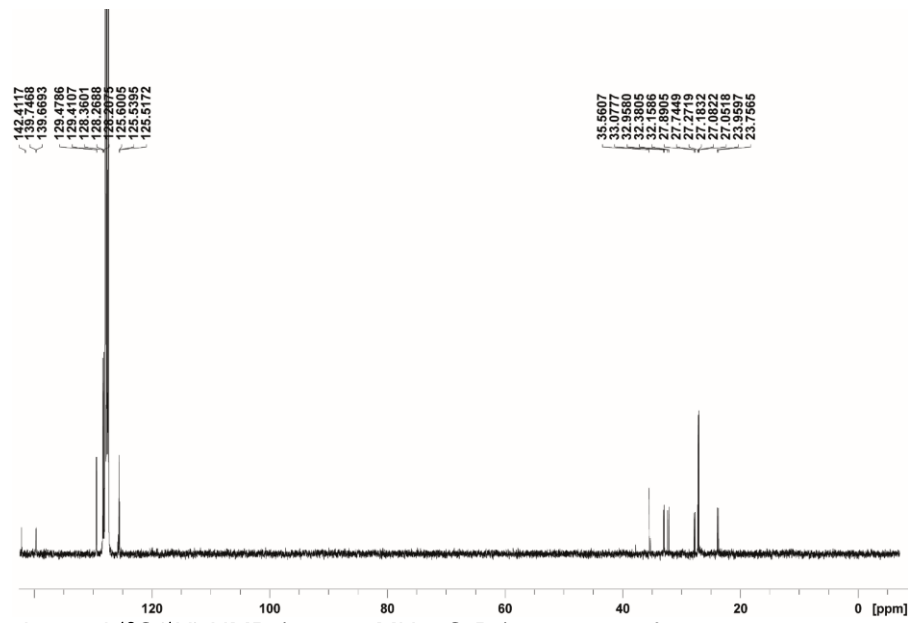


Fig. S32. Experimental $^{13}\text{C}\{^1\text{H}\}$ NMR (100.61 MHz, C_6D_6) spectrum of **6**.

$\text{SP}^t\text{BuBn}((\text{CH}_2)_3\text{Bn})$ (**6'**)

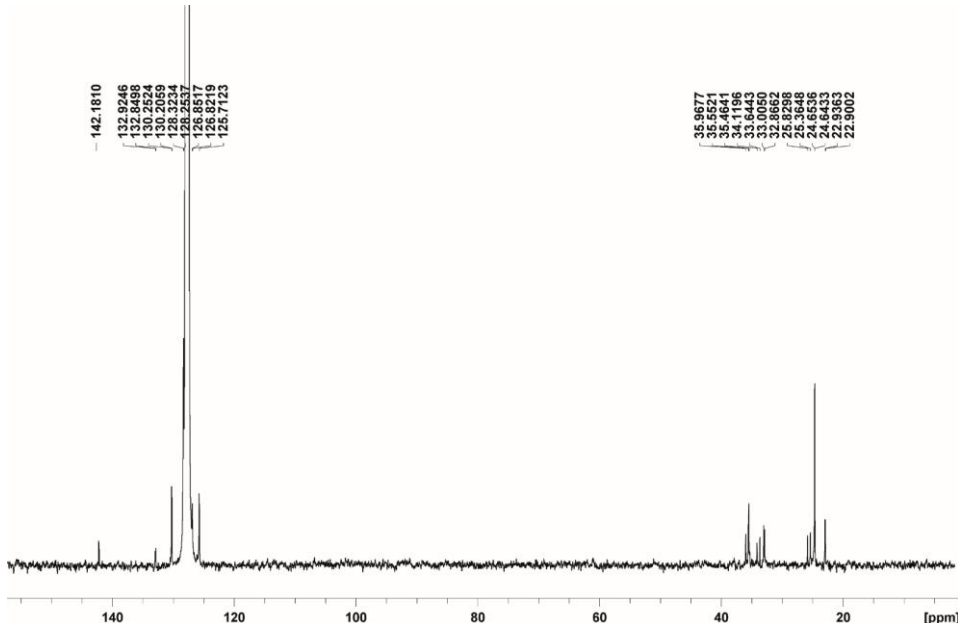


Fig. S33. Experimental $^{13}\text{C}\{^1\text{H}\}$ NMR (100.61 MHz, C_6D_6) spectrum of **6'**.

Crystallographic details

[K(18c6)(thf)][Cp*Fe(η^4 -P₅-C≡CPh)] (1c): There are two molecules of **1c**, two by 18-c-6 coordinated K cations and two THF solvent molecules in the asymmetric unit. One of these THF molecule is disordered over two positions (50:50). Further are both P₅ ligands disordered over two positions (94:6; 92:8). The restraints SADI and SIMU were applied to model these disorders. The structure in solid state is given in **Figure S34 and S35**. Crystallographic and refinement data are summarized in **Table S15**.

[Cp*Fe(η^4 -P₅'Bu(CH₂)₃Br)] (2a): The asymmetric unit contains one molecule of **2a** without any disorder. The structure in solid state is given in **Figure S36**. Crystallographic and refinement data are summarized in **Table S15**.

[Cp*Fe(η^4 -P₅Me(CH₂)₃Br)] (2b): The asymmetric unit contains one molecule of **2b**. Compound **3b** co crystallizes with another compound in the ratio (90:10). The second compound features a P₅Me(CH₂)₃Br ligand where one substituent migrated to a neighboring phosphorus atom. The SADI and SIMU restraints were applied to model this disorder. The structure in solid state is given in **Figure S37**. Crystallographic and refinement data are summarized in **Table S15**.

[Cp*Fe{ η^4 -P₅(-C≡CPh)Me}] (2c): The asymmetric unit contains one molecule of **2c** without any disorder. The structure in solid state is given in **Figure S38**. Crystallographic and refinement data are summarized in **Table S15**.

[Cp*Fe(η^4 -P₅Me(CH₂)₃CN)] (2d): The asymmetric unit contains one molecule of **3d**. Furthermore, compound **1** co-crystallizes at the same position and can only be distinguished by the disordered middle deck, with a distribution of 5:95. The structure in solid state is given in **Figure S39 and S40**. Crystallographic and refinement data are summarized in **Table S15**.

[Cp*Fe{(η^4 -P₅Me(CH₂)₄Br)}] (2e): The asymmetric unit contains one molecule of **2e**. Compound **3b** co crystallizes with another compound in the ratio (90:10). The second compound features a P₅Me(CH₂)₄Br ligand where one substituent migrated to a neighboring phosphorus atom. The SADI and SIMU restraints were applied to model this disorder. The structure in solid state is given in **Figure S41**. Crystallographic and refinement data are summarized in **Table S15**.

[(Cp*Fe)₂{ μ , $\eta^{4:4}$ -P₅'Bu(CH₂)₃P₅'Bu}] (3a / 3a'): The asymmetric unit contains one molecule of **3a** and **3a'** which co-crystallizes and a distribution of 92:8, respectively. The structures in solid state are depicted in **Figure S42, S43 and S44**. The unit cell contains 2 uncoordinated molecules of dichloromethane and 3 molecules of *n*-hexane which were removed with the implemented tool *SQUEEZE* due to unresolvable disorder. Crystallographic and refinement data are summarized in **Table S16**.

[(Cp*Fe)₂{ μ , $\eta^{4:4}$ -P₅Me(CH₂)₃P₅Me}] (3b): The asymmetric unit contains one molecule of **3b**. One Cp* ligand is disordered over two positions with a distribution of 58:42. To

describe the disorders the SIMU restrain is applied. The structure in solid state is given in **Figure S45**. Crystallographic and refinement data are summarized in **Table S16**.

[(Cp*Fe)₂{ μ , $\eta^{4:4}$ -P₅Me(CH₂)₄P₅Me}] (3c): The asymmetric unit contains half a molecule of **3c**. The Cp* ligand is disordered over two positions with a distribution of 60:40. The structure in solid state is given in **Figure S46**. The unit cell contains 1.5 uncoordinated molecules of dichloromethane which were removed with the implemented tool *SQUEEZE* due to unresolvable disorder. Crystallographic and refinement data are summarized in **Table S16**.

[(Cp*Fe)₂{ μ , $\eta^{4:4}$ -P₅^tBu(CH₂)₃P₅Me}] (4): The asymmetric unit contains one molecule of **4** without any disorder. The structure in solid state is given in **Figure S47**. Crystallographic and refinement data are summarized in **Table S16**.

[Cp*Fe(η^4 -P₅^tBu(CH₂)₃PPh₂)] (5): The asymmetric unit contains two molecules of **5**. The P₅ middle decks are disordered over two positions in both molecules with a distribution of 65:35 / 76:24, respectively. As well as the middle decks, both Cp* ligands is disordered over two positions with a distribution of 85:15 in both molecules. In addition to this, the *n*-propyl-di-phenyl-phosphine residue is disorder over two positions. Thereby, the occupancy is 77:23 / 85:15, respectively. To describe the disorders the SADI and SIMU restraints are applied. Since the distribution, bond lengths, and bond angles are very similar, only one molecule in solid state is depicted in Figure **S48** and **S49** and its bond lengths and angles are presented in Table **S38** and **S39**. Crystallographic and refinement data are summarized in **Table S17**.

SP^tBuBn((CH₂)₄Ph) (6'): The asymmetric unit contains one molecule of **6'** without any disorder. The structure in solid state is given in **Figure S50**. Crystallographic and refinement data are summarized in **Table S17**.

[Cp*Fe{ η^4 -P₅((CH₂)₃CN)₂}] (7): The asymmetric unit contains one molecule of **7**. The P₅ middle decks are disordered over two positions with a distribution of 97:3. Since the carbon atoms of part 2 cannot be resolved, due to the low occupation, only the bond lengths and angles of part 1 are presented in Table **S42** and **S43**. The structure in solid state is given in **Figure S51** and **S52**. Crystallographic and refinement data are summarized in **Table S17**.

[[Cp*Fe{ η^4 -P₅((CH₂)₃CN)₂}]ZnBr₂] (8): The asymmetric unit contains one molecule of **8** without any disorder, forming a linear polymer when grown. Since the measured crystal was twinned, a HKLF5 refinement was applied (BASF 0.368). The structure in solid state is given in **Figure S53**. Crystallographic and refinement data are summarized in **Table S17**.

CCDC-2247948 (**1c**), CCDC-2041983 (**2a**), CCDC-2247949 (**2b**), CCDC-2247950 (**2c**), CCDC-2041982 (**2d**), CCDC-2247951 (**2e**), CCDC-2041984 (**3a**), CCDC-2247952 (**3b**), CCDC-2247953 (**3c**), CCDC-2041985 (**4**), CCDC-2041986 (**5**), CCDC-2247954 (**6'**), CCDC-2247955 (**7**), and CCDC-2247956 (**8**), contain the supplementary crystallographic data for this paper. These data can be obtained free of charge at www.ccdc.cam.ac.uk/conts/retrieving.html (or from the Cambridge Crystallographic Data Centre, 12 Union Road, Cambridge CB2 1EZ, UK; Fax: + 44-1223-336-033; e-mail: deposit@ccdc.cam.ac.uk).

Table S15. Crystallographic details of **1c** and **2a-d**.

Compound	1c	2a	2b	2c	2d
CCDC Formula	2247948 C ₃₄ H ₅₂ FeKO ₇ P ₅	2041983 C ₁₇ H ₃₀ BrFeP ₅	2247949 C ₁₄ H ₂₄ BrFeP ₅	2247950 C ₁₉ H ₂₃ FeP ₅	2041982 C _{14.75} H _{23.55} FeN _{0.95} P ₅
$D_{\text{calc}}/\text{g cm}^{-3}$	1.364	1.558	1.595	1.455	1.425
μ/mm^{-1}	6.192	2.816	12.027	9.316	1.160
Formula Weight	1645.11	525.02	482.94	462.07	424.89
Colour	Metallic dark green	dark brown	dark red	green	clear dark brown
Shape	Block	needle	plate	plate-shaped	block
Size/mm ³	0.37×0.15×0.11	0.27×0.10×0.07	0.21×0.12×0.03	0.39×0.21×0.06	0.33×0.20×0.17
T/K	123.00	123(1)	122.9(2)	123.00(10)	123
Crystal System	monoclinic	monoclinic	orthorhombic	monoclinic	monoclinic
Flack Parameter	/	/	-0.008(7)	/	/
Hooft Parameter	/	/	-0.003(5)	/	/
Space Group	<i>P</i> 2 ₁ / <i>c</i>	<i>P</i> 2 ₁ / <i>m</i>	<i>P</i> 2 ₁ 2 ₁ 2 ₁	<i>P</i> 2 ₁ / <i>n</i>	<i>P</i> 2 ₁ / <i>c</i>
<i>a</i> /Å	20.3442(5)	11.2089(5)	8.1330(2)	9.53044(5)	14.2369(3)
<i>b</i> /Å	26.2921(5)	11.4407(4)	9.6956(2)	14.14435(7)	9.0210(2)
<i>c</i> /Å	15.0828(3)	18.1308(8)	25.5069(6)	16.21683(8)	16.3159(5)
<i>a</i> °	90	90	90	90	90
<i>b</i> °	96.721(2)	105.764(4)	90	105.2398(5)	109.044(3)
<i>g</i> °	90	90	90	90	90
V/Å ³	8012.2(3)	2237.60(17)	2011.33(8)	2109.183(19)	1980.78(9)
<i>Z</i>	4	4	4	4	4
<i>Z'</i>	2	1	1	1	1
Wavelength/Å	1.54184	0.71073	1.54184	1.54184	0.71073
Radiation type	CuK _α	MoK _α	CuK _α	CuK _α	MoK _α
$Q_{\min}/^{\circ}$	3.362	3.499	3.466	4.213	3.231
$Q_{\max}/^{\circ}$	66.600	32.281	74.916	74.357	32.255
Measured Refl's.	41460	13109	6543	51123	19036
Ind't Refl's	14019	7434	3431	4256	6439
Refl's with $ I > 2(I)$	10664	6052	3190	4200	5702
R_{int}	0.0652	0.0222	0.0322	0.0337	0.0189
Parameters	1010	255	259	232	214
Restraints	279	0	69	0	0
Largest Peak	0.659	1.046	0.888	0.858	1.173
Deepest Hole	-0.535	-0.440	-1.150	-0.435	-0.490
GooF	1.085	1.064	1.071	1.074	1.051
wR ₂ (all data)	0.1963	0.0807	0.1398	0.0801	0.0883
wR ₂	0.1829	0.0752	0.1361	0.0799	0.0851
R_1 (all data)	0.0981	0.0483	0.0551	0.0289	0.0385
R_1	0.0754	0.0349	0.0510	0.0287	0.0328

Table S16. Crystallographic details of **2e**, **3a-c** and **4**.

Compound	2e	3a	3b	3c	4
CCDC Formula	2247951 C ₁₈ H ₃₂ BrFeP ₅	2041984 C _{40.5} ClFe ₂ H ₇₆ P ₁₀	2247952 C ₂₅ H ₄₂ Fe ₂ P ₁₀	2247953 C _{27.5} Cl ₃ Fe ₂ H ₄₇ P ₁₀	2041985 C ₂₈ H ₄₈ Fe ₂ P ₁₀
D _{calc} / g cm ⁻³	1.493	1.432	1.470	1.460	1.443
μ/mm ⁻¹	10.146	1.037	11.252	11.265	10.494
Formula Weight	539.04	1019.86	763.98	905.40	806.06
Colour	black	dark green	brownish green	green	dark green
Shape	sticks	block	plate-shaped	plate-shaped	needle
Size/mm ³	0.89×0.125×0.096	0.57×0.32×0.29	0.33×0.05×0.03	0.23×0.11×0.03	0.50×0.12×0.09
T/K	122.9(2)	123(1)	123.01(10)	123.00(10)	123(1)
Crystal System	monoclinic	monoclinic	monoclinic	monoclinic	triclinic
Flack Parameter	/	/	/	/	/
Hooft Parameter	/	/	/	/	/
Space Group	P2 ₁ /n	P2 ₁ /c	P2 ₁ /c	P2 ₁ /n	P-1
a/Å	14.6139(4)	15.5101(3)	14.3913(2)	8.6991(2)	8.8375(4)
b/Å	8.2362(3)	12.8109(2)	8.09300(10)	9.0109(2)	14.5973(7)
c/Å	20.3049(5)	24.2981(3)	30.4026(3)	26.6182(8)	16.2499(8)
a°	90	90	90	90	63.684(5)
b°	101.048(2)	101.4490(10)	102.9490(10)	99.170(3)	89.773(4)
g°	90	90	90	90	81.732(4)
V/Å ³	2398.66(13)	4731.92(13)	3450.91(7)	2059.85(9)	1855.28(17)
Z	4	4	4	2	2
Z'	1	1	1	0.5	1
Wavelength/Å	1.54184	0.71073	1.54184	1.54184	1.54184
Radiation type	CuK _α	MoK _α	CuK _α	CuK _α	CuK _α
Q _{min} /°	4.1160	3.370	2.983	5.157	5.069
Q _{max} /°	75.0100	34.549	75.279	74.066	71.725
Measured Refl's.	8203	55081	36548	15304	12816
Ind't Refl's	4840	18675	6922	3980	7024
Refl's with I > 2(l)	4136	13489	6330	3136	6125
R _{int}	0.0757	0.0309	0.0353	0.0622	0.0289
Parameters	289	525	441	273	375
Restraints	84	126	120	52	0
Largest Peak	1.772	1.098	0.851	0.827	0.555
Deepest Hole	-0.758	-0.448	-0.571	-0.371	-0.543
GooF	1.055	1.026	1.044	1.082	1.030
wR ₂ (all data)	0.1862	0.1252	0.1255	0.1626	0.0919
wR ₂	0.1764	0.1141	0.1226	0.1532	0.0870
R ₁ (all data)	0.0761	0.0687	0.0509	0.0655	0.0434
R ₁	0.0678	0.0458	0.0471	0.0532	0.0356

Table S17. Crystallographic details of **5**, **6'**, **7** and **8**.

Compound	5	6'	7	8
CCDC Formula	2041986 C ₂₉ H ₄₀ FeP ₆	2247954 C ₂₁ H ₂₉ PS	2247955 C ₁₈ H ₂₇ FeN ₂ P ₅	2247956 C ₁₈ H ₂₇ Br ₂ FeN ₂ P ₅ Zn
<i>D</i> _{calc} / g cm ⁻³	1.322	1.158	1.443	1.775
<i>m/mm⁻¹</i>	6.812	2.178	1.046	11.978
Formula Weight	630.28	344.47	482.11	707.30
Colour	dark green	colourless	dark brown	green
Shape	block	block-shaped	block	plate-shaped
Size/mm ³	0.30×0.18×0.15	0.20×0.09×0.05	0.28×0.22×0.18	0.11×0.07×0.02
T/K	123(1)	99.99(10)	123(1)	100.02(10)
Crystal System	triclinic	monoclinic	monoclinic	monoclinic
Flack Parameter	/	/	/	/
Hooft Parameter	/	/	/	/
Space Group	<i>P</i> -1	<i>P</i> 2 ₁ / <i>c</i>	<i>P</i> 2 ₁ / <i>c</i>	<i>P</i> 2 ₁ / <i>c</i>
<i>a</i> /Å	11.7026(6)	13.5196(3)	12.6279(3)	20.1798(6)
<i>b</i> /Å	14.3826(5)	6.25270(10)	13.0636(3)	9.3717(3)
<i>c</i> /Å	18.9471(7)	23.3769(6)	13.8564(3)	14.2681(4)
<i>a</i> °	85.336(3)	90	90	90
<i>b</i> °	85.053(4)	91.391(2)	103.793(2)	101.165(3)
<i>g</i> °	88.352(4)	90	90	90
V/Å ³	3165.9(2)	1975.56(7)	2219.92(9)	2647.30(14)
<i>Z</i>	4	4	4	4
<i>Z'</i>	2	1	1	1
Wavelength/Å	1.54184	1.54184	0.71073	1.54184
Radiation type	CuK _α	CuK _α	MoK _α	CuK _α
<i>Q</i> _{min} /°	3.726	3.270	3.322	4.467
<i>Q</i> _{max} /°	73.574	74.458	32.430	74.907
Measured Refl's.	32841	19848	20964	9190
Ind't Refl's	12335	3959	7231	9190
Refl's with I > 2(l)	9948	3575	6242	7281
<i>R</i> _{int}	0.0356	0.0250	0.0216	.
Parameters	1206	212	258	268
Restraints	753	0	6	0
Largest Peak	0.670	0.662	0.519	0.909
Deepest Hole	-0.766	-0.300	-0.294	-1.155
GooF	1.068	1.047	1.037	1.109
w <i>R</i> ₂ (all data)	0.1471	0.1110	0.0729	0.1533
w <i>R</i> ₂	0.1432	0.1075	0.0693	0.1448
<i>R</i> ₁ (all data)	0.0737	0.0473	0.0377	0.0705
<i>R</i> ₁	0.0626	0.0427	0.0293	0.0542

[K(18c6)(THF)][Cp*Fe(η^4 -P₅-C≡CPh)] (1c)

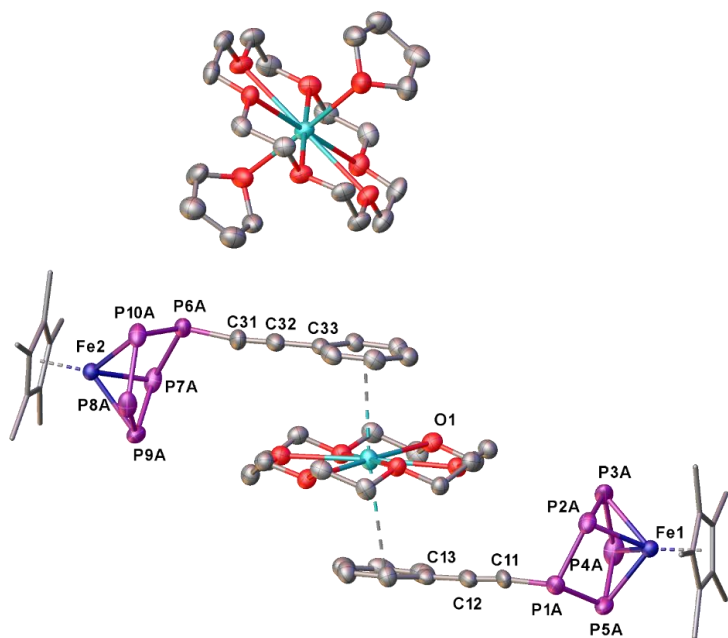


Fig. S34. Molecular structure of **1c** with thermal ellipsoids at 50% probability level. The hydrogen atoms are omitted for clarity. The Cp* ligands are drawn in the wire frame model.

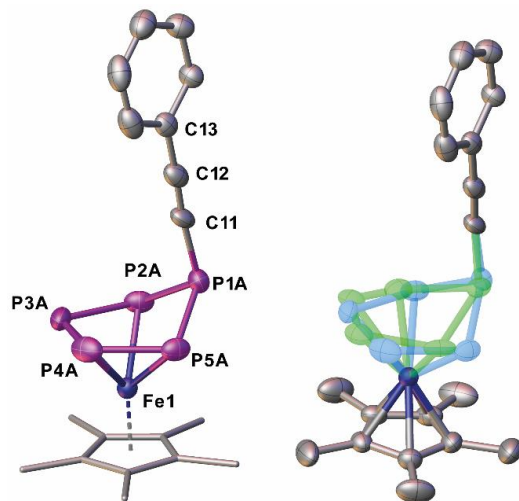


Fig. S35. Side view of the molecular structure of **1c** with thermal ellipsoids at 50 % probability level. The disorder is highlighted blue (Part 1) and green (Part 2). The hydrogen atoms are omitted for clarity. The Cp* ligand is drawn in the wire frame model.

Table S18. Selected bond lengths of **1c**.

Atom-Atom	Length [Å]
P1A-P2A	2.142(5)
P1A-P5A	2.162(3)
P2A-P3A	2.187(3)
P3A-P4A	2.127(4)

Atom-Atom	Length [Å]
P1A-C11	1.782(7)
Fe1-P2A	2.322(3)
Fe1-P3A	2.312(2)
Fe1-P4A	2.338(2)

P4A-P5A	2.142(3)
---------	----------

Fe1-P5A	2.317(2)
---------	----------

Table S19. Selected angles of **1c**.

Atom-Atom-Atom	Angle [°]
P5A-P1A-P2A	93.56(16)
P3A-P2A-P1A	107.09(16)
P4A-P3A-P2A	103.14(13)

Atom-Atom-Atom	Angle [°]
P3A-P4A-P5A	103.82(11)
P4A-P5A-P1A	107.18(14)

[Cp*Fe{η⁴-P₅'Bu(CH₂)₃Br}] (2a)

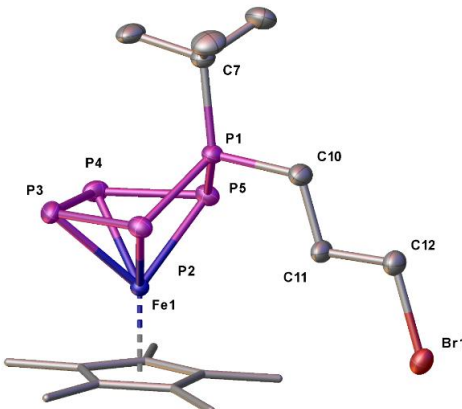


Fig. S36. Molecular structure of **2a** with thermal ellipsoids at 50% probability level. The hydrogen atoms are omitted for clarity. The Cp* ligand is drawn in the wire frame model.

Table S20. Selected bond lengths of **2a**.

Atom-Atom	Length [Å]
P1-P2	2.1580(7)
P2-P3	2.1461(8)
P3-P4	2.1594(11)
P4-P5	2.1461(8)
P1-P5	2.1580(7)
P1-C7	1.871(3)
C12-Br1	1.950(3)

Atom-Atom	Length [Å]
Fe1-P2	2.3425(6)
Fe1-P3	2.3334(6)
Fe1-P4	2.3334(6)
Fe1-P5	2.3425(6)
Fe1-P1	3.1105(9)
P1-C10	1.838(3)

Table S21. Selected angles of **2a**.

Atom-Atom-Atom	Angle [°]
P1-P2-P3	99.57(3)
P2-P3-P4	104.662(19)
P4-P5-P1	99.57(3)
P5-P1-C10	120.16(5)
C10-P1-C12	103.94(14)

Atom-Atom-Atom	Angle [°]
P3-P4-P5	104.662(19)
P5-P1-P2	97.53(4)
P5-P1-C7	120.16(5)
P2-P1-C7	120.16(5)
P2-P1-C10	107.04(7)

[Cp*Fe{η⁴-P₅Me(CH₂)₃Br}] (2b)

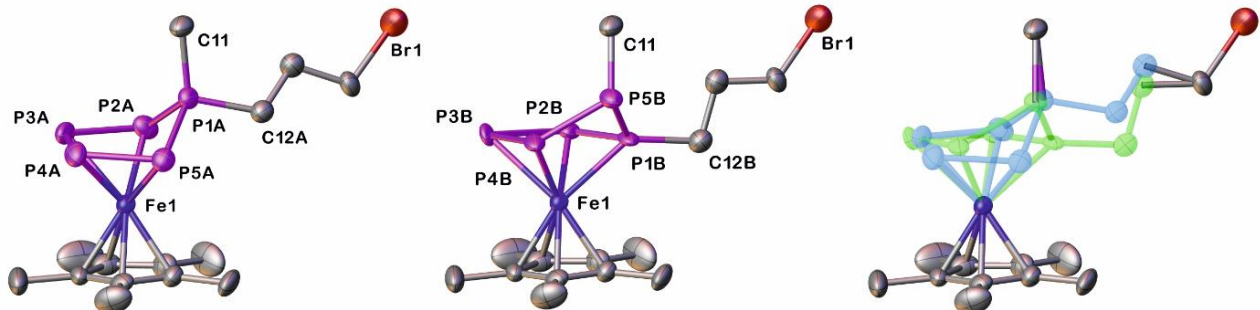


Fig. S37. Molecular structure of **2b** (left part) and **2b'** (middle part) with thermal ellipsoids at 50% probability level. The hydrogen atoms are omitted for clarity. The disorder is highlighted blue (Part 1) and green (Part 2). The Cp* ligands are drawn in the wire frame model.

Table S22. Selected bond lengths of **2b** and **2b'**.

Atom-Atom	Length [Å]	Atom-Atom	Length [Å]
Part 1 – 2b			Part 2 – 2b'
P1A-P2A	2.129(3)	P1B-P2B	2.07(4)
P1A-P5A	2.142(3)	P1B-P5B	2.11(3)
P2A-P3A	2.147(4)	P2B-P3B	2.34(8)
P3A-P4A	2.143(11)	P3B-P4B	2.33(8)
P4A-P5A	2.119(9)	P4B-P5B	2.18(3)
P1A-C11	1.817(8)	P1B-C12B	1.84(3)
P1A-C12A	1.842(9)		

Table S23. Selected angles of **2b** and **2b'**.

Atom-Atom-Atom	Angle [°]	Atom-Atom-Atom	Angle [°]
Part 1 – 2b			Part 2 – 2b'
P5A-P1A-P2A	98.89(14)	P7-P8B-P9B	98.3(4)
P3A-P2A-P1A	99.49(14)	P8B-P9B-P10B	106.1(6)
P4A-P3A-P2A	103.9(2)	P9B-P10B-P11B	101.6(8)
P3A-P4A-P5A	106.0(3)	P11B-P7-P8B	91.9(8)
P4A-P5A-P1A	99.1(3)	P8B-P7-C30	129.2(3)

[Cp*Fe{η⁴-P₅(-C≡CPh)Me}] (2c)

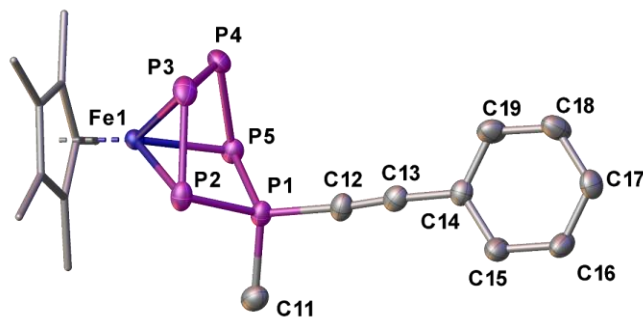


Fig. S38. Molecular structure of **2c** with thermal ellipsoids at 50% probability level. The hydrogen atoms are omitted for clarity. The Cp* ligand is drawn in the wire frame model.

Table S24. Selected bond lengths of **2c**.

Atom-Atom	Length [Å]
P1-P5	2.1405(6)
P1-P2	2.1425(6)
P1-C12	1.7582(18)
P1-C11	1.821(2)

Atom-Atom	Length [Å]
P2-P3	2.1419(7)
P4-P4	2.1538(7)
C13-C12	1.197(3)
P5-P4	2.1399(6)

Table S25. Selected angles of **2c**.

Atom-Atom-Atom	Angle [°]
P5-P1-P2	93.56(16)
C12-P1-P5	107.09(16)
C12-P1-P2	103.14(13)

Atom-Atom-Atom	Angle [°]
C12-P1-C11	103.82(11)
C11-P1-P5	107.18(14)
P1-C12-C13	175.74(18)

[Cp*Fe{η⁴-P₅Me(CH₂)₃CN}] (2d)

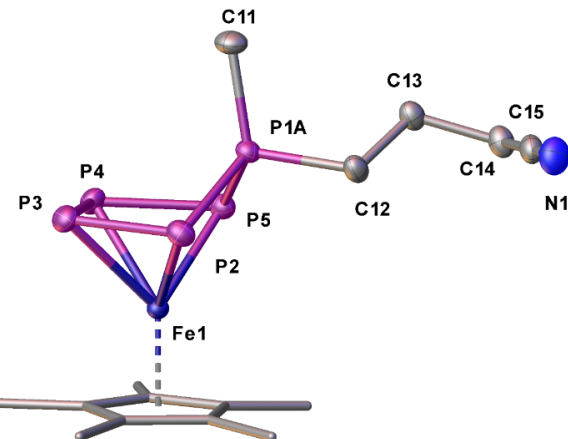


Fig. S39. Molecular structure of **2d** with thermal ellipsoids at 50% probability level. The hydrogen atoms are omitted for clarity. The Cp* ligand is drawn in the wire frame model.

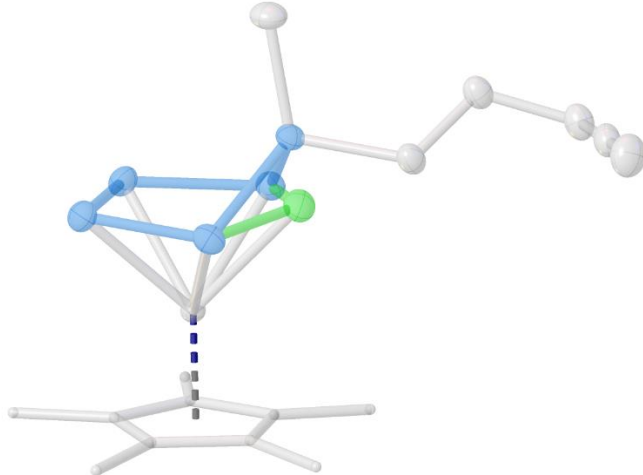


Fig. S40. Side view of the mixed crystal of **I** and **2d** with thermal ellipsoids at 50% probability level. The disordered P_5 middle decks are highlighted green (**I**) and blue (**3a**). The Cp^* ligand is drawn in the wire frame model.

Table S26. Selected bond lengths of **2d**.

Atom-Atom	Length [Å]
P1A–P2	2.1462(6)
P2–P3	2.1465(6)
P3–P4	2.1589(6)
P4–P5	2.1384(6)
P1A–P5	2.1499(5)
P1A–C11	1.8214(17)
N1–C15	1.142(2)

Atom-Atom	Length [Å]
Fe1–P2	2.3340(4)
Fe1–P3	2.3355(4)
Fe1–P4	2.3422(4)
Fe1–P5	2.3199(5)
Fe1–P1A	3.0591(5)
P1–C12	1.8284(16)

Table S27. Selected angles of **2d**.

Atom-Atom-Atom	Angle [°]
P1A–P2–P3	97.27(2)
P2–P3–P4	105.34(2)
P4–P5–P1	105.8(3)
P5–P1A–C11	118.98(6)
C10–P1A–C12	106.50(8)

Atom-Atom-Atom	Angle [°]
P3–P4–P5	104.28(2)
P5–P1A–P2	98.48(2)
P5–P1A–C11	118.98(6)
P5–P1A–C12	106.70(6)
P2–P1A–C11	118.07(6)

[Cp*Fe{η⁴-P₅Me(CH₂)₄Br}] (2e)

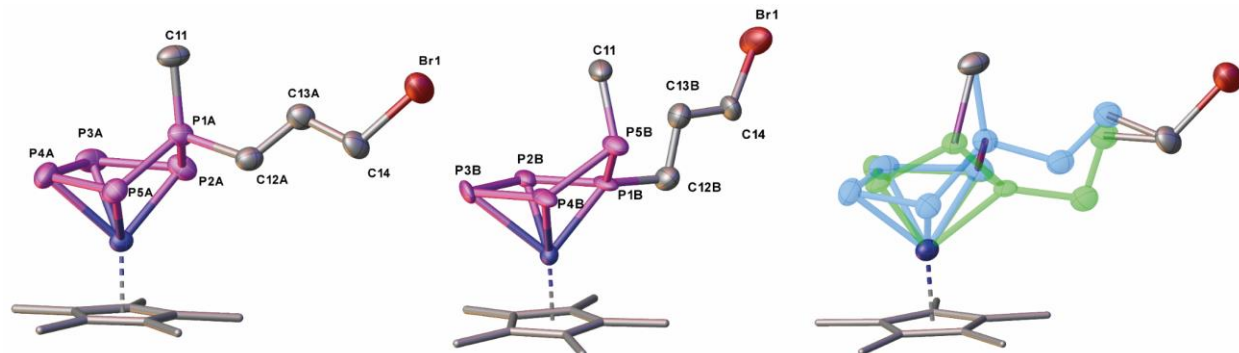


Fig. S41. Molecular structure of **2e** (left part) and **2e'** (middle part) with thermal ellipsoids at 50% probability level. The hydrogen atoms are omitted for clarity. The disorder is highlighted blue (Part 1) and green (Part 2). The Cp* ligands are drawn in the wire frame model.

Table S28. Selected bond lengths of **2e** and **2e'**.

Atom-Atom	Length [Å]	Atom-Atom	Length [Å]		
Part 1 – 2e			Part 2 – 2e'		
P1A-P2A	2.142(3)	C11-P5B	1.88(2)		
P1A-P5A	2.129(3)	C12A-C13A	1.526(14)		
P1A-C11	1.817(8)	P4B-P5B	2.18(3)		
P1A-C12A	1.842(9)	P5B-P1B	2.11(3)		
P2A-P3A	2.119(9)	P1B-P2B	2.07(4)		
P3A-P4A	2.143(11)	P1B-C12B	1.84(3)		
P5A-P4A	2.147(4)	C14-Br1	1.938(8)		

Table S29. Selected angles of **2e** and **2e'**.

Atom-Atom-Atom	Angle [°]	Atom-Atom-Atom	Angle [°]		
Part 1 – 2e			Part 2 – 2e'		
P5A-P1A-P2A	98.89(14)	P5B-P4B-P3B	115(3)		
C11-P1A-P2A	120.0(3)	C11-P5B-P4B	117.6(13)		
C11-P1A-P5A	117.8(4)	C11-P5B-P1B	100.2(12)		
C11-P1A-C12A	107.5(4)	P1B-P5B-P4B	84.8(11)		
C12A-P1A-P2A	106.6(3)	C13B-C12B-P1B	103(3)		

$[(\text{Cp}^*\text{Fe})_2\{\mu,\eta^{4:4}\text{-P}_5^t\text{Bu}(\text{CH}_2)_3\text{P}_5^t\text{Bu}\}]$ (3a)

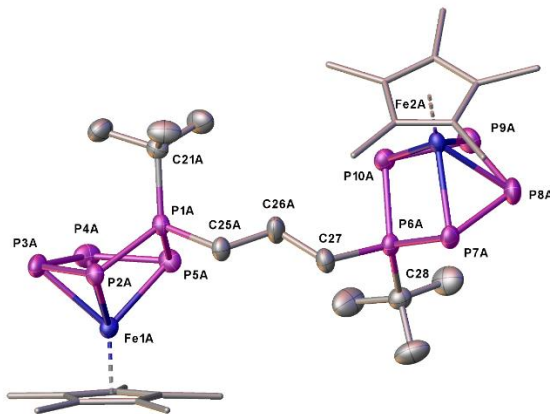


Fig. S42. Molecular structure of 3a with thermal ellipsoids at 50% probability level. The hydrogen atoms are omitted for clarity. The Cp^* ligands are drawn in the wire frame model.

$[(\text{Cp}^*\text{Fe})_2\{\mu,\eta^{4:4}\text{-P}_5^t\text{Bu}(\text{CH}_2)_3\text{P}_5^t\text{Bu}\}]$ (3a')

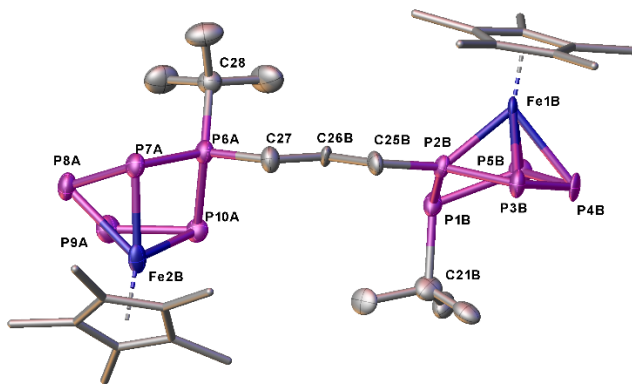


Fig. S43. Molecular structure of 3a' with thermal ellipsoids at 50% probability level. The hydrogen atoms are omitted for clarity. The Cp^* ligands are drawn in the wire frame model.

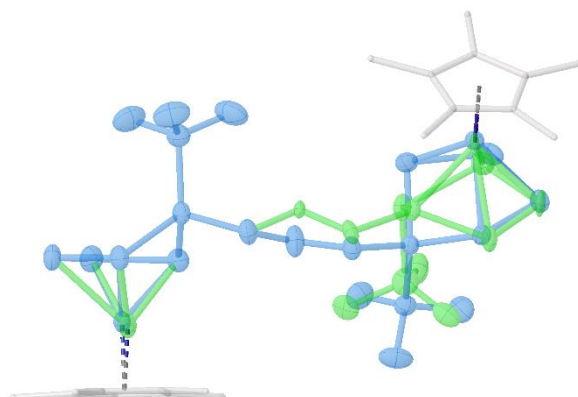


Fig. S44. Molecular structure of 3a, highlighted blue (Part 1), and 3a', highlighted green (Part 2), with thermal ellipsoids at 50 % probability level. The hydrogen atoms and solvent molecules are omitted for clarity.

Table S30. Selected bond lengths of **3a** and **3a'**.

Atom-Atom	Length [Å]	Atom-Atom	Length [Å]
Part 1 – 3a		Part 1 – 3a'	
P1A–P2A	2.1514(9)	P6A–P7A	2.1503(7)
P2A–P3A	2.1422(15)	P7A–P8A	2.1419(8)
P3A–P4A	2.1518(18)	P8A–P9A	2.1499(9)
P4A–P5A	2.1422(11)	P9A–P10A	2.1361 (8)
P1A–P5A	2.1454(7)	P6A–P10A	2.1508(7)
P1A–C21A	1.876(2)	P6A–C28	1.870(2)
P1A–C25A	1.847(2)	P6A–C21	1.848(2)
Part 2 – 3a'		Part 2 – 3a'	
P1B–P2B	2.098(9)	P6A–P7A	2.1503(7)
P2B–P3B	2.140(10)	P7A–P8A	2.1419(8)
P3B–P4B	2.179(19)	P8A–P9A	2.1499(9)
P4B–P5B	2.140(18)	P9A–P10A	2.1361 (8)
P1B–P5B	2.213(12)	P6A–P10A	2.1508(7)
P1B–C21B	1.98(3)	P6A–C28	1.870(2)
P2B–C25B	1.84 (2)	P6A–C21	1.848(2)

Table S31. Selected angles of **3a** and **3a'**.

Atom-Atom-Atom	Angle [°]	Atom-Atom-Atom	Angle [°]
Part 1 – 3a		Part 1 – 3a'	
P1A–P2A–P3A	100.49(5)	P6A–P7A–P8A	100.91(3)
P2A–P3A–P4A	104.81(4)	P8A–P9A–P10A	105.20(3)
P1A–P5A–P2A	98.58(3)	P9A–P10A–P6A	100.71(3)
P2A–P1A–C21A	120.23(7)	P7A–P6A–C28	119.33(7)
P2A–P1A–C25A	104.01(8)	C27–P6A–C28	106.91(10)
P5A–P1A–C21A	118.92(7)	C21A– P1A–C25A	108.59(10)
Part 2 – 3a'		Part 2 – 3a'	
P6A–P7A–P8A	100.91(3)	P1B–P2B–P3B	119.5(4)
P7A–P8A–P9A	105.20(3)	P2B–P3B–P4B	95.1(6)
P9A–P10A–P6A	100.71(3)	P4B–P5B–P1B	111.3(7)
P7A–P6A–C28	119.33(7)	P2B–P1B–C21B	111.9(9)
C27–P6A–C28	106.91(10)	P2B–P1B–C25B	114.4(9)
C21A– P1A–C25A	108.59(10)	P5B–P1B–C21B	113.9(10)

[(Cp*Fe)₂{ μ , $\eta^{4:4}$ -P₅Me(CH₂)₃P₅Me}] (3b)

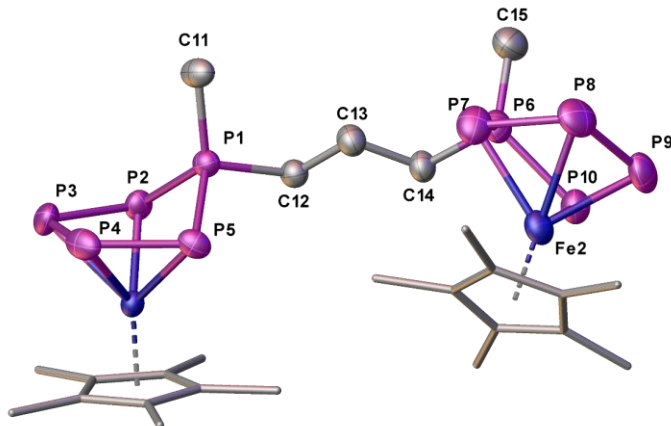


Fig. S45. Molecular structure of **3b** with thermal ellipsoids at 50% probability level. The hydrogen atoms are omitted for clarity. The Cp* ligands are drawn in the wire frame model.

Table S32. Selected bond lengths of **3b**.

Atom-Atom	Length [Å]
P1-P2	2.1407(12)
P2-P5	2.1417(11)
P2-P3	2.1394(13)
P1-C11	1.816(3)
P6-C14	1.829(3)
P6-C15	1.814(4)
P7-P8	2.1360(16)

Atom-Atom	Length [Å]
P1-C12	1.824(3)
P4-P5	2.1358(14)
P6-P10	2.1488(14)
P6-P7	2.1290(15)
P9-P10	2.1361(14)
P3-P4	2.1488(16)
P9-P8	2.1434(19)

Table S33. Selected angles of **3b**.

Atom-Atom-Atom	Angle [°]
P2-P1-P5	98.46(4)
C12-P1-P2	105.49(11)
C12-P1-P5	105.89(11)
C11-P1-P2	119.77(14)
C11-P1-P5	119.09(12)
C14-P6-P7	106.83(12)
C15-P6-P7	118.38(16)

Atom-Atom-Atom	Angle [°]
C11-P1-C12	106.74(15)
P1-P2-P3	99.61(5)
P5-P4-P1	99.46(5)
P6-P7-P10	100.00(6)
C14-P6-P10	103.83(12)
C15-P6-P10	121.22(16)
C15-P6-C14	105.10(18)

[(Cp*Fe)₂{ μ , $\eta^{4:4}$ -P₅Me(CH₂)₄P₅Me}] (3c)

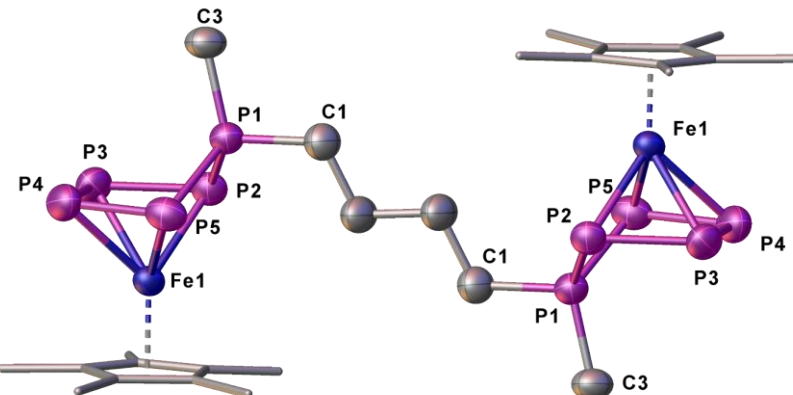


Fig. S46. Molecular structure of **3c** with thermal ellipsoids at 50% probability level. The hydrogen atoms are omitted for clarity. The Cp* ligands are drawn in the wire frame model.

Table S34. Selected bond lengths of **3c**.

Atom-Atom	Length [Å]
P1-P2	2.1479(14)
P1-P5	2.1419(13)
P1-C3	1.812(4)
P1-C1	1.826(4)

Atom-Atom	Length [Å]
P2-P3	2.1356(15)
P3-P4	2.1620(17)
P4-P5	2.1523(18)

Table S35. Selected angles of **3e**.

Atom-Atom-Atom	Angle [°]
P2-P1-P5	97.01(5)
C3-P1-P2	117.83(15)
C3-P1-P5	118.61(15)
C3-P1-C1	102.88(19)
P3-P2-P1	97.95(6)

Atom-Atom-Atom	Angle [°]
P2-P3-P4	104.18(6)
P1-P5-P4	97.69(6)
P5-P4-P3	104.19(6)
C1-P1-P2	110.59(14)
C1-P1-P5	110.03(14)

$[(\text{Cp}^*\text{Fe})_2\{\mu,\eta^{4:4}\text{-P}_5^\text{tBu}(\text{CH}_2)_3\text{P}_5\text{Me}\}]$ (4)

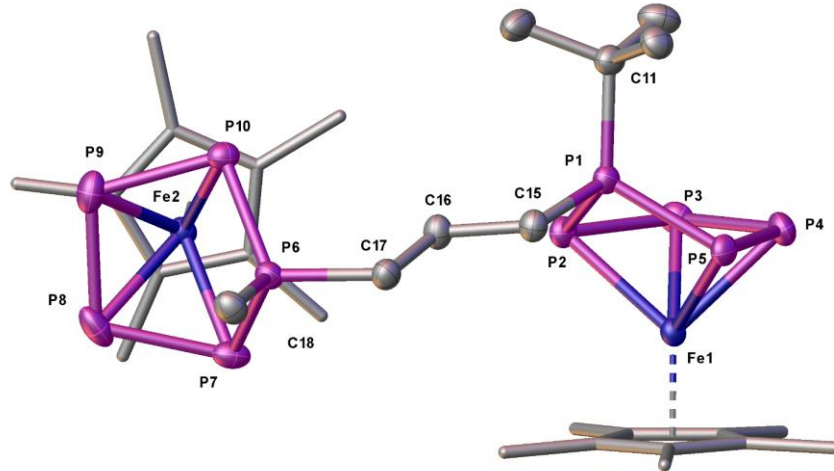


Fig. S47. Molecular structure of **4** with thermal ellipsoids at 50% probability level. The hydrogen atoms are omitted for clarity. The Cp^* ligands are drawn in the wire frame model.

Table S36. Selected bond lengths of **4**.

Atom-Atom	Length [Å]
P1–P2	2.1482(8)
P2–P3	2.1370(9)
P3–P4	2.1484(10)
P4–P5	2.1444(10)
P1–P5	2.1455(9)
P1–C11	1.874(3)
P1–C18	1.817(3)

Atom-Atom	Length [Å]
P6–P7	2.1451(9)
P7–P8	2.1491(11)
P8–P9	2.1639(12)
P9–P10	2.1450(10)
P6–P10	2.1514(9)
P6–C17	1.835(3)
P1–C15	1.849(3)

Table S37. Selected angles of **4**.

Atom-Atom-Atom	Angle [°]
P1–P2–P3	101.02(4)
P2–P3–P4	105.30(4)
P4–P5–P1	100.73(4)
P5–P1–C15	104.54(9)
P2–P1–C15	104.88(9)
C11–P1–C15	107.36(12)
P6–P7–P8	96.71(4)
P7–P8–P9	104.27(4)
P9–P10–P6	97.12(4)
P10–P6–C18	118.35(10)
C18–P6–C17	102.70(13)

Atom-Atom-Atom	Angle [°]
P3–P4–P5	105.16(4)
P5–P1–P2	99.33(3)
P5–P1–C11	117.90(8)
P2–P1–C11	121.08(9)
P2–P1–C15	104.88(9)
P8–P9–P10	103.78(4)
P17–P6–P7	96.46(3)
P17–P6–C18	102.70(13)
P7–P6–C17	111.75(9)
P7–P6–C18	118.35(10)
C17–P6–P10	111.57(9)

[Cp*Fe(η^4 -P₅^tBu(CH₂)₃PPh₂)] (5)

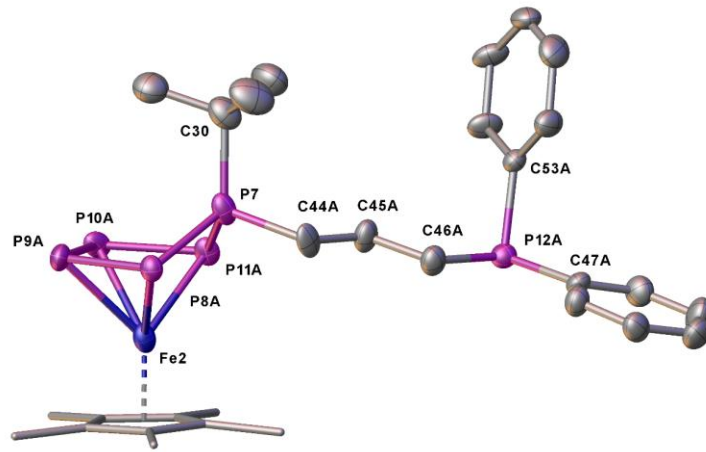


Fig. S48. Molecular structure of **5** with thermal ellipsoids at 50% probability level. The hydrogen atoms are omitted for clarity. The Cp* ligand is drawn in the wire frame model.

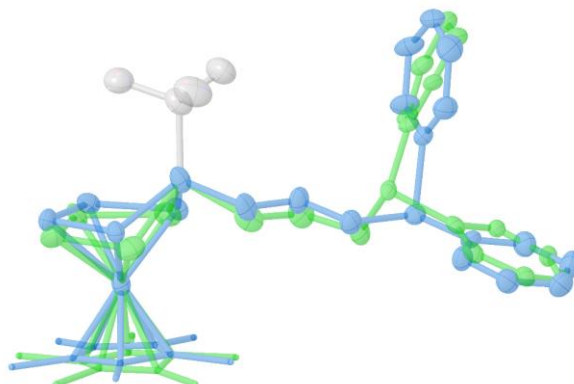


Fig. S49. Molecular structure of **5** with thermal ellipsoids at 50% probability level. The hydrogen atoms are omitted for clarity. The disorder is highlighted blue (Part 1) and green (Part 2). The Cp* ligand is drawn in the wire frame model.

Table S38. Selected bond lengths of **5**.

Atom-Atom	Length [Å]	Atom-Atom	Length [Å]
Part 1		Part 2	
P7-P8A	2.147(3)	P7-P8B	2.205(10)
P8A-P9A	2.139(3)	P8B-P9B	2.130(11)
P9A-P10A	2.148(4)	P9B-P10B	2.123(11)
P10A-P11A	2.137(5)	P10B-P11B	2.134(14)
P7-P11A	2.140(4)	P7-P11B	2.172(14)
P7-C30	1.867(6)	P7-C30	1.867(6)
P7-C44A	1.829(5)	P7-C44B	1.858(19)
P12A-C46A	1.839(6)	P12B-C46B	1.838(18)
P12A-C53A	1.853(6)	P12B-C53B	1.81(3)
P12A-C47A	1.828(5)	P12B-C47B	1.79(3)

Table S39. Selected angles of 5.

Atom-Atom-Atom	Angle [°]	Atom-Atom-Atom	Angle [°]
Part 1			2
P7-P8A-P9A	101.14(12)	P7-P8B-P9B	98.3(4)
P8A-P9A-P10A	104.90(16)	P8B-P9B-P10B	106.1(6)
P9A-P10A-P11A	106.0(2)	P9B-P10B-P11B	101.6(8)
P11A-P7-P8A	100.1(2)	P11B-P7-P8B	91.9(8)
P8A-P7-C30	118.15(19)	P8B-P7-C30	129.2(3)
P11A-P7-C30	119.7(3)	P11B-P7-C30	122.8(9)
C30-P7-C44A	106.7(3)	C30-P7-C44B	117.9(15)
C46A-P12A-C53A	102.4(3)	C46B-P12B-C53B	102.3(15)
C46A-P12A-C47A	102.5(3)	C46B-P12B-C47B	100.5(14)
C47A-P12A-C53A	98.9(3)	C47B-P12B-C53B	102.3(15)

SP^tBuBn((CH₂)₃Bn) (6')

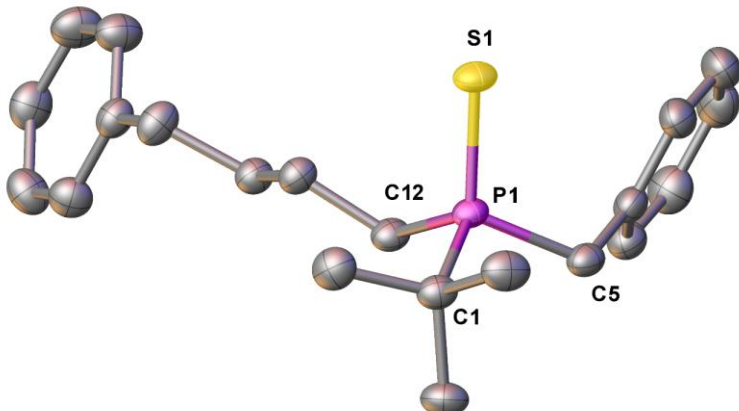


Fig. S50. Molecular structure of 6' with thermal ellipsoids at 50% probability level. The hydrogen atoms are omitted for clarity.

Table S40. Selected bond lengths of 6'.

Atom-Atom	Length [Å]	Atom-Atom	Length [Å]
P1-S1	1.9575(6)	P1-C12	1.8253(18)
P1-C1	1.8600(18)	P1-C5	1.8280(19)

Table S41. Selected angles of 6'.

Atom-Atom-Atom	Angle [°]	Atom-Atom-Atom	Angle [°]
C1-P1-S1	112.49(6)	C12-P1-C5	103.10(8)
C12-P1-S1	112.40(6)	C5-P1-S1	113.49(6)
C12-P1-C1	110.13(8)	C5-P1-C1	104.58(8)

[Cp*Fe{η⁴-P₅((CH₂)₃CN)₂}] (7)

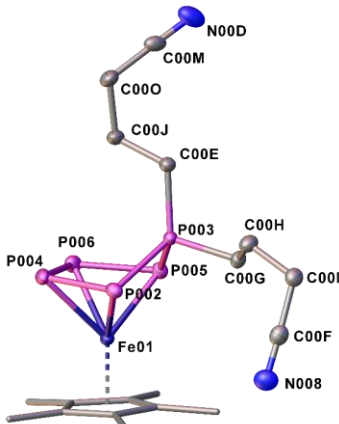


Fig. S51. Molecular structure of **7** with thermal ellipsoids at 50% probability level. The hydrogen atoms are omitted for clarity. The Cp* ligand is drawn in the wire frame model.

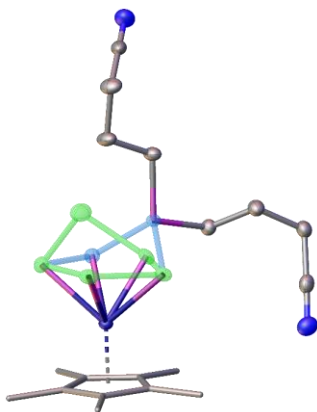


Fig. S52. Molecular structure of **7** with thermal ellipsoids at 50% probability level. The hydrogen atoms are omitted for clarity. The disorder is highlighted blue (Part 1) and green (Part 2). The Cp* ligand is drawn in the wire frame model.

Table S42. Selected bond lengths of **7**.

Atom-Atom	Length [Å]
P002-P003	2.1478(5)
P002-P004	2.1482(5)
P003-P005	2.1498(5)
P003-C00E	1.8341(13)

Atom-Atom	Length [Å]
P003-C00G	1.8360(13)
P004-P006	2.1614(5)
P005-P006	2.1446(5)

Table S43. Selected angles of **7**.

Atom-Atom-Atom	Angle [°]
P003-P002-P004	99.561(19)
P002-P003-P005	98.259(18)
C00E-P003-P002	117.94(5)
C00E-P003-P005	122.24(5)
C00E-P003-C00G	104.96(6)

Atom-Atom-Atom	Angle [°]
C00G-P003-P002	105.14(4)
C00G-P003-P005	106.90(4)
P002-P004-P006	104.727(19)
P005-P006-P004	104.643(19)

[{Cp*Fe{η⁴-P₅((CH₂)₃CN)₂}ZnBr₂

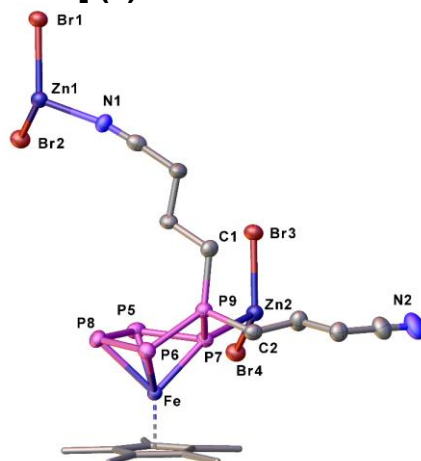


Fig. S53. Molecular structure of **8** with thermal ellipsoids at 50% probability level. The hydrogen atoms are omitted for clarity. The Cp* ligand is drawn in the wire frame model.

Table S44. Selected bond lengths of **8**.

Atom-Atom	Length [Å]
P9-P7	2.141(2)
P7-P5	2.143(3)
P5-P8	2.140(3)
P8-P6	2.137(3)
P6-P9	2.168(2)

Atom-Atom	Length [Å]
N1-Zn1	2.053(6)
Zn1-Br1	2.3533(12)
Zn1-Br2	2.3653(12)
P7-Zn2	2.4296(18)

Table S45. Selected angles of **8**.

Atom-Atom-Atom	Angle [°]
Br1-Zn1-Br2	121.57(5)
Br3-Zn2-P7	106.06(6)
Br4-Zn2-P7	108.40(6)

Atom-Atom-Atom	Angle [°]
N1-Zn1-Br1	109.88(18)
N1-Zn1-Br2	102.69(18)
N1-Zn1-P7	107.60(17)

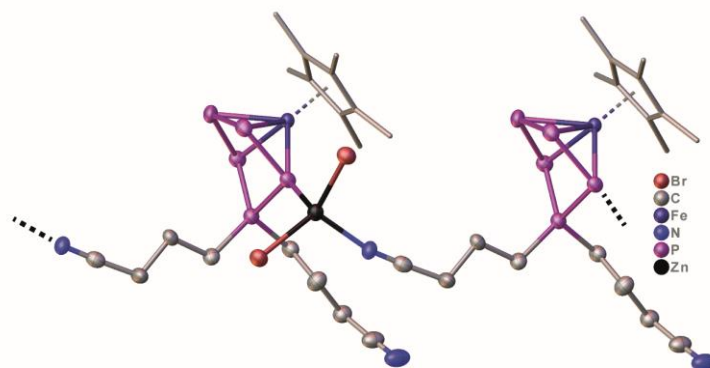
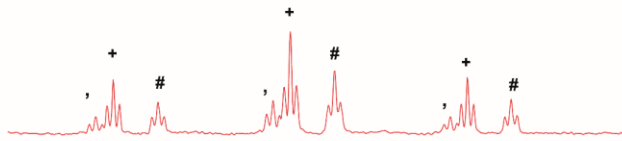


Fig. S54. Molecular structure of **8** as a grown structure with thermal ellipsoids at 50% probability level. The Cp* ligand is drawn in the wire frame model.

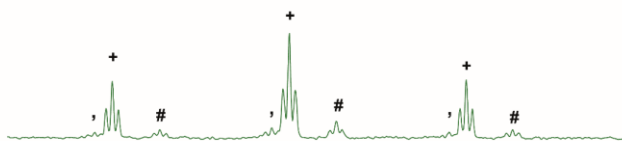
Additional information

NMR Investigations

$^{31}\text{P}\{\text{H}\}$ (THF/C₆D₆ cap); reaction in THF; starting at r.t;
1 eq Br₂(CH₂)₃



$^{31}\text{P}\{\text{H}\}$ (THF)/C₆D₆ cap; reaction in THF; starting at r.t;
10 eq Br₂(CH₂)₃



$^{31}\text{P}\{\text{H}\}$ (C₆D₆); reaction in THF; starting at -80 °C;
1 eq Br₂(CH₂)₃

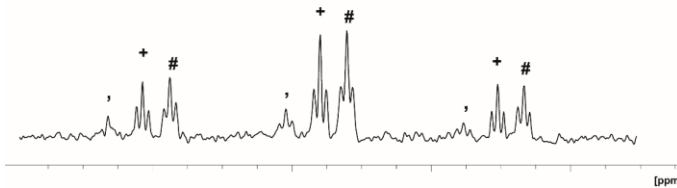
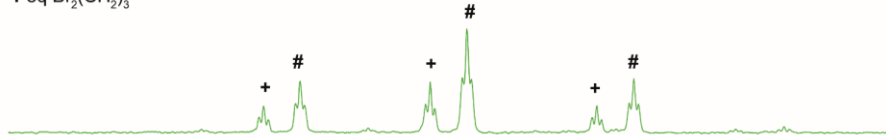
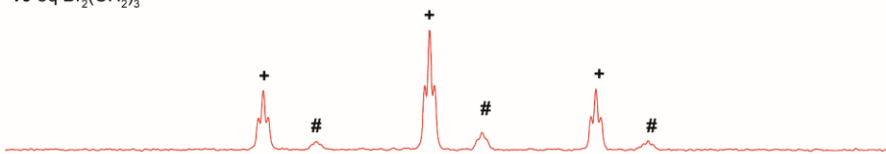


Fig. S55. $^{31}\text{P}\{\text{H}\}$ NMR Spectra (161.98 MHz)/ Cutout: Reaction of **1a** with 1,3-dibromopropane at different reaction conditions (shifts are normalized for better overview) (+ = **2a**; # = **3a**; ' = **3a'**).

$^{31}\text{P}\{\text{H}\}$ (C₆D₆); reaction in THF; starting at -80 °C;
1 eq Br₂(CH₂)₃



$^{31}\text{P}\{\text{H}\}$ (THF)/C₆D₆ cap; reaction in THF; starting at -80 °C;
10 eq Br₂(CH₂)₃



$^{31}\text{P}\{\text{H}\}$ (DME/C₆D₆ cap); reaction in DME; starting at -50 °C;
1 eq Br₂(CH₂)₃

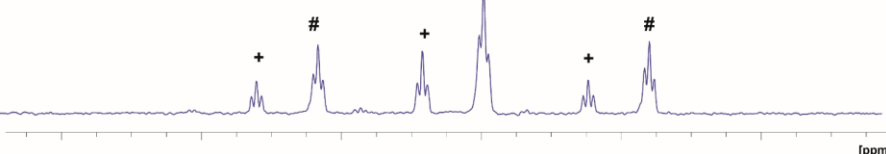


Fig. S56. $^{31}\text{P}\{\text{H}\}$ NMR Spectra (161.98 MHz)/ Cutout: Reaction of **1b** with 1,3-dibromopropane at different reaction conditions (shifts are normalized for better overview) (+ = **2b**; # = **3b**).

$^{31}\text{P}\{\text{H}\}$ (C_6D_6); reaction in THF; starting at -80 °C;
1 eq $\text{Br}_2(\text{CH}_2)_3$

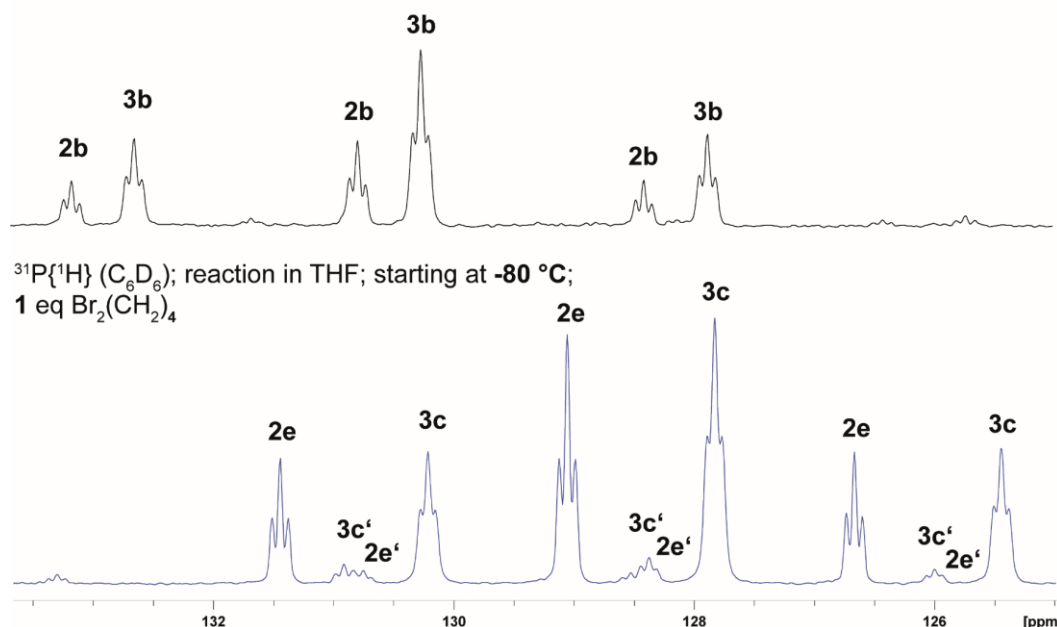


Fig. S57. $^{31}\text{P}\{\text{H}\}$ NMR Spectra (161.98 MHz)/ Cutout: Reaction of **1b** with 1,3-dibromopropane (top) and 1,4-dibromobutane (button).

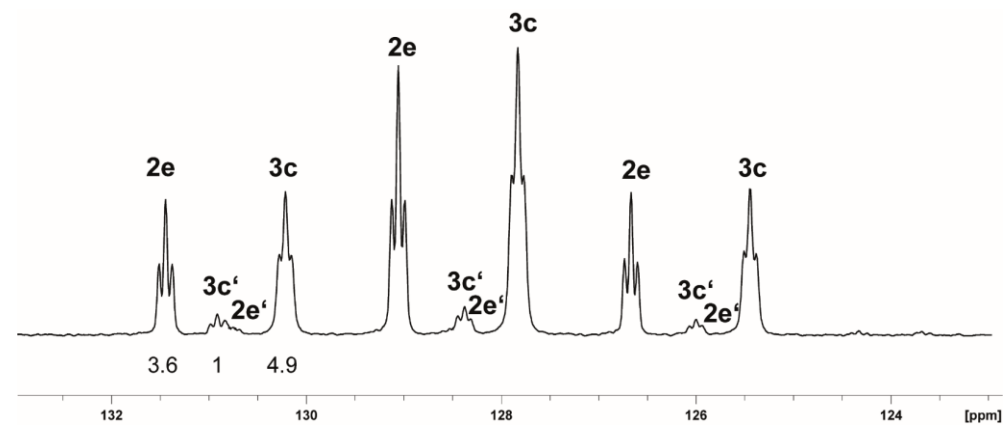


Fig. S58. $^{31}\text{P}\{\text{H}\}$ NMR Spectra (161.98 MHz)/ Cutout: Reaction of **1b** with 1,4-dibromobutane.

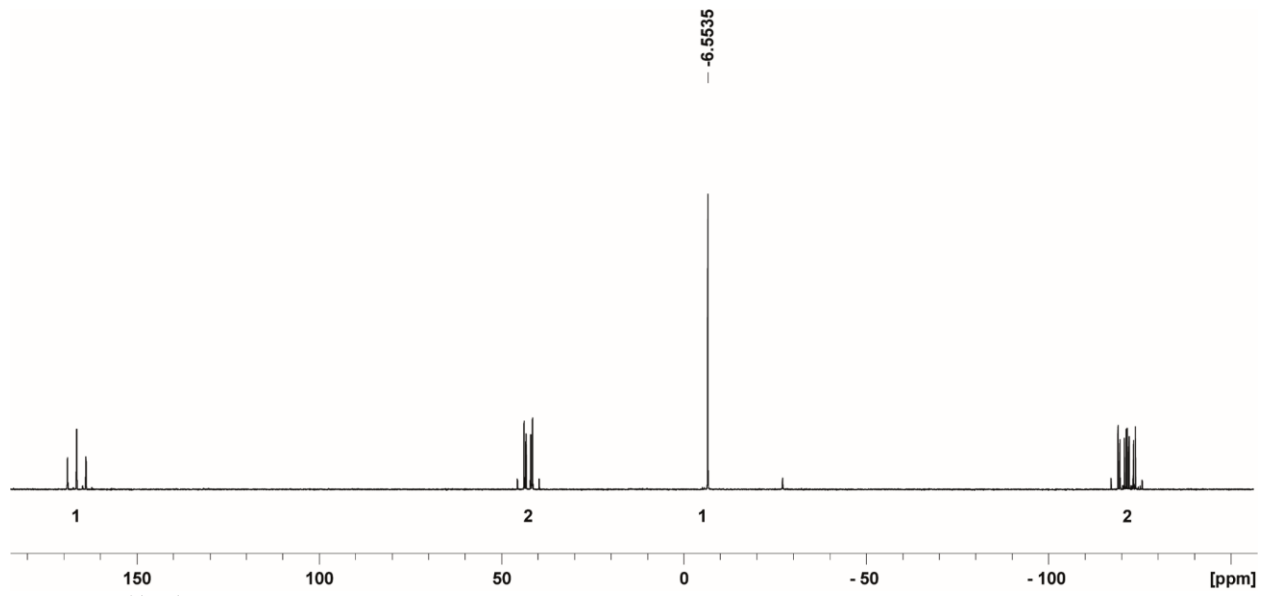


Fig. S59. $^{31}\text{P}\{^1\text{H}\}$ NMR Spectra (161.98 MHz, THF/C₆D₆ capillary): Reaction of **2a** with LiPCy₂.

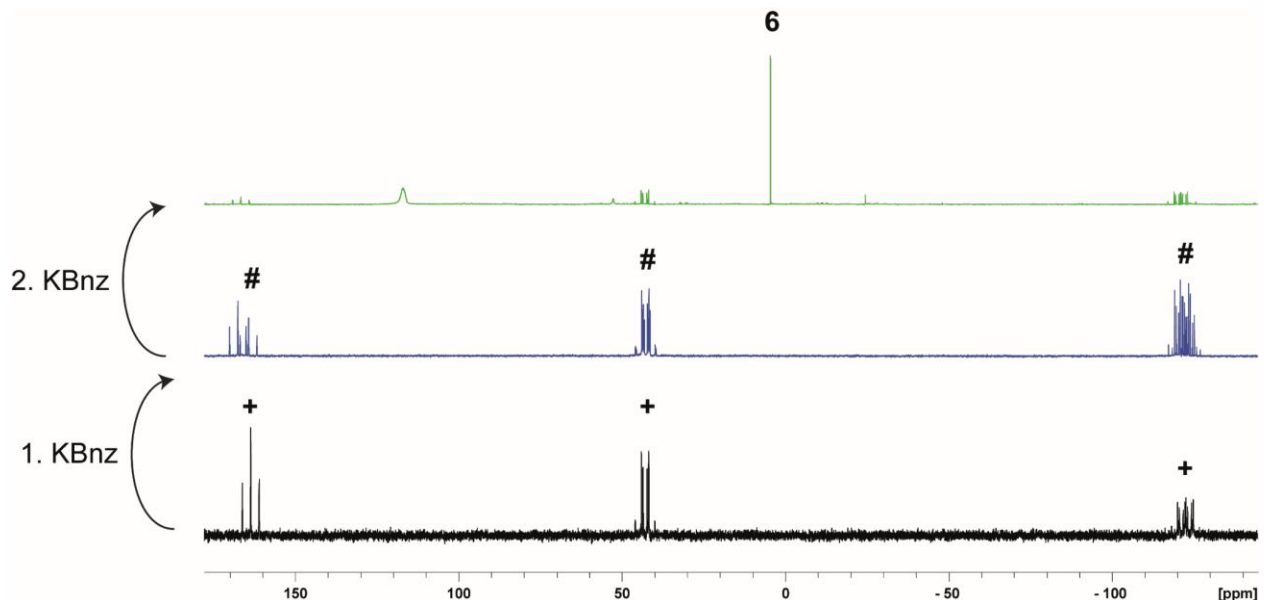


Fig. S60. $^{31}\text{P}\{^1\text{H}\}$ NMR Spectra (161.98 MHz, C₆D₆ or THF/C₆D₆ capillary (middle spectra)): Reaction of **2a** with successive 2 eq KBn (+ = **2a**; # = [$\text{Cp}^*\text{Fe}\{\eta^4\text{-P}_5'\text{Bu}(\text{CH}_2)_3\text{Bn}\}$]).

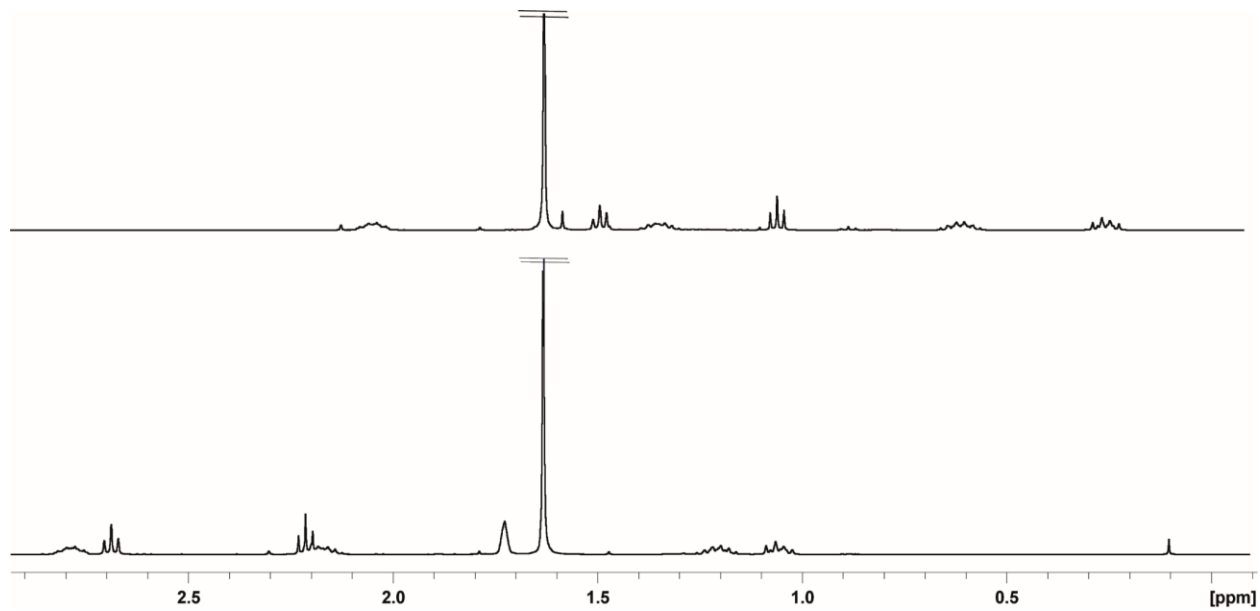


Fig. S61. ¹H NMR Spectra (400.13 MHz)/ Cutout: Complex 7 (top, C₆D₆) and Complex 8 (bottom, THF-d₈).

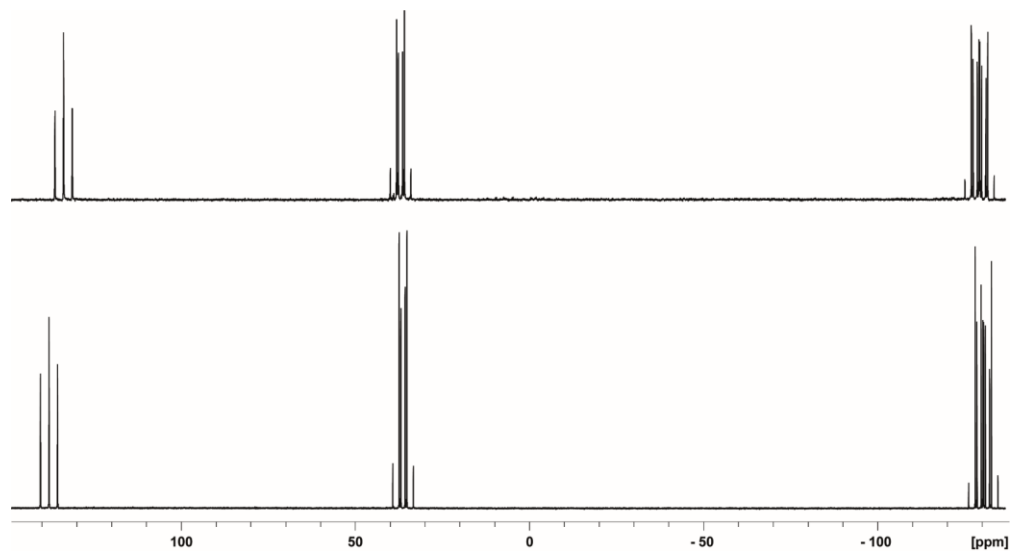


Fig. S62. ³¹P{¹H} NMR Spectra (161.98 MHz): Complex 7 (top, C₆D₆) and Complex 8 (bottom, THF-d₈).

Cyclovoltammogram

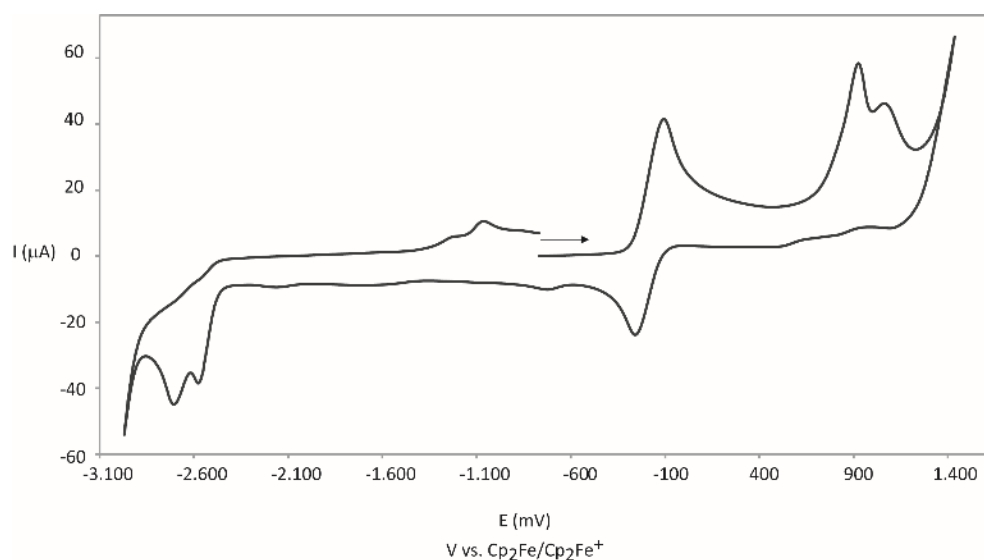


Fig. S63. CV of compound $[(\text{Cp}^*\text{Fe})_2\{\mu,\eta^{4:4}\text{-P}_5\text{tBu}(\text{CH}_2)_3\text{P}_5\text{Me}\}]$ (**4**)

Computational details

DFT calculations were carried out using the ORCA program.⁵ The geometries were optimised using the B3LYP⁶⁻⁹ functional together with the def2-TZVP basis set¹⁰ and the RIJCOSX¹¹ approximation. The dispersion effects have been incorporated by using the charge dependent atom-pairwise dispersion correction D4¹² as implemented in Orca. The nature of the stationary points has been proofed by frequency analysis at the B3LYP-D4/def2-SVP level of theory, which show no imaginary frequencies.

Thermodynamic data for **3** (B3LYP-D4/def2-SVP):

```
-----
GIBBS FREE ENERGY
-----
The Gibbs free energy is G = H - T*S

Total enthalpy           ... -7150.78057949 Eh
Total entropy correction ... -0.13824262 Eh   -86.75 kcal/mol
-----
Final Gibbs free energy ... -7150.91882210 Eh

For completeness - the Gibbs free energy minus the electronic energy
G-E(el)                 ... 0.71506087 Eh   448.71 kcal/mol
```

Thermodynamic data for **3'** (B3LYP-D4/def2-SVP):

```
-----
GIBBS FREE ENERGY
-----
The Gibbs free energy is G = H - T*S

Total enthalpy           ... -7150.77005460 Eh
Total entropy correction ... -0.13966935 Eh   -87.64 kcal/mol
-----
Final Gibbs free energy ... -7150.90972395 Eh

For completeness - the Gibbs free energy minus the electronic energy
G-E(el)                 ... 0.71289328 Eh   447.35 kcal/mol
```

Table S46. Total energies (final single point energy) for all optimized geometries (B3LYP/def2-TZVP level of theory).

	total energy [Ha]
3a	-7154.469496830940
3a'	-7154.459987063832

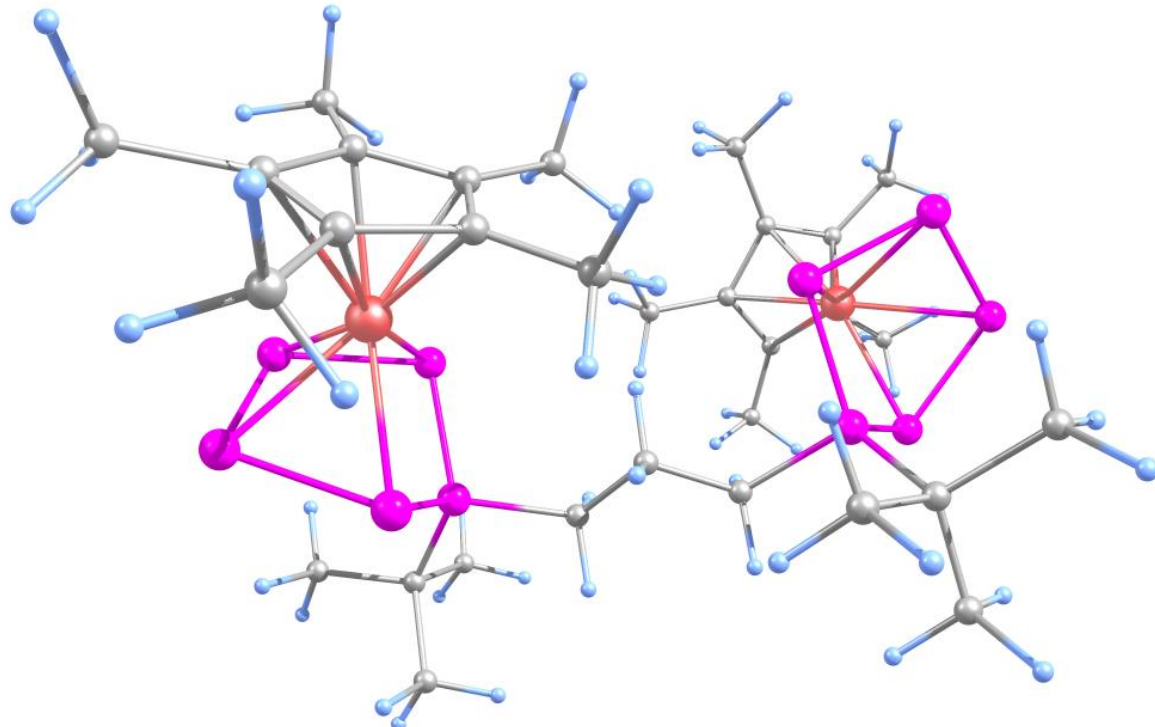


Table S47. Optimized geometries of **3a** XYZ coordinated in angstroms. B3LYP/def2-TZVP level of theory.

Fe	-3.89612574913573	-0.34794107283859	-0.61397446189609
Fe	3.63878182935633	-0.93015456651920	0.03386623664552
P	2.72596583662703	1.98428443911075	-0.52709583226963
P	-2.47904750898578	0.81931439164679	1.76771144278261
P	-2.19519222764702	-1.11688757919114	0.85454683120389
P	-4.33696150249641	1.46780725569684	0.85823333857024
P	3.70173633760971	1.14423265424407	1.21948218773384
P	2.72794677903173	0.24770188512820	-1.83115559561846
P	-4.17304981108793	-1.98700026386107	1.05252360169387
P	-5.55491174509278	-0.31893907396633	1.05164816421054
P	5.51300238333341	0.44490453845484	0.22559716143593
P	4.87589528166990	-0.14511013519568	-1.77451950245137
C	-2.75704189038912	-0.22898915852495	-2.36893429247994
C	-3.74009641237626	0.80886054258807	-2.36061504617170
C	2.29073391794523	-2.55494505457827	0.0051292819991
C	2.50776470107320	-2.10965326839348	1.34692690368712
C	-5.03686394142918	0.19910881981853	-2.26082044292164
C	-4.85189239364236	-1.22466109185548	-2.21200947448532
C	3.91484353088382	-2.21091106027846	1.62563312402477
C	0.17146498395089	1.34587488646333	0.68506972878698
H	0.07594117430131	0.43153067628905	0.08295905563726
H	0.69395367599429	1.05910343916883	1.60829499788266
C	-2.31589299830187	1.00938776240778	3.63896481285955
C	4.5620932779603	-2.72549334119760	0.45120656677535
C	-3.44128425776155	-1.49073391666385	-2.27377367067324
C	3.55642221939502	-2.93205418438149	-0.5525536519323
C	0.97905999020489	2.39146087873303	-0.08078545291381
H	1.02413260663825	3.32772445123772	0.49897022792544
H	0.46760790058279	2.63329733103882	-1.02617384514508
C	-2.69115112053084	2.44953574614726	4.01632789732006
H	-1.97217538710364	3.18643291444912	3.62464214135845
H	-3.69420405867065	2.71627072296564	3.64764707322029
H	-2.69676759444189	2.55038796615007	5.11483899566725
C	1.45641649189169	-1.72089622063759	2.33625991562819
H	0.52554835846223	-1.41414014276806	1.84268734374579
H	1.20571780033101	-2.57503250832909	2.99116351141586
H	1.79325447873039	-0.89792011945588	2.98329620212600
C	-1.21629681617293	1.92902377130274	0.98514511883186
H	-1.68697372826550	2.25103295146045	0.04431993631708
H	-1.13142981035002	2.82779699692140	1.61714269391292
C	-6.34481357035571	0.92725496762155	-2.27412848423879

H	-7.14174414177934	0.33246993353545	-1.80631330896582
H	-6.28348293653178	1.88073314521188	-1.72748993869308
H	-6.65802531299513	1.15885854848086	-3.30782938145936
C	3.36638193875112	3.63683685344448	-1.21289012029019
C	-3.47472562501108	2.27426111282028	-2.51703829850012
H	-4.21331367301737	2.88310247491656	-1.97687337609788
H	-2.47886509192531	2.54947004595706	-2.13910851464098
H	-3.51233134100339	2.56495775387648	-3.58227418415085
C	-1.28373402863463	-0.04389176057037	-2.55826435844719
H	-0.94222634043921	0.93803104427093	-2.20159225599459
H	-0.69903910744720	-0.80875904085939	-2.03302256039088
H	-1.01727143492772	-0.10580841634408	-3.62847393962158
C	-2.78910623066653	-2.83825460314679	-2.30028207807962
H	-1.82256998154093	-2.82761975003145	-1.77549620258395
H	-3.41785457177005	-3.59903545291230	-1.81616478961656
H	-2.59941782580890	-3.16736903779599	-3.33736409547827
C	-3.30671626147096	0.02210961448595	4.27546085102345
H	-4.34177040725422	0.23088866524621	3.96679096039081
H	-3.07714602946781	-1.01731980953922	3.99715702004004
H	-3.25086201641440	0.10536437864543	5.37409675928465
C	4.56717734053382	-1.90061538299555	2.93661646325379
H	4.07419368425839	-1.05592544585631	3.44148681920147
H	4.52035493112992	-2.76789004951645	3.61915692387473
H	5.62586919510979	-1.63305338309244	2.80687519247078
C	-5.94237268587966	-2.24854965654429	-2.15864340318297
H	-5.60824932475562	-3.16651741348056	-1.65421601291025
H	-6.81737170953091	-1.87339520635478	-1.60828113246234
H	-6.27538482185921	-2.52259790071164	-3.17539657651192
C	0.97235294487392	-2.70633931575721	-0.68431839391206
H	0.60412030409464	-3.74354415009104	-0.58721469912241
H	0.20473668981612	-2.05153390287631	-0.25321299685478
H	1.04984414340455	-2.48215398769093	-1.75790381601353
C	-0.88306060409607	0.67436413830048	4.07081995560187
H	-0.59284372939834	-0.33878940738243	3.75531843437300
H	-0.14604720549080	1.38688156236279	3.66956756878283
H	-0.81230067288057	0.71382345227039	5.17120215212140
C	6.01479033707361	-3.05909139300167	0.31164526404586
H	6.36727292752861	-2.89369849689484	-0.71689339968466
H	6.63709302534768	-2.44085812638212	0.97377170419649
H	6.19757815841632	-4.11863898654852	0.56414216365363
C	3.76405130419111	-3.51490618347219	-1.91649353886732
H	3.54224272245728	-4.59719447208472	-1.91921159736249
H	3.10743969054357	-3.04306702040378	-2.66310841889203
H	4.79920306819607	-3.38178094553984	-2.25941176225676
C	4.76670042226113	3.43727144033872	-1.81024381495882
H	5.48787417508745	3.08980039170756	-1.05800897026522
H	4.76171033691015	2.70801040030851	-2.63258989184910
H	5.12207631794461	4.40306457201739	-2.20814199320806
C	3.44799184853727	4.64132793126242	-0.05275425562757
H	2.46092764084933	4.88762323843146	0.36840268635858
H	4.08478368274756	4.26018503288130	0.76094914726248
H	3.89178802794604	5.58324637349836	-0.41682164768497
C	2.40797921088174	4.11994907416431	-2.31329158946251
H	2.84443207062695	4.99971917099148	-2.81517893366004
H	2.25023837467637	3.34413725775405	-3.08057697352942
H	1.42774951173002	4.42367586028766	-1.91699958778658

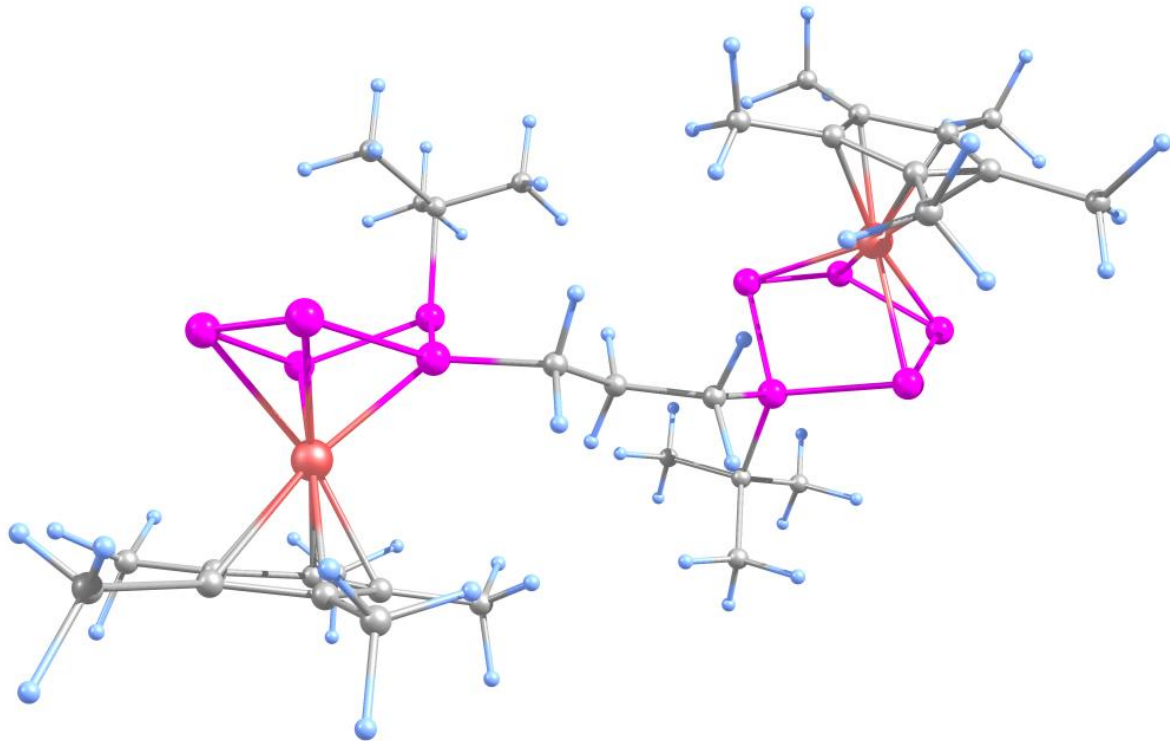


Table S48. Optimized geometries of **3a'** XYZ coordinated in angstroms. B3LYP/def2-TZVP level of theory.

P	2.44539429396336	-1.63150957727077	-0.56624568811845
P	4.18288554905658	-2.04334067820079	0.65771698796980
P	2.96365208327462	0.27643072547505	-1.44506134814584
P	4.99665829204042	-0.11733571562264	-2.10576091782546
P	5.78669842928416	-1.60216182730581	-0.74054111708681
C	-4.32237036143721	-2.24994338320505	0.38198718623868
C	-5.33180200510359	-1.87981478722743	-0.56168471750866
C	5.90456882100594	0.67531086779285	1.80330498644082
C	4.01448111218912	1.91223624064214	1.27041770714961
C	1.14366169286186	-1.22648153870422	0.68585548081296
H	0.92909878608511	-2.13436335313511	1.27145493601319
H	1.64959550734042	-0.52058589788193	1.36094249627807
C	6.22403434941569	1.50674247722723	0.67625895592743
C	-4.75460713578247	-1.83756867816226	1.68922442226243
C	4.53812100801846	0.93199169561136	2.16921381468231
C	-6.4011151443794	-1.24215540508671	0.16011120758601
C	5.05361762857041	2.26953552324628	0.34261859775758
C	-6.04310618885554	-1.21646867600004	1.55024634252320
C	1.77814016247471	-2.99504408952664	-1.69782683345156
C	-5.3143831682299	-2.17901106220682	-2.02835648606342
H	-5.91112955956582	-1.45039438949540	-2.59385684404720
H	-5.72855671759738	-3.18402732498262	-2.2273446343647
H	-4.29350907848526	-2.15156602182003	-2.43677773946805
C	-3.07215104715659	-3.00939190196026	0.05856241335920
H	-2.68905422174062	-2.74902650353494	-0.93848857165326
H	-3.26459419454801	-4.09712517395346	0.06411121213906
H	-2.27426420893490	-2.81761432026169	0.79028543792085
C	2.64994271871682	2.52607539906659	1.32835018930718
H	2.28814654446457	2.80471165518175	0.32915910024345
H	2.65663277982481	3.43940679667960	1.94984010339740
H	1.91173942532892	1.83914097206686	1.76822626880270
C	-4.03406753943925	-2.07875170717262	2.97994122758041
H	-2.94907351147422	-2.18154906597152	2.82874551624690
H	-4.38340920060708	-3.00911255819940	3.46210638930850
H	-4.19111712202257	-1.25416962275161	3.69018625512406

C	-6.88036700776841	-0.68406234984916	2.67067693049336
H	-6.25607306035811	-0.28643806848906	3.48388699477691
H	-7.52136006686509	-1.47684283467343	3.09530203072705
H	-7.53432782036340	0.13222664366207	2.33248045973471
C	-7.67814381059893	-0.74349647176478	-0.44139718414848
H	-8.1533830542165	0.01587136764541	0.19516188462643
H	-8.39816254708470	-1.56935878961601	-0.57956104707206
H	-7.50347166941354	-0.28397570960381	-1.42577149573560
C	6.83575019641436	-0.25363723817978	2.51794643197242
H	6.31107687510651	-1.15313999510042	2.87440528021003
H	7.28949050395642	0.23622353845723	3.39787561324072
H	7.65161009446840	-0.58908975925541	1.86211070781385
C	3.82532628074685	0.33611420621362	3.34360314097039
H	2.73427557065571	0.33150311033001	3.20259347247082
H	4.03215466853183	0.91713632359573	4.26024911232908
H	4.13962669787124	-0.70114998704447	3.52620905676131
C	2.99613377967194	-3.62019020649078	-2.39740561334597
H	3.68950827071049	-4.07965516215501	-1.67743088737660
H	3.55998543841537	-2.87070144113783	-2.97246627685665
H	2.65278651178877	-4.40220755155561	-3.09555764627982
C	4.93998246371744	3.30128235450712	-0.73600717061683
H	5.13695507582520	4.31351954466305	-0.34010639820062
H	3.93281140674601	3.31030333285774	-1.17981629439039
H	5.65445496076508	3.11326352092027	-1.55001141733605
C	1.05524627317668	-4.04880097333975	-0.84810021505148
H	0.78720277967868	-4.91346892321613	-1.47874771326316
H	0.12336618645440	-3.66205803049342	-0.40775870012113
H	1.69803016936052	-4.42153227451632	-0.03341914010069
C	7.557133151711428	1.59787018126467	0.00142421765325
H	7.45202756875091	1.85123648829434	-1.06332941227567
H	8.09942808516848	0.64320172382533	0.05829678368944
H	8.18658256762026	2.37322060175883	0.47278206330806
C	0.84605731885567	-2.37481435049682	-2.75052224056930
H	0.53432005192236	-3.15666062888461	-3.46380457465272
H	1.35841214252534	-1.58383655286562	-3.31980286038210
H	-0.06467235468716	-1.93857400685041	-2.31675528212024
P	-2.51021934669681	1.39616820129440	-1.52976635049044
P	-2.60324477658315	0.63741222191977	0.48179291482486
C	-1.83769831025607	3.17808446685466	-1.59137998222399
C	-2.01773358773538	3.63053972810982	-3.04972347568192
H	-1.48100309545854	2.97167071297804	-3.75132413689115
H	-1.62540113808869	4.65441236927941	-3.17824127513084
H	-3.08200792441164	3.64264792094999	-3.33676553256952
C	-0.34625282526864	3.08932364673840	-1.23101323753738
H	-0.20471139097553	2.76442725522005	-0.18753026391548
H	0.12585387549892	4.08270986923097	-1.32981914914440
H	0.20436127958791	2.39227102801642	-1.88306998585895
C	-2.5608227977087	4.13610373769510	-0.64312468725614
H	-3.63448164797064	4.19981118788662	-0.87342916224385
H	-2.12952564173566	5.14897662916362	-0.73538403770925
H	-2.46596988865205	3.82023688042076	0.40627983929713
P	-4.73317678199069	1.28548835324196	-1.42812107771082
P	-5.47012892374880	2.00635151595480	0.50825779559798
P	-3.91371958134012	1.56751956566209	1.93079060974306
Fe	-4.64041281480067	-0.18990346022601	0.44389789471545
Fe	4.67565660190309	0.24017766646437	0.19432640181534
C	-0.13177116942396	-0.60734020216688	0.11646696641590
H	-0.70437063700491	-1.35912154645079	-0.44474881579102
H	0.13063479379826	0.17749995634143	-0.60910571972749
C	-1.02250727489472	-0.00112532009759	1.20185183414550
H	-0.50478170073378	0.82328204389501	1.71854231720777
H	-1.29420467520964	-0.74664515414315	1.96655219697078

References

- 1 E. S. S. A, L. Lochmann and J. Trekoval, *J. Organomet. Chem.*, 1987, **326**, 1–7.
- 2 O. J. Scherer and T. Brück, *Angew. Chem. Int. Ed.*, 1987, **26**, 11987.
- 3 M. V. Butovskiy, G. Balázs, M. Bodensteiner, E. V. Peresypkina, A. V. Virovets, J. Sutter and M. Scheer, *Angew. Chem. Int. Ed.*, 2013, **52**, 2972–2976.
- 4 S. Reichl, E. Mädl, F. Riedlberger, M. Piesch, G. Balázs, M. Seidl and M. Scheer, *Nat. Commun.*, 2021, **12**, 5774.
- 5 a) ORCA - An Ab Initio, DFT and Semiempirical electronic structure package, Version 5.0; b) F. Neese, *WIREs Comput Mol Sci.*, 2012, **2**, 73–78; b) F. Neese, *WIREs Comput Mol Sci.*, 2017, **8**, e1327.
- 6 A. D. Becke, *J. Chem. Phys.*, 2005, **98**, 5648–5652.
- 7 S. H. Vosko, L. Wilk and M. Nusair, *Can. J. Phys.*, 1980, **58**, 1200–1211.
- 8 C. Lee, W. Yang and R. G. Parr, *Phys. Rev. B*, 1988, **37**, 785–789.
- 9 P. J. Stephen, F. J. Devlin, C. F. Chabalowski and M. J. Frisch, *J. Phys. Chem.*, 1994, **98**, 11623–11627.
- 10 F. Weigend and R. Ahlrichs, *Phys. Chem. Chem. Phys.*, 2005, **7**, 3297–3305.
- 11 F. Neese, F. Wennmohs, A. Hansen and U. Becker, *Chem. Phys.*, 2009, **356**, 98–109.
- 11 a) E. Caldeweyher, S. Ehlert, A. Hansen, H. Neugebauer, S. Spicher, C. Bannwarth, S. Grimme, *J. Chem. Phys.* **2019**, *150*, 154122; b) E. Caldeweyher, C. Bannwarth, S. Grimme, *J. Chem. Phys.* **2017**, *147*, 034112.
- 13 L. J. Bourhis, O. V Dolomanov, R. J. Gildea, J. A. K. Howard and H. Puschmann, *J. Appl. Crystallogr.*, 2009, **42**, 339–341.
- 14 G. M. Sheldrick, *Acta Crystallogr. Sect. A*, 2015, **71**, 3–8.
- 15 G. M. Sheldrick, *Acta Crystallogr. Sect. C*, 2015, **71**, 3–8.